INFLUENCE OF ATOMIC STRUCTURE ON PLASTIC DEFORMATION IN TECTOSILICATE CALCIUM-ALUMINOSILICATE, MAGNESIUM-ALUMINOSILICATE, AND CALCIUM-GALLIOSILICATE GLASSES

A Dissertation

Presented to the Faculty of the Graduate School

of Cornell University

In Partial Fulfillment of the Requirements for the Degree of

Doctor of Philosophy

by

Lisa A. Lamberson

August 2016

INFLUENCE OF ATOMIC STRUCTURE ON PLASTIC DEFORMATION IN TECTOSILICATE CALCIUM-ALUMINOSILICATE, MAGNESIUM-ALUMINOSILICATE, AND CALCIUM-GALLIOSILICATE GLASSES

Lisa A. Lamberson, Ph. D.

Cornell University 2016

Calcium Aluminosilicate glasses are of great industrial importance and are the basis for such products as liquid crystal display (LCD) substrates and Corning® Gorilla® glass due to their mechanical attributes such as high hardness and scratch resistance. It is widely known that silicate glasses deform by two mechanisms, shear and densification. However, it still remains unclear what are the microscopic mechanisms of shear deformation and what microscopic processes cause glasses to transform from one mode of deformation to the other.

In this work we explored a series of tectosilicate calcium aluminosilicate glasses. Hardness results, obtained from nanoindentation without fracture, for these glasses show a clear shift from shear deformation in glasses with < 80 mole% SiO_2 to densification deformation in glasses with > 80 mole% SiO_2. Shear deformation in these glasses is proposed to be aided by the movement of non-bridging oxygen (NBO) contained in the glass. Higher coordinated Al species, such as $Al^{(V)}$, are proposed to prevent the movement of NBO and thereby increase the glass hardness. The deformation mechanism must shift from a lower energy shear process to a higher

energy densification process, as indicated by 100% SiO_2, which deforms primarily by densification, having the highest hardness, when NBO are no longer available.

We further show that by making atom substitutions, such as Mg for Ca and Ga for Al, we can change the overall hardness and the concentration at which the deformation mode transitions from shear to densification in these glass systems. The overall hardness increases at high SiO_2 content when Ca is substituted with a higher field strength atom, Mg, due to an increased amount of higher coordinated Al and the stronger Mg-NBO bond, both of which prevent the NBO from participating in shear. In Ga containing glasses the weaker bond strength of Ga-O over Al-O allows shear to occur not only by movement of NBO but also by movement of Ga-O bonds, decreasing the hardness at low SiO_2 content. The shift from shear to densification at lower SiO_2 content in the Mg case is thought to result from a more difficult shear process along with a more open structure, due to the smaller size of Mg over Ca, and in the Ga case the shift from shear to densification occurs at the same place as it does for calcium aluminosilicate glasses.

BIOGRAPHICAL SKETCH

Lisa Lamberson is from Corning, NY. Lisa has a B.A. from Keuka College in Biochemistry/Biology and a M.S. from Alfred University in Glass Science and Engineering. Lisa has worked for Corning Incorporated for the past 15 years. Her work has ranged from developing measurement systems for fiber optics and planar photonic devices to developing new glass compositions for Corning businesses. Lisa currently works in the Glass Research department at Corning Incorporated.

ACKNOWLEDGMENTS

I would like to thank Dr. Baker, Dr. Mauro and Dr. Ellison for their guidance and helpful ideas throughout this research project. It is thanks to them that this research was so successful. I would like to thank Dr. Randy Youngman for all of his help with NMR data and interpretation. He was an invaluable resource for me and I could not have done this project without him. I would like to thank the EMP group at Corning for all of the glass melting and the finishing shop for the glass processing. I would also like to thank Corning Incorporated and the Glass Research department for their financial support throughout this process. I would like to thank Dr. Bob Morena, Dr. Charlene Smith and Dr. Nick Borrelli for their support and encouragement, without which I would not have been able to succeed in this adventure. Dr. Bob Morena specifically, has been a profound influence. His guidance, encouragement and support in my role within the Glass Research department at Corning Incorporated are primarily responsible for my desire to go on for a PhD in materials engineering. I will forever be grateful for all of the knowledge and wisdom he has provided me over the past 14 years.

I would like to thank my parents, Richard and Ellen French, for being such a great support system. Without them I would not be where I am today. Also I would like to thank my husband, Derwin Lamberson, for always supporting me and encouraging me to follow my dreams. Lastly, I would like to thank my children, Ella and Adler, for their patience during this long journey.

TABLE OF CONTENTS

LIST OF FIGURES

LIST OF TABLES

CHAPTER 1

INTRODUCTION

Glasses have been long sought after because of their environmental friendliness, transparency and durability. These factors have enabled them to be used in a variety of products such as the skywalk at the Grand Canyon, enabling people to look down through glass floors from high heights. Glasses are also utilized in such products as container glass, spacecraft windows and most recently in mobile hand held devices. All of the aforementioned products require better structural reliability and mechanical integrity of the glass to prolong its lifetime. If the structural mechanisms in glasses that lead to superior mechanical properties could be identified for silicate glasses, new potentially easier to melt glasses could be designed to mimic the silicate structure which provides the desirable mechanical properties.

It has been known since the 1970's that glasses have the ability to plastically deform. This plastic deformation is noticed in such things as pile-up, lateral displacement of material around an indentation impression, scratches, grooves in glass with the absence of cracking or chipping, and more recently in a process known as ductile regime grinding.[(2)]In the latter case the plasticity of glasses is specifically taken advantage of in order to produce finished glass parts that have improved shape accuracy and optical surface quality.[(1)] It has also been found that plastic flow is a more energetically favorable material removal process as opposed to the conventional fracture process used in standard grinding and polishing techniques.[(2)] For these

reasons much research has been conducted recently on brittle materials and glasses specifically[1-3], to develop ductile machine grinding methods which can take advantage of the plastic regime in these materials.

All of the current research in ductile machine grinding however, has been focused on developing machine settings and parameters which will remove the very surface layer (10-100 nm) of material.[3] It was found that at this low depth of cut one could avoid the brittle regime and stay completely in the ductile regime for glasses. These studies on ductile regime grinding aim to determine the ductile to brittle transition in glasses but do not go into depth on the underlying mechanisms of plasticity in glasses. My research was focused on identifying these underlying mechanisms and understanding how they work in glasses.

Plasticity in general is the result of breaking and reforming of bonds with neighboring atoms. Since the types of atoms and bonds associated with them are crucial to understanding plasticity it is crucial to know what the glass structure looks like. Specifically, what atom species are present in the glass structure and the polyhedral arrangements the atoms are found in. It is also important to know how polymerized the glass structure is, or in other words, if there are non-bridging oxygen (NBO) present. This information can be determined by the use of ^{27}Al Triple quantum magic angle spinning nuclear magnetic resonance (^{27}Al 3Q MAS NMR). This is a technique which has been widely used in the literature to provide structural information on glasses.[4-6] From the knowledge of the species, bond types and polyhedral configurations of the atoms, we can identify which species are most likely to break and re-form contributing to the plastic deformation or hardness. It is from this

knowledge that we can begin to draw a picture of how the atoms would rearrange in the structure accommodating permanent deformation.

The glass composition I have chosen to study is the calcium aluminosilicate (CAS) one, because of its industrial importance. This glass composition is the backbone for the liquid crystal display glasses that are used in flat screen televisions. I investigated simplistic versions of the calcium aluminosilicate glasses by using glass compositions that have a 1:1 ratio of CaO to Al_2O_3. These are glasses that are of the nominal composition $(CaO + Al_2O_3)_{1-x} + (SiO_2)_x$.

In order to understand what effect the different species in the glass have on the plastic deformation behavior of the glass I varied the SiO_2 content systematically while maintaining a 1:1 ratio of CaO to Al_2O_3. This systematic variation provides information on the importance of density of bonds vs. strength of bonds in relation to plastic behavior and hardness of glasses.

Since I am interested in the plastic deformation behavior of tectosilicate calcium aluminosilicate glasses specifically, I used the measurement of hardness as determined by point contact of a sharp pyramidal indenter. This is a method commonly employed for investigating plastic deformation and fracture in glasses. This technique is relatively easy to perform and hardness is a good measure of plasticity as hardness is the resistance of a material to permanent deformation. I selected nanoindentation as an indentation technique that will ensure plastic deformation without fracture. Previous data by Gross and Tomozawa[7] showed in similar glasses using Vickers indentation that onset of cracking begins at forces around 1.96 N, however, they use a description of onset of cracking which states that the load at

which 2 out of 4 possible cracks stemming from the corners of a diamond shaped indentation is the crack onset load. Since I wanted to avoid any and all cracking I used indentation loads much lower than this. Nanoindentation is performed at very low loads on the order of 0.01N. This technique has been shown to produce reliable and repeatable data without causing fracture. Fracture would cause our results to have an artificially low hardness and will also impact our ability to understand the plastic behavior of these glasses as fracture in the indentations would confound the results and make analysis on plastic behavior more difficult.

This thesis is structured in the following manner. First I provide background information going over all relevant material needed to fully understand the current status of plasticity in glasses and how it is measured. I then describe the calcium aluminosilicate glass system and what we found for hardness and modulus along with the glass structure as determined by ^{27}Al 3Q MAS NMR. I then discuss these results with respect to plastic deformation and propose a possible mechanism for the observed deformation. The same investigative method was applied to systems where the Mg was swapped for Ca and the Ga was swapped for Al. These substitutions enable the understanding of the underlying mechanisms of plastic deformation in glasses by targeting the effects of NBO on shear and glass structure on densification.

REFERENCES

1. P.S. Sreejith, B.K.A. Ngoi, "Material Removal Mechanisms in Precision Machining of New Materials." *International J. of Machine Tools and Manufacturing* **41**, 1831-1843 (2001).

2. T.G. Bifano, T.A. Dow, R.O. Scattergood, "Ductile-Regime Grinding: A new Technology for Machining Brittle Materials." *J. of Engineering for Industry* **113**, 184-189 (1991).

3. W.J. Wills-Moren, K. Carlisle, P.A. McKeown, P. Shore, "Ductile Regime Grinding of Glass and Other Brittle Materials by use of Ultra-Stiff Machine Tools." *SPIE,* **1333,** 126-135 (1990).

4. L. M. Thompson and J.F. Stebbins."Non-Stoichiometric Non-Bridging Oxygens and Five Coordinated Al in Alkaline Earth Aluminosilicate Glasses: Effect of Modifier Cation Size." *J. Non-Cryst. Solids,* **358,** 1783-1789 (2012).

5. L. M. Thompson and J. F. Stebbins."Non-Bridging Oxygen and High-Coordinated Aluminum in Metaluminous and Peraluminous Calcium and Potassium Aluminosilicate Glasses: High Resolution ^{17}O and ^{27}Al MAS NMR Results." *American Minerologist,* **96**, 841-853 (2011).

6. D. R. Neuville, L. Cormier and D. Massiot."Al Coordination and Speciation in Calcium Aluminosilicate Glasses: Effects of Composition Determined by ^{27}Al MQ-MAS NMR and Raman Spectroscopy." *Chemical Geology,* **229,** 173-185 (2006).

7. T.M. Gross, M. Tomozawa, A. Koike, "A glass with high crack initiation load: Role of fictive temperature-independent mechanical properties. *J. non-cryst. Sol.* **355,** 563-568 (2009).

CHAPTER 2

BACKGROUND

In order to construct a good experimental study on plasticity in $(CaO+ Al_2O_3)_{1-x} + (SiO_2)_x$ glasses, where x is the moles of CaO and Al_2O_3 in the glass, we must have a good understanding of what is already known about how glasses plastically deform. We will also have to understand what people currently know about the structure of $CaO\text{-}Al_2O_3\text{-}SiO_2$ glasses. For these reasons a thorough discussion of all of the relevant material needed in order to understand the experiments conducted and the results obtained from those experiments in this thesis is provided in this chapter. This information includes discussions on the silica anomaly, the different deformation mechanisms found in silica containing glasses, how fracture occurs in silica containing glasses, the nanoindentation technique, previously reported hardness and indentation modulus data for similar glasses, different techniques for looking at glass structure, and relevant structural information on calcium aluminosilicate glasses.

2.1. Silica Anomaly

In the experiments discussed in Chapters 4, 5 and 6, we have glasses that contain varying amounts of silica from roughly 35 mole% to 100 mole%. The glasses at low SiO_2 content, below 80 mole%, are considered "normal" glasses.[(1)] Normal glasses have large amounts of modifying ions and a more dense structure. Glasses with SiO_2 contents > 80 mole% are considered to be "anomalous" glasses.[(1)] Anomalous glasses are typically characterized as being made up primarily of network formers, which have

---

* Figures reproduced from;
2. M.R. Vukcevich**,** *J. Non-Cryst. Solids*, **11**, 25-63, 1953.
27. Oliver, Pharr, *J. Mater. Res.*, 19 [1] 3-20, 2004.

a more open network structure containing strong covalent bonds. These structural differences between "normal" and "anomalous" glasses impact several different glass properties including hardness.

The silica anomaly is a set of phenomena observed in tetrahedrally coordinated glasses, more specifically in glasses with silica content greater than about 80 mole%, which have open network structures made up of strong covalent bonds, and are characterized by several anomalous properties[(1)] including unusually low thermal expansion at low temperatures, positive temperature gradient and negative pressure gradient of bulk modulus, and deformation mainly by densification when indented with a diamond tip indenter (as opposed to "normal" glasses, which deform by shear).[(1-2)]

Since the Si-O bond distance in glass was found to always be the same, 1.61 ± 0.01 Å, no matter how the glass is processed, it was determined that the most likely cause for the observed anomalous property characteristics described above is the transverse bending of the Si-O-Si bond framework between network tetrahedron as proposed by H.T. Smyth in 1953.[**(1-3)**] The transverse bending will lead to a decrease in the Si-Si distance resulting in a contraction of the network as shown in Figure 2.1a. This contraction of the network leads to a negative coefficient of thermal expansion (CTE) at low temperatures. At high temperatures, the other modes normally associated with dilatation, shown in Figure 2.1b, will become excited resulting in a positive CTE.[**(2-3)**]

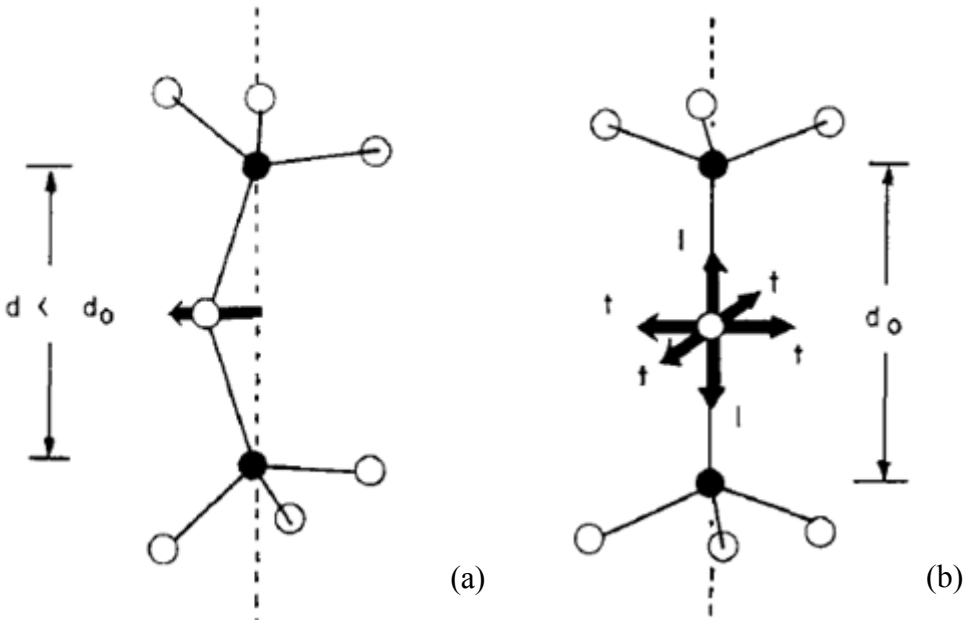

Figure 2.1: a) Effects of transverse oxygen oscillations on thermal expansion of silica b) Vibration modes of an independent oxygen oscillator in silica polymorphs. [2]

However, M.R. Vukcevich felt that the above description was problematic as it does not include any well-defined parameters that are characteristic of the vitreous network.[2] All of the modes considered above would also exist in the crystalline form at the same frequencies.[2] So he came up with a two Potential Energy (PE) minimum model[2] Unlike silica crystals that are characterized by a well-defined Si-O-Si angle, ϕ, (hereafter defined as oxygen angle), silica glasses are characterized by a broad distribution of oxygen angles, as shown in Figure 2.2. The two potential energy minimum model suggests that, even though silica glass is made from a network of randomly oriented tetrahedral, there is still a preference for certain oxygen angles.

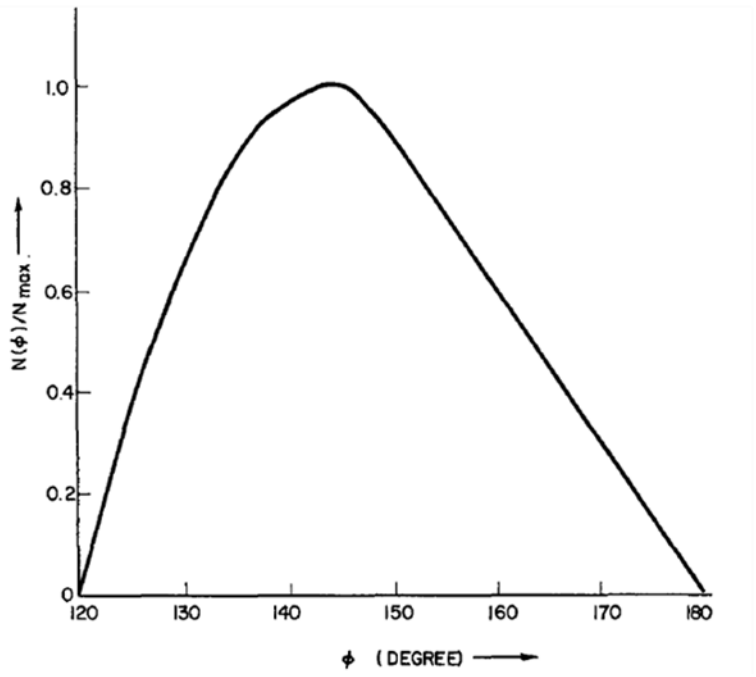

Figure 2.2: Average distribution of oxygen bond angles in vitreous silica at R.T. $N(\phi)/N_{max}$ is the number of oxygen angles at a given value/the maximum number of oxygen angles found in fused silica.[2]

These oxygen bond angles are grouped around two different values—ϕ_α^o , which is a low temperature, high density phase of crystalline silica and ϕ_β^o ,which is a high temperature, low density phase in crystalline silica—that are separated by a small energy barrier.[2] In fused silica, which has an average Si-O atom separation distance, *r*, of 1.61 Å, ϕ_α^o is found to have a value of 138° and ϕ_β^o is found to have a value of 145°. At any given temperature and pressure there will be oxygen angles distributed around these two angles.[2] A change in the stress or temperature of fused silica will result in a change in the ratio of ϕ_α^o and ϕ_β^o states, resulting in anomalous macroscopic behavior.[2]

Vukcevich[2] determined that instead of looking at the standard central force model, which states that potential energy of a crystal depends only on the distance between the atoms and has a single minimum at the equilibrium spacing, r_o, for silica we should be looking at a potential energy curve with two minima. This was determined based on evidence that some silica crystals have, at different temperatures, two equilibrium phases indicating that the potential energy must have two minima.[2] Figure 2.3a shows the proposed potential energy diagram, which plots potential energy (h) as a function of change in angle, ϕ, instead of change in Si-O distance, r. This diagram is applicable when r_α, the distance of the Si-O bond for the α phase, and r_β, the distance of the Si-O bond for the β phase, are equivalent, which was found to be always true in silica containing glasses. Figure 2.3b shows the free energy, g, as a function of ϕ at varying temperatures of vitreous silica. The entropy term is what changes the relative free energy of the two minima.[2]

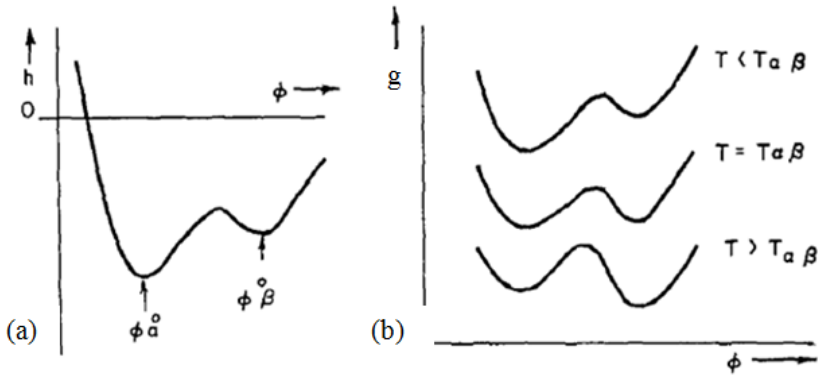

Figure 2.3: a) Simplified central force potential applicable when $r^\circ_\alpha = r^\circ_\beta$. Minima refer to α and β modifications of silica crystals. b) Free energy as a function of ϕ for $\alpha \leftrightarrows \beta$ solid state displacive transformation. [2]

This two PE minimum theory would explain the pressure dependence of compressibility because an applied pressure will result in some of the ϕ_β^o jumping over the energy barrier to ϕ_α^o. Each of these jumps will result in two of the tetrahedron coming closer together and contraction of the glass structure. As the pressure continues to increase, the activation barrier between the two states will become smaller and will result in more ϕ_β^o angles transforming to ϕ_α^o causing the compressibility of the glass to increase with pressure. However, at a specific pressure, all of the ϕ_β^o will have transformed to ϕ_α^o, resulting in a decrease in compressibility with increasing pressure from this point on. Experimental data in Figure 2.4 indicate that this maximum point in compressibility as a function of pressure occurs at 30 Kbar or 3 GPa.[2]

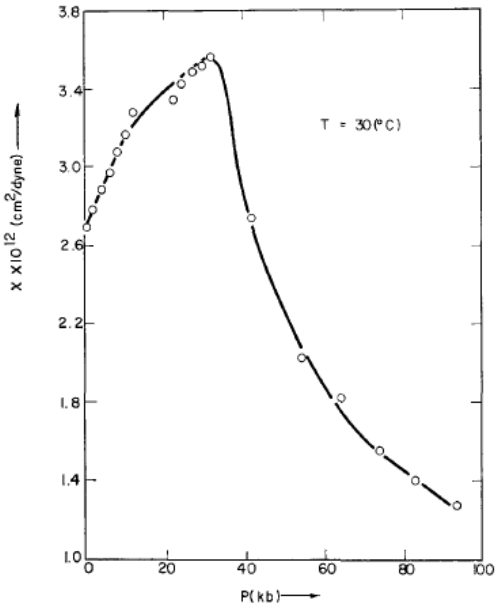

Figure 2.4: R.T. compressibility of vitreous silica as a function of pressure.[2]

This theory of two potential energy minima in bond angles, ϕ_{β}^{o} and ϕ_{α}^{o}, can be qualitatively justified by analyzing the geometry of bonds in different silicates. It is known that in SiO_4 tetrahedron the Si-O bonding is partially ionic and partially covalent. The SP_3 hybridization, oxygen charge repulsion, and steric hindrance of the Si-O bond all favor a tetrahedron shape. On the other hand, the orientation of two tetrahedron next to each other will be less resistant to smaller changes because the oxygen angle can change and will change to minimize the angular potential energy.[4] Hence, this oxygen angle change is the main cause of the observed anomalous behavior in thermal expansion coefficient and compressibility in silica-containing glasses at all temperatures. The degree of the silica anomaly is directly proportional to the silica content in the glass.

2.2. Mechanical Properties

2.2.1. Mechanisms of plastic deformation in glass:

It has been known since the 1800's based on Victorian glassware that glass can hold lasting impressions. This indicated that glass was sufficiently plastic enough to take an impression. Taylor, in 1949, using a diamond indenter tip showed that he could produce a crack free, permanent indentation in glass.[5] He further found that there was a rim of piled-up material around the depression.[5] The presence of pile-up material has since been reported by several others and is considered to be a way of confirming the presence of shear deformation in glasses. Following up on the discovery of a permanent deformation in glass upon indentation with a sharp indenter, Ernsberger looked at several silicate glasses and identified areas under the indentation impression

which had higher index of refraction compared to that of the surrounding glass.[6] He identified these areas by taking an indented piece of glass and reducing its thickness to about 0.5 mm by grinding and polishing the side opposite the indentation impression. He then submerged the sample in index oil matched to the refractive index of the specimen glass and, using an interference microscope, was able to measure the fringe motion associated with the density change of the glass structure in the region beneath the indentation. From this observation he deduced that glasses deform by densification rather than plastic or shear flow process. According to Ernsberger, densification cannot be considered plastic deformation, as it does not require the breaking and reforming of bonds; instead it is the rearrangement of atoms to a more close packed state[7]. Therefore he concluded that glasses do not deform plastically.[6] We know this to be inaccurate as subsequent research into plasticity in glass as measured by sharp point contact under load has shown that glasses which have a minimum amount of modifiers do in fact deform by shear flow dominated processes. Peter in 1970 performed indentations on 3 different silicate glasses (fused silica, binary alkali-silicate, and a ternary alkali/alkaline-earth-silicate glass) and was able to show that not only do all 3 glasses exhibit densification deformation but that the ternary glass also exhibits shear deformation.[8] It was based upon this finding that Peter came to the conclusion that glasses with a minimum number of network modifiers will exhibit shear flow deformation.[8] He based this conclusion on the observation of pile-up of material around the indentation impression, which is an indication of a lateral displacement process, and cannot be imagined without having flow.[8] Peter was also the first to identify a system of curved lines that he believed developed during the last

stage of the formation of the densified region under the indentation impression. This system of curved lines resembles a "rosette pattern" which is very much like the slip line systems occurring in theoretically well-known problems of plasticity.[8]

2.2.1.1. Mechanisms for shear deformation in glass

It is difficult to think about a dislocation model for amorphous materials, so Peter suggested a type of rate process, such as the influence of shear on viscosity, to describe how shear deformation could be occurring.[8] He believed that potential barriers of various activation energies occur in glasses with network modifiers. During shearing the potential barriers will be reduced in the direction of effective shear stress. This will facilitate the transition of an atom to a neighboring potential well.[8] This is a plausible explanation in glass because there are groups of atoms around network modifiers, which will be strongly bound to each other but loosely bound to the surroundings with the exception of one atom. It is at this site that a local stress concentration is generated providing energy for the motion of this group of atoms.[8] This proposed mechanism of plastic flow is consistent with what people have proposed in the past, which is that slip in glasses is associated with regions which are not well connected such as those containing NBO and modifiers.[1]

In 1974, by studying metallic glasses, J.J. Gilman recognized that dislocation motion can play a leading role in flow of glasses, as dislocations do not need a uniform lattice for their definition. He believes that in "perfect" glasses nucleation might be the limiting step. However if it is not the critical step then the resistance to the propagation of dislocations is important. [9] Assuming we have a homogeneous

glass, the resistive stress can be calculated by assuming the critical feature is that atoms at dislocation cores must be sheared past one another irreversibly. The shearing process is accompanied by some average dilation if the atoms are densely randomly packed.[9] The energy required for the dilation is provided by the work done by dislocation motion. The dilation will originate at a point of weakness (ionic bond, modifier atom) and spread in a shear plane. This observed dilation will facilitate slip in the material. [9] A substantial amount of strain energy is liberated in the volume of the sheared region.[10] Part of this energy will go to the creation of dilation which enables the atoms to glide past each other, however the remaining portion will appear as heat. The resulting local temperature rise may account for the occurrence of inhomogeneous shear in silicate glasses.[10]

2.2.1.2. Mechanisms for densification deformation in glass

The other form of deformation identified in glasses is densification deformation, which is a contraction of material under the indenter tip during loading, that results in bonds bending to a more close packed structure.[11-13] There will not be any evidence of pile up around the indentation impression with this form of plastic deformation as it is not displacive in nature.[12,14] Densification deformation is the characteristic form of deformation for glasses that have open structures, low packing density, and little to no modifier ions present in the structure.[11,13] Glasses that exhibit densification deformation, such as fused silica, are considered to be "anomalous" glasses.[11]

2.2.1.3. Transition from Plastic Deformation to Fracture

It has been shown by several authors that glass under point loading will transition from plastic to fracture.[8,16-21] According to Lawn, this transition from plastic to fracture occurs because as the indenter begins to contact a specimen surface, the elastic stresses build up rapidly until the cohesive strength of the solid is exceeded.[16] These elastic stresses are a result of mismatch between the plastically deformed volume and the surrounding elastically deformed material.[17] At this point local plasticity occurs and takes the form of discrete slip events, called shear faults which occur at relatively high stress levels on the order of ($H/E > 0.1$) where E is elastic modulus.[16] The shear fault will propagate in the subsurface of the material, somewhat relaxing contact pressure as it does so. However, as the indenter continues to penetrate, the stresses will build up again, and the process will repeat itself. This repetitive process is what causes the inherent discreteness in the observed fault pattern.[16]

The fault lines will follow curved shear stress trajectories, and intersection lines between the fault surfaces provide high stress concentration sites for initiation of corner radial cracks.[16] (How the cracks are nucleated from the intersecting shear lines has been studied in greater detail by Hagan and Swain and will be discussed in more detail in the following section, fracture formation in glasses.) Kato and co-workers also found that radial crack nucleation is governed by the residual stress induced by plastic deformation in glasses during indentation with sharp indenters.[18] They further

concluded that as plastic deformation increases with applied load, the residual stress will reach a critical value at some point beneath indentation and cracks will initiate.[18]

The above theories on transition from plastic to fracture with a self-similar indenter tip cannot be true, because a self-similar tip will have geometrical similarity in the stress fields. This means that the contact pressure during indentation remains independent of size.[15] Therefore there must be another explanation as to why there is a transition from plastic to fracture in glasses when using self-similar indenter tips.

Lawn has a fracture mechanics argument which explains how a characteristic fixed length scale is what causes the transition from plastic to fracture in brittle materials.[16] He states that this critical value or threshold condition for crack formation can be estimated to occur when a critical dimension a_* is exceeded.

$$a_* = \left(T_0/2\chi H\right)^2 , \tag{1}$$

where T_0 is the toughness of the glass, H is the indentation hardness, and

$$\chi = \varepsilon \left(E/H\right)^{1/2} (cot\,\phi)^{2/3} , \tag{2}$$

where E is the elastic plastic geometry coefficient and ϕ is the indenter half angle.[16] Lawn arrives at this critical condition a_* by considering that for sharp indenters the deformation depression diagonal

$$a = \left(P/2H\right)^{1/2} , \tag{3}$$

where *P* is indenter load and for fracture to occur the radial crack length,

$$C = (\chi P/T_0)^{2/3}. \quad (4)$$

As one can see, C varies more strongly than a with indenter load, P. Therefore there is a critical dimension $a_* = c_*$ below which radial cracks are surpressed.[16]

The depth at which the fracture threshold occurs varies, depends on the glass composition under study. This is believed to be a result of the amount of densification deformation the glass undergoes during indentation. Densification is thought to reduce residual stress around the indentation, and thereby prevent cracks from initiating.[19] All glasses according to Peter are believed to undergo some amount of densification.[8] The amount of densification a glass undergoes however, will vary based on composition.[20] For instance, Yoshida found that in two glasses classified as "normal" the indentation volume resulting from densification varied from 3% for soda lime glass to 61% for float glass.[20] In a so called "anomalous glass" the indentation volume from densification is near 100%. According to Sellappan the densified region is found in the area of contact of the indenter with the glass and in a region typically about $^1/_3$ of the indentation depth.[21]

Sellappan used Poisson's ratio as a way of predicting which deformation mode, densification or plastic deformation by shear, will predominate in the glass composition under investigation.[21] He found that when a glass had a Poisson ratio, υ, of less than 0.2, densification prevails and limits residual stress. As υ increases, shear becomes easier and, for $\upsilon > 0.3$, enhances crack initiation resistance at a fixed amount of compaction.[21] Based on this criteria he believed that the ideal glass for crack

resistance under indentation would have a large amount of densification and some shear deformation. He however, felt that this type of glass would be a challenge to make as glasses which exhibit large amounts of densification contain highly cross-linked networks and are therefore resistant to shear.[21]

2.2.1.4. Fracture formation in Glass

In 1978 Hagan and Swain took Peter's findings of shear bands or shear flow in glasses one step further by studying the shear bands (rosette pattern) in greater detail to determine how cracks are nucleated.[22] They did this by etching samples after indentation and looking at them in a microscope.[22]They were able to determine that beneath the indent was a system of interacting shear bands, which are responsible for the nucleation of radial cracks. They further suggest that on the shear bands are over-constrained atomic bonds which are the nucleation sites for lateral cracks.[22] The sub surface median cracks are nucleated as a result of the interaction of two shear bands, similar to piling up of dislocations in two intersecting slip planes resulting in crack nucleation in crystals, which was suggested by Stokes, et. al. in 1958.[22] These shear band interactions most likely take place at local weaknesses (regions with modifiers as Peter suggested) in highly strained regions beneath the indenter. Once the median cracks are nucleated they will continue to propagate in a direction roughly parallel to shear stress trajectories.[23] This will help to minimize the number of strong covalent bonds which would need to be broken.

Hagan in 1980 took a closer look at crack nucleation in soda-lime silicate glasses.[23] He found that the shear bands in glasses intersected at 110° instead of the

90° predicted by plastic theory. This difference can be explained by the modification of the silicate structure from ideal plastic behavior as a result of the densification which takes place.[23] He identified the following three effects of shear band interaction, shown in Figure 2.5: (a) No distortion at the intersection point, (b) a kink, or shear displacement, in one of the bands, or (c) a short kink in both interacting shear bands. [23]

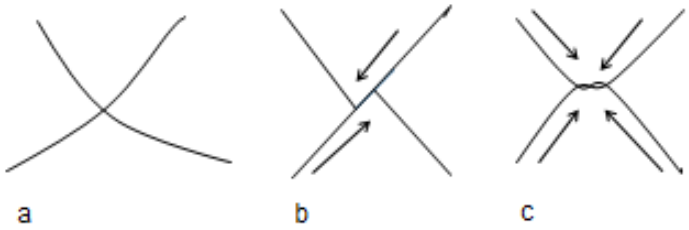

Figure 2.5: Schematic representation of intersection of shear bands and shear displacement formation (kink).

According to Hagan, the kinks represent the magnitude of different shear displacements.[23] He showed that one shear band may produce kinks of different magnitudes in several intersecting shear bands, which is a result of shear displacements varying along shear bands, or more likely because the strains in intersecting lines are different.[23] The formation of kinks also indicates that all shear bands do not form at the same time. Kinks are genuine shear displacements on shear bands, which can be likened to jog formation from intersecting dislocations. In this sense the kink on one shear band represents the magnitude of the burgers vector of the second shear band.[23] The intersection and kinking of these shear bands will result in the increasing difficulty to slip on the kinked shear band. Attempts to slip past a kink can result in void or crack formation. However, if a void or crack does not form, the

strain that is no longer possible on kinked shear band can be accommodated by activating slip on another shear band in the neighborhood of the kinked shear band.[23

Nucleation of cracks and fracture happens very differently in "anomalous" glasses (such as fused silica). Ernsberger[10], Peter[8], and Hagan & Swain[24] all showed that beneath an indentation in fused silica there is no evidence of shear flow ("rosette pattern"). All that is visible is a densified region, which was shown by a refractive index change in the material directly beneath indentation. The deformation process was determined to be dominated by stresses resulting from elastic strains with the exception of the initial compaction or densification of the material directly below the indentation.[24] Hagan believed that median cracks in fused silica result from the expansion of the compacted zone with increasing indenter load rather than from interacting shear bands which are not visible in fused silica. Lateral cracks on the other hand are formed by the mismatch of strain at the boundary of the compacted zone during unloading.[24] The dominant cracks (cone cracks) observed in fused silica Hagan said result from radial surface stresses which are tensile in nature. He states that the tensile stresses initiate shallow surface flaws at the contact area during loading and as the load increases new cracks will form at the new contact area. These new cracks are prevented from propagating into the bulk because of the compacted region which is under hydrostatic pressure. Therefore, these surface ring cracks initiating outside the contact area and developing outside the deformed zone in the glass are the ones which become fully grown cone cracks.[24]

2.2.2. Nanoindentation

Nanoindentation is a simple yet powerful method for evaluating elastic modulus, hardness and toughness of a variety of materials at very small scales.[25] One of nanoindentation's greatest advantages is that it can be used to measure mechanical properties and the load displacement data can be used to calculate hardness rather than having to image hardness impressions, which allows for measurements at the submicron level.[25] Today the most widely used analysis for nanoindentation data is that of Oliver and Pharr.[26-28] The Oliver and Pharr method is based on using a geometrically self-similar tip like the Berkovich triangular pyramid indenter. However, in recent years the methodology on nanoindentation has been refined so it can now be applied to other axisymmetric tip shapes such as the sphere.[27] A schematic representation of a typical load/unload vs. displacement curve using a Berkovich tip is shown in Figure 2.6. In Figure 2.6, P represents the load and h is the displacement relative to initial un-deformed surface.[27-28] For modeling and analysis purposes, deformation during loading is considered to be both elastic and plastic leaving behind the permanent hardness impression. Unloading is considered to be elastic. For this reason materials that recover plastically during unloading cannot be measured by this technique. The three most important parameters measured from the load vs. displacement curve are P_{max}, $h_{max,}$ and dP/dh. The parameter dP/dh is equal to contact stiffness S and is the slope of the elastic unloading curve. Hardness and indentation modulus can be determined from these three points so the accuracy with which these can be measured is very important.[27-28]

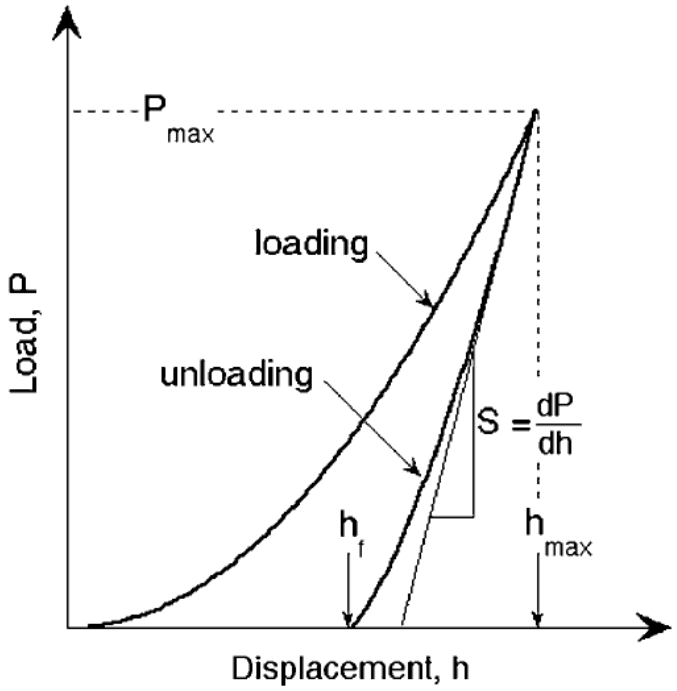

Figure 2.6: Schematic of nanoindentation load displacement data showing important measured parameters.[27]

Hardness and indentation modulus are measured by the unloading process as shown in Figure 2.7. The basic assumption in this analysis is that the contact area of the indent can be described by models for indentation of a flat elastic half space by rigid punches of simple geometry.[27-28] The downside of this method is it does not account for pile-up at the periphery of the indent which can occur in some softer elastic/plastic materials. If the following relation, $h_f/h_{max} < 0.7$, where h_f is the contact depth after indenter removal shown below in Figure 2.7 and h_{max} is the contact depth at maximum load, then there is very little pile-up in the sample and the Oliver and Pharr method can be used to obtain accurate results for *A*, contact area. However

if h_f/h_{max} > 0.7 then pile-up is found in the sample and the Oliver and Pharr analysis can lead to an underestimation of A by as much as 50%.[26]

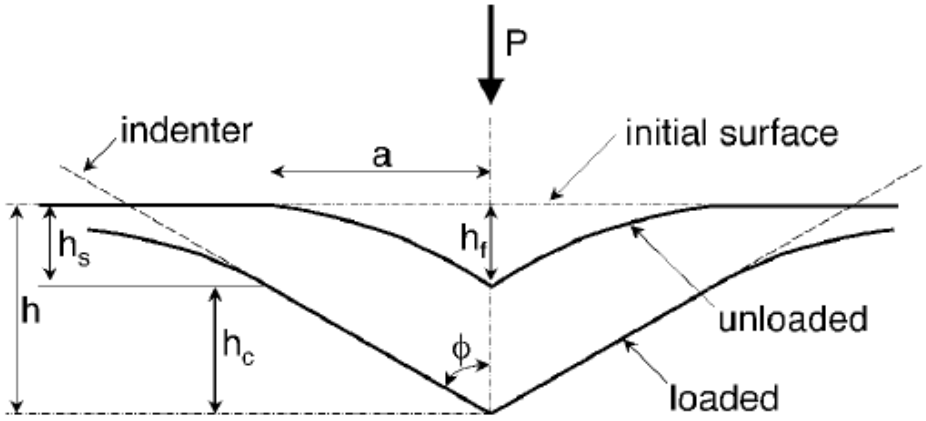

Figure 2.7: Schematic of unloading process showing parameters used in characterizing contact geometry. [27]

If one neglects pile-up of material the amount of sink-in can be approximated by the following equation:

$$h_s = \epsilon \frac{P_{max}}{S}. \quad (5)$$

ϵ is a constant that depends on the geometry of the indenter. For a Berkovich tip ϵ = 0.75. Based on the above schematic, h_c, the depth along which contact is made between the indenter and the sample will be:

$$h_c = h_{max} - \epsilon \frac{P_{max}}{S}. \quad (6)$$

The contact area A will then be

$$A = F(h_c), \quad (7)$$

where $F(d)$ is the area function which is carefully calculated for the specific indenter tip being utilized for the measurement. Once all of the above values are determined, the hardness of the sample can be found by:

$$H = \frac{P_{max}}{A}. \quad (8)$$

Measurement of the contact modulus, E_{eff} is then determined by its relationship to contact area, A, and measured unloading stiffness, S.

$$S = \frac{2}{\sqrt{\pi}} E_{eff} \sqrt{A}\,, \quad (9)$$

where E_{eff} is defined by,

$$E_{eff} = \frac{1}{E_{eff}} = \frac{1-\upsilon^2}{E} + \frac{1-\upsilon_i^2}{E_i}. \quad (10)$$

E_{eff} takes into account that elastic displacements occur in both the sample with E (Young's modulus) and υ (Poisson's ratio) and the indenter with E_i and υ_i.[27-28]

2.2.3. Summary of nanoindentation data

During nanoindentation, normal and anomalous glasses will exhibit different behaviors in deformation. Anomalous glasses will densify under a load and normal glasses will exhibit shear flow under load.[14] The difference in deformation is believed to be related to the free volume in the glass structure. As the amount of free volume decreases in the glass the deformation mechanism will change from densification to shear flow and result in pile-up during indentation. The anomalous behavior of densification has also been hypothesized to be a result of elastic compression accompanied by shear stress during indentation, resulting in

entanglement of portions of the glass network. This entanglement will result in an incomplete volume recovery during unloading of the indenter tip.[29] It has been found in fused silica that local densification under the indenter tip can reach as high as 20%.[30] In anomalous glasses such as vitreous silica, densification hardening and shear hardening are also observed.

The shear flow behavior of normal glasses on the other hand, is a result of plastic flow preferentially occurring along shear bands which are located in areas that are modifier rich, with ionically bonded interfaces between anions. These shear bands can also be created in areas that are composed of modifiers associated with non-bridging oxygen.[29] One way of determining the amount of free volume in a glass structure is to look at the Poisson's ratio. The more free volume in the glass structure, the lower the Poisson ratio.[21] Pile-up during indentation has been shown to cause an overestimation of hardness by up to 60% and indentation modulus by up to 16%.[13] In order to avoid this overestimation pile-up will have to be looked at very carefully and taken into consideration when calculating hardness and indentation modulus.

Some evidence exists that the deformation mechanism a glass exhibits can be altered not only by the glass structure but also by the sharpness of the indenter tip. A blunter indenter tip will cause the amount of densification exhibited by the glass to increase at the expense of plastic flow.[29]

2.3. STRUCTURE

2.3.1. Measurement Techniques

In order to look at the structure of glasses, several different measurement techniques have been utilized. Some of the more frequently used measurement techniques are as follows, high energy XRD, Neutron scattering, Raman spectroscopy, Infrared spectroscopy, and solid state Nuclear Magnetic Resonance (NMR). High Energy XRD is able to obtain information on short, nearest neighbor bonding arrangements such as the polyhedral unit (i.e. Si tetrahedron), Neutron diffraction is a complimentary technique to X-ray diffraction in that it also provides short to medium range information but neutron diffraction can detect lighter atoms and atoms with similar X-ray scattering cross sections that x-ray diffraction cannot distinguish. Raman and Infrared spectroscopy are complimentary spectroscopic techniques which take advantage of the way in which molecules vibrate when impacted by a light source. The different vibration modes absorb light differently and therefore result in changes in the collected spectrum. From Raman and IR absorption techniques we can gain information on the types of bonds and symmetry of bonds in a specimen. Lastly there is solid state nuclear magnetic resonance (NMR). This technique exploits the magnetic properties of certain atomic nuclei. NMR can provide information on structure, dynamics, reaction state, and chemical environment of molecules.

2.3.1.1. XRD and Neutron Diffraction

In glasses there is no long range structure like there is in crystalline materials, therefore X-ray diffraction (XRD) will result in a broad single peak versus the sharp peaks observed for crystalline materials that have well defined atom positions and lattice structures. This makes XRD more challenging to use for determining structure in glasses. However, with the use of high energy synchrotron X-rays we now have the ability to reach higher wave-vectors and reduce unwanted experimental effects such as absorption and multiple scattering, allowing us to obtain useful information on glass structure.[31] We can obtain information such as the average interatomic distance (i.e. Si-O, Al-O), also known as the pair distribution function (PDF) or radial-pair distribution function, which is independent of orientation, (r-PDF), and the number of atoms around a given atom (coordination number). The PDF or r-PDF are calculated directly from the scattering measurements by use of a Fourier transform.

High energy X-rays from synchrotron sources have also enabled the development of X-ray absorption near-edge structure (XANES). In XANES the low energy side of an absorption spectrum is sensitive to the geometrical arrangement of the environment surrounding the atom of interest, due to multiple scattering events. Analysis of the absorption data obtained from XANES can provide not only the pair distribution function but also an n-particle distribution function, because of the multiple scattering events.[32] This has become especially useful for glasses as absorption patterns obtained from XANES measurements can provide information on

not only short, referring to nearest neighbor bonding such as bonding arrangement of Si with O, but also medium range order, which is related to ring structure.

Neutron diffraction is a complimentary technique to XRD. They differ in that instead of X-ray photons scattering from or interacting with the electron cloud of the material the neutrons are scattered by the nuclei. There are two main advantages to neutron scattering. 1) neutrons scatter from nuclei thus the scattering efficiency is proportional to neutron-nucleus interaction. This would mean that light nuclei which have low X-ray scattering power can have strong neutron scattering power. This would allow us to look at atoms such as O in the glass structure. 2) When a material contains two atoms with similar atomic numbers the two atoms will have similar X-ray scattering power and will be difficult to distinguish from one another; however, in neutron scattering those same two atoms are likely to have very different neutron scattering power so they can be easily distinguished from one another. The following examples demonstrate how the use of high energy XRD and neutron diffraction have provided useful information on glass structure and more specifically on aluminosilicate glass structure.

V. Petkov was able to use high resolution, real space atomic pair distribution functions (PDF), obtained from high energy XRD, to resolve the Si-O and Al-O bonds at *r* (atomic spacing) = 1.61Å and *r* =1.75 Å respectively.[31] This ability to distinguish between Al-O and Si-O has allowed for the separate study of the Si-O and Al-O coordination. Being able to distinguish between Si-O and Al-O has been a problem in the past because Si and Al have similar scattering cross sections in both x-rays and neutrons.[31] The atomic PDF represented by:

$$G(r) = 4\pi\,[p(r) - p_0] \tag{11}$$

provides the deviation of the local, $p(r)$, from the average, p_0, atomic number density and this is how atomic PDF describes atomic arrangement in materials. More specifically the atomic PDF is the sine Fourier transform of the experimentally observable total structure factor $S(Q)$ i.e.,[18]

$$G(r) = \left(2/\pi\right)\int_{Q=0}^{Qmax} Q[S(Q) - 1]\,Sin(Qr)dQ \tag{12}$$

Where (Q_r) is the magnitude of the wave vector. The structure factor related to the elastic part of total diffracted intensity, $I_{el}\,(Q)$ as follows:

$$S(Q) = \left.1 + [I^{el}(Q) - \sum c_i\,|f_i(Q)|^2]\right/|\sum c_i f_i\,(Q)|^2 \tag{13}$$

Where c_i is the atomic concentration and f_i is the atomic scattering factor for species type i. In order for the data to be useable one needs to measure $I^{el}\,(Q)$ to a high value of $Q/Q_{max} \geq 40$ Å^{-1}.[31] The samples are measured in symmetric transmission geometry at low temperature, 20 K to minimize vibration and improve the PDF's. Also a bent double Laue Si (111) crystal monochromator is used to monochromatize the white beam and deliver photons of 80.6 KeV.[18] Experimental data shows structure factors exhibiting prominent oscillations up to Q = 40 Å^{-1}. Oscillations of this magnitude can only come from the presence of well-defined coordination polyhedral in the aluminosilicate glass structure.[31]

Experimental PDF results on glasses of the family $(CaO + Al_2O_3)_{1-X} + (SiO_2)_X$

($0 \leq x \leq 1$), were able to show evidence of both Si and Al atoms being tetrahedrally coordinated with oxygen on average. This indicates that the glass network would be a continuous tetrahedral network in glasses containing Al_2O_3 and CaO of up to about 25 mole%.[31,33] This is evidenced by wide angle XRD scattering results for a glass with an Anorthite composition ($CaO\text{-}Al_2O_3\text{-}2SiO_2$). The glass structure was found to be composed of a 3 dimensional network of interconnected SiO_4 and AlO_4^- tetrahedron that are arranged in 4 membered rings with the Ca^{2+} ions balancing the negative charge of the AlO_4^- tetrahedron.[32-34]

As the concentration of CaO and Al_2O_3, in $(CaO + Al_2O_3)_{1-x} + (SiO_2)_X$ glasses continues to increase one would expect the network to begin to break down, and as the amount of CaO and Al_2O_3 becomes larger than the amount of SiO_2 in the network, the number of non-bridging oxygen (NBO) in the first coordination sphere of Si would presumably increase. However, evidence from high energy XRD studies suggests that the Al-O network remains free of NBO as Al will enter fully polymerized Q^4 sites, where Q represents a tetrahedron and the superscript (4 in this case) represents the amount of bridging oxygen bound to that tetrahedron, when added to the glass structure.[31,33,35] This result indicates that the breakdown of the glass network occurs by the creation of Si-O-Ca and not by Al-O-Ca bonds.[31,33,35] This means that at high modifier concentrations, Ca in this instance, some of the O in the Si tetrahedron become NBO and change from having two network former cation neighbors to only one. The development of NBO on the Si tetrahedron results in the reduction of Si-O bonds and reduces the amount of network formers around some of the O atoms

without creating any atomic vacancies.[31] Data suggests that Si remains in tetrahedral coordination even when the glass is modifier rich, indicating the lower Si-O coordination found in the data is a result of lower network connectivity and not a change of Si from tetrahedral coordination.[31]

In modifier rich, or high Ca containing alumino-silicate glasses the Al was found to reside in both Q^3 and Q^4 sites.[33] As the amount of Al in Q^3 sites increases with increasing Ca content in high Ca containing glasses the glass network begins to depolymerize.[33] One of the surprising findings is that the average coordination of O on Ca does not change. Ca maintains a well-defined and stable octahedral coordination with O, which will impact the way in which the tetrahedral backbone arranges in space.[31,33]

2.3.1.2. Magic Angle Spinning Nuclear Magnetic Resonance (MAS NMR)

NMR is a technique which exploits the magnetic properties of certain atomic nuclei, nuclei that have a non-zero spin. More specifically, NMR is a physical phenomenon in which nuclei in a magnetic field will absorb and re-emit energy in the form of electromagnetic radiation. This energy will be at a specific resonance frequency which is dependent on the magnetic properties of the isotope of the atom and on the strength of the applied magnetic field. The underlying principle of NMR involves two main steps. 1) a constant magnetic field is applied to the sample in order to polarize or align the magnetic nuclear spins. 2) A radio frequency pulse is then applied in order to perturb the alignment of the nuclear spins. The two fields are chosen to be perpendicular to each other in order to maximize the NMR signal strength. The

resulting response by the total magnetization of the nuclear spins is the exploited phenomenon. From this we can gain information on structure, chemical environment, dynamics and reaction state of molecules.

When looking at solids, however we do not get very good signal to noise ratio due to lack of signal averaging by thermal motion. In order to combat this issue samples are spun at a magic angle, φ_m of 54.74°, with respect to the direction of the magnetic field. Spinning the sample at the φ_m increases the resolution of the spectrum by cancelling out the dipolar interactions and partially cancelling out the quadrupolar interactions. The quadrupolar interactions, which are a result of a non-spherical charge distribution around a nucleus having a spin greater than ½ such as Al, are so large that they cannot be treated in just the first order; they require a second order treatment. The first order term is removed by magic angle spinning (MAS) , however the second order term cannot be removed this way as it has two zero points. A new technique called triple quantum magic angle spinning (3Q MAS) was developed which is able to switch quickly between two angles thereby removing the second order term and cancelling out the quadrupolar interaction.

MAS- NMR and 3QMAS-NMR spectroscopies has been used extensively to look at the structure of silicate glasses.[36-39] More specifically ^{29}Si, ^{27}Al NMR spectroscopy have been utilized to look at alumino-silicate glasses with alkali or alkaline-earth modifier cations. MAS NMR is sensitive to the local chemical structure in glasses which includes tetrahedral bond angles, bond distances and the number of bridging oxygen per atom.[36-39] From these two isotopes, ^{29}Si and ^{27}Al, we can learn a lot about the local environment of an alumino-silicate glass. These isotopes are

selected because they have a non-zero spin and can be used to probe the local environment. The absorption frequency of the probe nucleus will shift depending on the degree to which nearby electrons shield the probe nucleus from the external magnetic field. Different bonding sites or environments of the nuclei will shield the probe nucleus differently so the bonding environment of the probe nucleus can be deduced from the absorption frequency shift in the data.[38]

It is has been experimentally determined that most silicate glasses contain Si atoms in a tetrahedral formation with 4 oxygen atoms bound to each Si atom.[36] The tetrahedron are linked to each other by bridging or shared oxygen atoms. The more bridging oxygen (BO) atoms in the glass structure the more polymerized the structure will be. In order to describe this local degree of connectivity in a glass structure, the glass community refers to a Q^n species, where n is the number of bridging oxygen atoms per tetrahedron.[36] Any one glass may contain a variety of Q^n species. There are some drawbacks to this technique such as very broad peaks or heterogeneous broadening which is indicative of an amorphous structure. These broad peaks make it difficult to determine if there are more than one Q^n structure present. Glasses containing Al or alkaline-earths also have a broad single ^{29}Si NMR peak even when structural models of these glasses indicate more than one Q^n species must exist.[36] Another concern is glasses with similar structures cannot be adequately resolved since the number of structural species with different number of bridging oxygen atoms is equal to or greater than the number of resolvable peaks in the NMR spectrum. These

issues lead to a 5% error in peak location and up to 20% error in full width at half maximum.[36]

A long standing controversial question in glass science has been what is the coordination and environment around Al in Alumino-silicate glasses. Through the use of ^{27}Al 3QMAS NMR spectroscopy some insight has been gained in answering this question. In calcium-alumino-silicate glasses Al has been found to be mainly in tetrahedral sites, however, there is some evidence that 5 fold coordinated Al is present to some extent throughout the ternary except in the low Si percalcic region.[37] The role of Al is much more complex than that of Si in glasses as Al has a charge balancing requirement for AlO_4^- tetrahedron. This charge balancing requirement is usually satisfied by charge compensating alkali or alkaline-earth cations, however these non-framework or modifier cations will aid in the de-polymerization of the network by forming non-bridging oxygen (NBO). If there are more modifier cations than Al in the network then NBO in the glass network will result.[37,39] If there are few to no charge balancing cations present in the glass then Al will form 5 or 6 fold coordination complexes with oxygen to maintain charge neutrality in the glass. The concentration of Al^V in the glass will increase with decreasing alkaline-earth/Al_2O_3 ratio in glasses with constant Si content.[37] Al^{VI} has been detected in glasses which have alkaline-earth/Al_2O_3 ratios of 33.5, 48.03 and 50.40.[37] Experimental evidence suggest that up to 7% Al^V has been measured in some compositions such as Anorthite ($CaAl_2Si_3O_8$).[37] This may contradict the general theory that the Anorthite composition has a structure consisting of an alternating framework of Si and Al tetrahedral. This particular structure is believed to be a manifestation of the

Lowenstein's aluminum avoidance rule which states that Al-O-Al linkages between aluminate tetrahedral are not energetically favorable. This would suggest that in this particular composition every Si tetrahedron must be a Q^4 (4 Al) unit, which is a Si atom with 4 BO connect to Al atoms, with no NBO present.[38-39] However, some evidence suggests that the greater polarizing power of Ca over Na causes the breakdown of the Al avoidance principle and could result in having Si tetrahedron in Q^4 (3Al) units, which is a Si atom with 4 BO, 3 connecting to an Al atom and one to a Si atom.[38]

In glasses where a high amount of Al^V is found, it is believed that the Al will exist in a tricluster state which is a tri-coordinated oxygen linked with 3 Si, and 1 Al tetrahedral. This species is however, very difficult to detect so there is much controversy around if it really exists or not.[37] The first direct evidence of this tricluster structure was shown experimentally by using a ^{17}O, ^{27}Al heteronuclear multiple quantum correlation technique. In conclusion, NMR data indicates that Al is mainly in tetrahedral coordination, however higher order species of Al such as Al^V and Al^{VI} have been found to exist to some extent in most alumino-silicate glasses. It is believed that these higher order Al species may contribute to topological disorder of the glassy network which could have an impact on some physical properties of the glass.[37] The specific role of Al^V and Al^{VI} in the glass structure needs further investigation to truly understand the impact these species may have on the glass physical properties.

2.3.1.3. Infrared and Raman Spectra

Infrared (IR) and Raman spectroscopy are complimentary techniques for looking at glass structure. IR is an absorption technique that exploits the fact that molecules absorb specific frequencies that are characteristic of their structure. In order for a molecule to absorb in the IR, it must have a dipole moment, or have a vibration that creates a change in the dipole. Absorption occurs when the vibrational frequency of a bond is the same as the IR frequency. One can gain information about molecular structure of a sample by analyzing the position, shape and intensity of the peaks in the IR spectrum.

Raman spectroscopy, on the other hand, relies on inelastic scattering of monochromatic light. More specifically, laser light interacts with molecular vibrations, phonons, resulting in energy of laser photons being shifted up or down. This shift in the laser energy provides information about the vibrational modes in the sample. Vibrational information is specific to chemical bonds and symmetry of molecules. Raman spectroscopy provides a fingerprint for which a molecule can be identified. Raman spectroscopy is also able to see symmetrical bonds which IR cannot.

Lu-Gen Hwa[40] and Anand Agarwal[41] used IR reflectivity and polarized Raman scattering to analyze the structural role of Al in CaO-Al_2O_3-SiO_2 glasses. In low SiO_2 containing glasses Al was found to have some groups which contained four oxygen in a bridging configuration [AlO_4], and some which contained three bridging oxygen and one non-bridging oxygen [AlO_4]$^-$. All of the Si-O tetrahedral were found to have four non-bridging oxygen.[40] IR reflectance can also be used to look at the Si-

O-Si bond angle in the glass structure by analyzing the frequency shift of the band at roughly 1122cm^{-1}.[41]

2.3.2. Calcium Aluminosilicate Glass Structure

Calcium Aluminosilicate glasses are of great importance in industry as they are the foundation glass for liquid crystal display panels and cover panels for handheld devices among many other things. Aluminosilicate glasses are also important to geological processes as they are in almost all magmas. For these reasons it is of great interest to understand the structure of these types of glasses and how the structure impacts the mechanical properties, more specifically the hardness or plastic deformation mechanisms of these glasses. There has been an extensive amount of data on the structure of these glasses published in the last 20 or so years, however aspects of the glass structure still remain in question.

Silicate glass structure in general is considered to be a continuous network of corner-shared Si-O tetrahedron. A bridging oxygen atom (BO) is found at the vertex of each tetrahedron that is shared between two tetrahedral.[42] As another network former, such as Al^{3+}, is introduced to the silicate glass structure along with a modifier cation, such as Ca^{2+}, to balance charge, the glass structure will change. This change involves the partial replacement of Si-O tetrahedral with Al-O tetrahedral along with the emergence of non-bridging oxygen (NBO). The NBO links either a Si-O or an Al-O polyhedral unit to a Ca-based one. [43] However, in the instance that the modifier cation is added in a 1:1 ratio, based on charge, with the Al cation the glass structure should be fully connected with the absence of any NBO. The modifier cation in this

instance should act as a charge compensator allowing Al^{3+} to stay in tetrahedral configuration. In this instance the Ca ions would occupy interstitial sites in a random way and would not directly form part of the interconnected network.[42] Figure 2.8 below is an example of what the ideal structure should look like for a tectosilicate, two Al for one Ca, calcium Aluminosilicate glass.

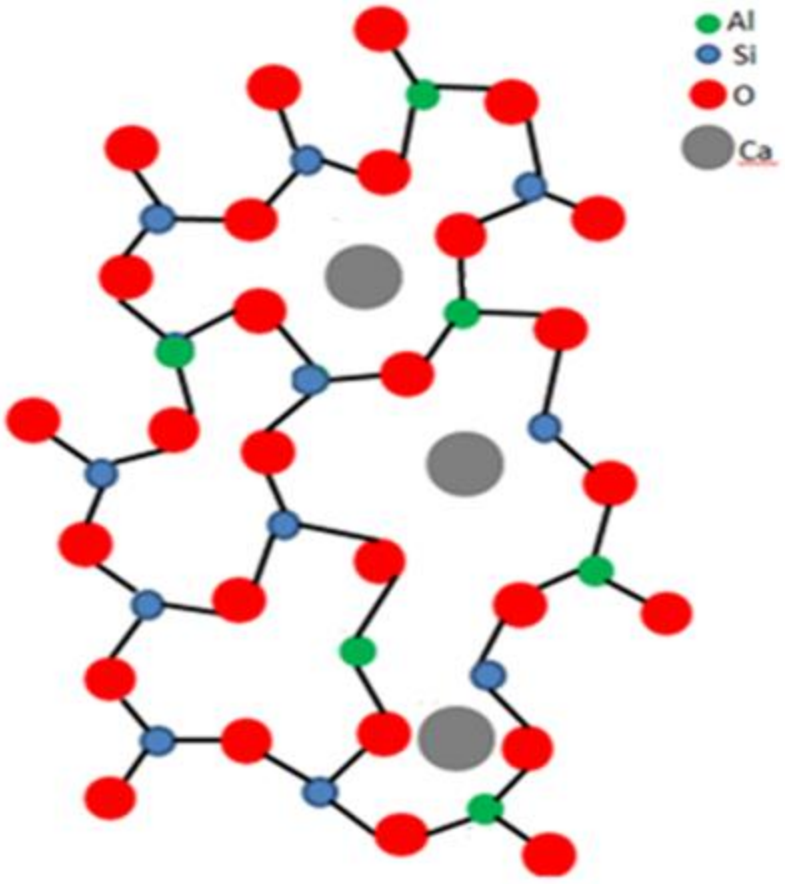

Figure 2.8: Ideal structure of a tectosilicate calcium Aluminosilicate glass, where Ca^{2+} occupies interstitial spaces in glass structure charge balancing two Al^{3+} ions.

Also, according to the Lowenstein's Al avoidance principle[44], Al will not enter the silicate structure randomly, instead it will occupy sites where it can share a BO with a Si. If it is found that two Al are connected by the same BO in the glass structure then

one of the Al must be of a higher coordination number such as five or six, towards O, otherwise if it was two Al tetrahedron connected to each other by a BO the structure would be less stable.[44] The lower stability resulting from the linkage of two Al tetrahedron by a BO is a result of unfavorable radius ratios. [44] More recent data from the last 20 or so years has provided a clearer picture of calcium aluminosilicate glasses showing how these glasses deviate from the above idealized structure.

The structure of calcium aluminosilicate glasses have been extensively studied using techniques such as magic angle spinning nuclear magnetic resonance (MAS NMR), Infra-Red Spectroscopy (IR), high energy x-ray diffraction (XRD), and neutron diffraction, as documented in the literature by researchers such as Stebbins[45], Neuville[37], Moesgaard[52], Himmel[34] and Cormier[33] to name a few. From the published structural information, a picture can be constructed of how the glass structure in calcium aluminosilicate glasses evolves as Ca and Al are added to the Si network. Starting from pure SiO_2 the glass structure is made up of SiO_4 tetrahedron that are fully connected by corner sharing, with each oxygen atom bonded to two Si atoms.[31,48] The Si-O bonds in glasses are more covalent in nature.[49] The addition of Al_2O_3 and CaO to the glass results in some of the SiO_4 tetrahedral in the glass backbone being replaced by $(AlO_4)^-$ with Ca^{2+} balancing the charge for two Al tetrahedral. [37,50-51] Al will only form tetrahedron in the presence of a cation which can act to balance the negative charge associated with the AlO_4 tetrahedron. As the amount of CaO and Al_2O_3 in the glass increases, the development of different Al species such as $Al^{(V)}$ and in some cases $Al^{(VI)}$ begins to form in the glass structure.[37,45-47,49,52-55] When $Al^{(V)}$ and $Al^{(VI)}$ forms in the glass structure, NBO

and/or oxygen triclusters (O atom bonded to three tetrahedron complexes, usually consisting of three Al or two Al and one Si tetrahedron) are also created as the Ca must be associated with either an AlO_4^- group or with a NBO to maintain the neutral charge.[45-46,54-55] If Ca does not act as a charge balancer for AlO_4^- then it will create NBO preferentially on the Si tetrahedral creating Si-O-Ca linkages.[31,50,54-56] $Al^{(V)}$ associates with three NBO, which each have a -1 charge and two bridging oxygen (BO) in the structure to compensate for the +3 charge on the Al.[48] At 50 mole% SiO_2 it is reported that the structure will be constructed of 4 membered rings with alternating SiO_4 and AlO_4^- tetrahedron. The alternation of Si and Al tetrahedron is a result of Lowenstein's aluminum avoidance rule [44] which states that Al-O-Al linkages are less energetically favorable compared to Al-O-Si linkages.[57] This alternating Si and Al tetrahedral structure is considered to be fully connected with octahedrally coordinated Ca located in interstitial spaces between the Si and Al network atoms.[34,38-39,58]At around 50 mole% SiO_2:25mole% Al_2O_3 the total amount of bridging oxygen associated with Al will be larger than the total number of bridging oxygen associated with Si leading to the breakdown of the Al avoidance principle.[47,56,58-59] Glasses with less than 40 mole% SiO_2 on the tectosilicate line in the calcium aluminosilicate glass family are found to have $Al^{(V)}$, NBO, Al-O-Al linkages, and Al triclusters, along with $Al^{(IV)}$ and $Si^{(IV)}$ species present .[31,37,46,52-53,55,59] The higher coordinated Al, such as $Al^{(V)}$, in tectosilicate glasses is either a result of the Al-O-Al linkages, which must occur when the Al concentration in the glass is greater than 50 mole%, having to contain an Al with a higher O coordination number in order to maintain stability[44] or a result of the inability of Ca, or the modifying ion, to be in

close enough proximity to the Al in order to charge balance the tetrahedral configuration. In the latter case the Al would have to take on higher coordination state in order to maintain overall charge neutrality in the glass.

In general calcium aluminosilicate glasses are of industrial importance as they are the backbone of glasses in modern applications such as LCD and handheld electronic devices. The high durability and strength of these glasses makes them the most attractive choice for these types of applications. With the increased need for stronger and stronger glasses it is becoming very important to understand not only the glass structure but also how that structure impacts the mechanical attributes.

In calcium Aluminosilicate glasses specifically, the glass structure has been extensively studied, however, since several different factors, such as melting conditions and cooling conditions, can impact the glass structure, it is of great importance to know how the structure of the particular glass affects the mechanical properties, specifically the hardness. Since we are very interested in understanding the microscopic mechanisms which cause the plastic behavior of calcium aluminosilicate glass, which is not known, we will need to be able to connect the specific structure of our glasses melted in our process to the measured hardness. This is the only way we will be able to begin elucidating the microscopic mechanisms for plastic deformation in glasses and more specifically in calcium aluminosilicate glasses.

In the following chapters, I report on work conducted to try and determine the microscopic mechanisms of plastic deformation in calcium aluminosilicate glasses by studying a series of tectosilicate calcium aluminosilicate glasses. We measured the load vs. displacement behavior of these glasses when indented with a Berkovich, three

sided pyramid, tip using the nanoindentation technique at low loads, thereby preventing fracture, and from this calculated the hardness and modulus of the glasses. Based on structural data obtained for each of the glasses from ^{27}Al 3Q MAS NMR, and information from literature on deformation mechanisms for similar glasses, we determined the deformation mechanisms for this specific series of glasses and how these mechanisms are controlled by the glass structure.

Having developed a theory on what microplastic mechanisms are at work in the calcium aluminosilicate glass series we tested our theory by substituting Mg for Ca to see how the higher field strength and smaller size of Mg impacts the glass structure and plastic deformation mechanisms. Lastly we substituted Ga for Al to determine if the larger size and lower bond strength of Ga-O causes the observed deformation mechanisms to alter in a predictable way based on knowledge of the proposed microplastic mechanisms determined from the original tectosilicate calcium aluminosilicate glass series.

REFERENCES

1. A. Arora, D.B. Marshall and B.R. Lawn, "Indentation, Deformation/Fracture of Normal and Anomalous Glasses." *J. Non-Cryst. Solids,* **31,** [3] 415-428 (1979).

2. M.R. Vukcevich, "A New Interpretation of the Anomalous Properties of Vitreous Silica." *J. Non-Cryst. Solids,* **11**, 25-63 (1972).

3. H.T. Smyth, H.S. Skogen, W.B. Harsell, "Thermal Capacity of Vitreous Silica." *J. of Am. Ceram. Soc.* **36,** [10] 327-328 (1953).]

4. T.G. Bifano, T.A. Dow, R.O. Scattergood, "Ductile-Regime Grinding: A new Technology for Machining Brittle Materials." *J. of Engineering for Industry* **113**, 184-189 (1991).

5. E.W. Taylor, "Plastic Deformation of Optical Glasses." *Nature,* **4139**, 323 (1949).

6. F.M. Ernsberger, "Role of Densification in Deformation of Glasses under Point Loading*." J. Amer. Ceram. Soc.* **51,** [10] 545-547 (1968).

7. K. Suzuki, Y. Benino, T. Fujiwara, T. Komatsu, "Densification Energy During Nanoindentation of Silica Glass." *J. Am. Ceram. Soc.* **85,** [12] 3102-104 (2002).

8. K.W. Peter, "Densification and Flow Phenomena of Glass In Indentation Experiments." *J. Non-Cryst. Solids* **5**, 103-115 (1970).

9. J.J. Gilman, "Mechanical Behavior of Metallic Glasses." *J. of App. Phys.* **46,** [4] 1625-1633 (1975).

10. F.M. Ernsberger, "Mechanical Properties of Glass." *Ibid* **25,** 293-321 (1977).

11. M.Bertoldi, V.M. Sglavo, "Soda-Borosilicate Glass: Normal or Anomalous Behavior Under Vickers Indentation?" *J. Non-Cryst. Solids* **344**, 51-59 (2004).

12. T. Rouxel, H. Ji, J.P. Guin, F. Augereau, B. Ruffle. "Indentation deformation mechanisms in Glass: Densification vs. Shear Flow." *J. App. Phys.* **107,** 094903 (2010).

13. A. Faivre, F. Despetis, F. Guillaume, P.Solignac."Role of Mobile Cations on Microplasticity in Alumino-Phosphate Glasses." *J. Am. Ceram. Soc.*, **93,** [10] 2986-2989 (2010).

14. J.A. Howell, J.R. Hellmann, C.L. Muhlstein,"Correlations Between Free Volume and Pile-up Behavior in Nanoindentation reference glasses." *Mater. Lett.* **62,** [14] 2140-2142 (2008).

15. B.R. Lawn and R.F. Cook, "Probing Material Properties with Sharp Indenters: A Retrospective." *J. Mater. Sci.* **47**, 1-22 (2012).

16. B.R. Lawn, "Fracture and Deformation in Brittle Solids: A Perspective on the Issue of Scale." *J. Mater. Res.* **19,** [1] 22-29 (2004).

17. R. Limbach, A. Winterstein-Beckmann, J. Dellith, D. Moncke and L. Wondraczek. " Plasticity, crack initiation and defect resistance in alkali-borosilicate glasses: From Normal to Anomalous Behavior." *J. Non-Cryst. Sol.*, **417-418** (2015) 15-27**.**

18. Y. Kato, H. Yamazaki, S. Yoshida, J. Matsuoka, "Effect of Densification on Crack Initiation Under Vickers Indentation Test." *J. of Non-Cryst. Sol.* **356**, 1768-1773 (2010).
19. Y. Kato, H. Yamazaki, S. Itakura, S. Yoshida, J. Matsuoka, "Load Dependence of Densification in Glass During Vickers Indentation Test." *J. Ceram. Soc. Of Japan* **119,** [2] 110-115 (2011).

20. S. Yoshida, J.C. Sangleboeuf, T. Rouxel, "Quantitative Evaluation of Indentation-Induced Densification in Glass." *J. Mater. Res.* **20,** [12] 3404-3412 (2005).

21. P. Sellappan, T. Rouxel, F. Celarie, E. Becker, P. Houizot, R. Conradt, "Composition Dependence of Indentation Deformation and Indentation Cracking in Glass." *Acta Materialia* **61, 5949-5965 (2013).**

22. J.T. Hagan and M.V. Swain, "The Origin of Median and Lateral Cracks Around Plastic Indents in Brittle Materials." *j. Phys. D.: Appl. Phys.* **11,** 2091-2102 (1978).

23. J.T. Hagan, "Shear Deformation Under Pyramidal Indentations in Soda-Lime Glass." *J. Mater. Sci.,* **15,** 1417-1424 (1980).

24. J.T. Hagan, "Cone Cracks Around Vickers Indentations in Fused Silica Glass." *J. Mater. Sci.,* **14**, 462-466 (1979).

25. B. R. Lawn, R. F. Cook, "Probing Material Properties with Sharp Indenters: A Retrospective." *J. Mater. Sci.,* **47**, 1-22 (2012).

26. G.M. Pharr, "Measurement of Mechanical Properties by Ultra-Low-Load Indentation." *Mater. Sci. Eng.,A*, **253**, 151-159 (1998).

27. W.C. Oliver and G.M. Pharr, “Measurement of Hardness and Elastic Modulus by Instrumented Indentation: Advances in Understanding and Refinements to Methodology.” *J. Mater. Res.*, **19,** [1] 3-20 (2004).

28. W.C. Oliver and G.M. Pharr, “An Improved Technique for Determining Hardness and Elastic Modulus Using Load and Displacement Sensing Indentation Experiments.” J. *Mater. Res.,* **7,** [6] 1564-1583 (1992).

29. T.M. Gross, ”Deformation and Cracking Behavior of Glasses Indented with Diamond Tips of Various Sharpness.” *J.Non-Cryst. Solids* **358,** [24] 3445-3452 (2012).

30. G. Kermouche, E. Barthel, D. Vandembroucq, and Ph. Dubujet, “Mechanical Modeling of Indentation-Induced Densification in Amorphous Silica.” *Acta Mater.,* **56,** [13] 3222-3228 (2008).

31. V. Petkov, S.J.L. Bilinge, S.D. Shastri and B. Himmel, “Polyhedral Units and Network Connectivity in Calcium Aluminosilicate Glasses From High Energy X-Ray Diffraction.” *Phys. Rev. Lett.,* **85,** [16] 3436-3439 (2000).

32. Z. Wu, C. Romano, A. Marcelli, A. Mottanu, G. Cibin, G. Della Ventura, G. Giuli, P. Courtial, D.B. Dingwell, “Evidence for Al/Si Tetrahedral Network in Aluminosilicate Glasses from Al K-edge X-ray-Absorption spectroscopy.” *Phys. Rev. B* **60,** [13] 9216-9219 (1999).

33. L. Cormier, D. R. Neuville, G. Calas.” Relationship Between Structure and Glass Transition Temperature in Low-Silica Calcium Aluminosilicate Glasses: The Origin of the Anomaly at Low Silica content.” *J. Am. Ceram. Soc.,* **88,** [8] 2292-2299 (2005).

34. B. Himmel, J. Weigelt, Th. Gerber, M. Nofz, “Structure of Calcium Aluminosilicate Glasses: Wide Angle X-Ray Scattering and Computer Simulation.” *J. Non-Cryst. Solids*, **136**, 27-36 (1991).

35. Z. Wu, C. Romano, A. Marcelli, A. Mottana, G. Cibin, G. Della Ventura, G. Giuli, P. Courtial and D.B. Dingwell, “Al/Si Tetrahedral Network in Aluminosilicate Glasses From Al K-Edge X-Ray Absorption Spectroscopy,” *Phys. Rev. B,* **60** [13] 9216- (1999).

36. E. Schneider, J.F. Stebbins, A. Pines, “ Speciation and Local Structure in Alkali and Alkaline Earth Silicate Glasses: Constraints from ^{29}Si NMR Spectroscopy.” *J. Non-Cryst. Solids*, **89,** 371-383 (1987).

37. D.R. Neuville, L. Cormier, V. Montouillout and D. Massiot, "Local Al Site Distribution in Aluminosilicate Glasses by 27Al MQMAS NMR." *J. Non-Cryst. Solids,* **353** [2] 180-184 (2007).

38. J. B. Murdoch, J. F. Stebbins, "High Resolution ^{29}Si NMR Study of Silicate and Aluminosilicate Glasses: The Effect of Network Modifying Cations." *American Minerologist,* **70**, 332-343 (1985).

39. A. Stamboulis, R.G. Hill, R. V. Law, "Characterization of the Structure of Calcium Aluminosilicate and Calcium Fluoro-Aluminosilicate Glasses by Magic Angle Spinning Nuclear Magnetic Resonance. (MAS-NMR)," *j. Non-Cryst. Solids,* **333**, 101-107 (2004).

40. L.Hwa, S.Hwang, L.Liu, "Infrared and Raman Spectra of Calcium Alumino-Silicate Glasses." *J. Non-Cryst. Solids,* **238,** 193-197 (1998).

41. A. Agarwal, M. Tomozawa, "Correlation of Silica Glass Properties with the Infrared Spectra," *J. Non-Cryst. Solids,* **209**, 166-174 (1997).

42. W. H. Zachariasen. "The Atomic Arrangement in Glass." *J. Am. Chem. Soc.* **54** [10] 3841-3851 (1932).

43. B. O. Mysen, "Structure and Properties of Silicate Melts." **Elsevier Amsterdam**, (1988)

44. W. Loewenstein, M. Lowenstein, Cia, "The Distribution of Aluminum in the tetrahedral of Silicates and Aluminates." *Am. Mineral.* **39**, 92-96 (1954).

45. L. M. Thompson and J. F. Stebbins."Non-Stoichiometric Non-Bridging Oxygens and Five Coordinated Al in Alkaline Earth Aluminosilicate Glasses: Effect of Modifier Cation Size." *J. Non-Cryst. Solids,* **358,** 1783-1789 (2012).

46. L. M. Thompson and J. F. Stebbins."Non-Bridging Oxygen and High-Coordinated Aluminum in Metaluminous and Peraluminous Calcium and Potassium Aluminosilicate Glasses: High Resolution ^{17}O and ^{27}Al MAS NMR Results." *American Minerologist*, **96**, 841-853 (2011).

47. D. R. Neuville, L. Cormier and D. Massiot."Al Coordination and Speciation in Calcium Aluminosilicate Glasses: Effects of Composition Determined by ^{27}Al MQ-MAS NMR and Raman Spectroscopy." *Chemical Geology,* **229**, 173-185 (2006).

48. A.K. Vurshneya, Fundamentals of Inorganic Glasses. **Academic Press Inc.**, San Diago, 1994.

49. C. I. Merzbacher, B. L. Sherriff, J. S. Hartman and W. B. White, "A High Resolution 29Si and 27Al NMR Study of Alkaline Earth Aluminosilicate Glasses." *J. Non-Cryst. Solids,* **124**, 194-206 (1990).

50. L. Cormier, D.R. Neuvile and G. Calas, "Structure and Properties of Low-Silica Calcium Aluminosilicate Glasses." *J. Non-Cryst. Solids,* **274**, 110-114(2000).

51. C. I. Merzbacher and W. B. White, "The Structure of Alkaline Earth Aluminosilicate Glasses as Determined by Vibrational Spectroscopy." *J. Non-Cryst. Solids*, **130**, 18-34 (1991).

52. M. Moesgaard, R.Keding, J. Skibsted and Y. Yue."Evidence of Intermediate-Range Order Heterogeneity in Calcium Aluminosilicate Glasses." *Chem. Mater.,* **22**, 4471-4483 (2010).

53. A. Tandia, N. T. Timofeev, J. C. Mauro, and K. D. Vargheese."Defect Mediated Self-Diffusion in Calcium Aluminosilicate Glasses: A molecular Modeling Study." *J. Non-Cryst. Solids*, **357**, 1780-1786 (2011).

54. J.F. Stebbins, J.V. Oglesby and S. Kroeker."Oxygen Triclusters in Crystalline CaAl4O7 (grossite) and in Calcium Aluminosilicate Glasses: ^{17}O NMR." *American Minerologist*, **86,** 1307-1311 (2011).

55. K. Zheng, F. Yang, X. Wang and Z. Zhang."Investigation of Self-Diffusion and Structure in Calcium Aluminosilicate Slags by Molecular Dynamics Simulations." *Mater. Sci. and App.,* **5** [?] 73-80 (2014).

56. M. Benoit and S.Ispas. "Structural Properties of Molten Silicates from Ab Initio Molecular-Dynamics Simulations: Comparison Between CaO-Al2O3-SiO2 and SiO2." *Phys. Rev. B.,***64**, 224205-1-224205-10 (year).

57. W. Loewenstein, "The Distribution of Aluminum in the Tetrahedra of Silicates and Aluminates." *American Minerologist*, **39,** 92-96 (1954).

58. S. K. Sharma, J.A. Philpotts and D.W. Matson. "Ring Distributions in Alkali and Alkaline-Earth Aluminosilicate Framework Glasses – A Raman Spectroscopic Study." *J. Non-Cryst. Solids*, **71**, 403-410 (1985).

59. S. K. Lee and J.F. Stebbins," The Structure of Aluminosilicate Glasses: High-Resolution 17O and 27Al MAS and 3Q MAS NMR Study." *J. Phys. Chem. B.,* **104**, 4091-4100 (2000).

CHAPTER 3

EXPERIMENTAL PROCEDURES

3.1. Specimen preparation

Glasses were made from 99.99% purity SiO_2, 99.98% purity Al_2O_3 , 99.9% purity $CaCO_3$, 99.992% MgO and 99.999% Ga_2O_3 powders. Glasses of 80 mole% SiO_2 or less were melted in Pt^{90}/Rh^{10} covered crucibles at 1600°C in a globar furnace for 12-16 hours and then the glass was poured on a metal table and rolled with a metal roller. The roller served to break the glass up into small pieces which were then re-melted at 1650°C for 6 hrs in Pt^{90}/Rh^{10} covered crucibles. This double melting process helps to ensure good glass homogeneity. After the second melt the glasses were poured into patties. The poured glass patties were annealed at 700°C for 2 hours and then cooled to room temperature at 2°C/min. These glasses showed no evidence of visible phase separation or gaseous inclusions. Glasses were checked in a polariscope for any evidence of residual stress. Glasses that contain greater than 80 mole% SiO_2 were melted in iridium crucibles in an induction furnace at 2000°C for 12 to 16 hours. The glasses were then core drilled out of the crucible and ground up and re-melted in the same set-up for an additional 6 hours. The glasses were annealed in-crucible at 800°C for 2 hours and then allowed to cool to room temperature at 5°C/min and then core drilled out. These glasses did not contain any visible phase separation, however they did have gaseous inclusions which were several mm apart and were therefore not a

concern for nanoindentation experiments. The glasses were checked in a polariscope for evidence of residual stress.

Rectangular samples $10\ mm\ \times\ 10\ mm\ \times\ 1\ mm$ were cut on a precision diamond saw from the annealed glass. The samples were mounted on plate with Unibond 5.0 Adhesive wax. The samples were then Lapped with 22 μm alumina powder on a steel plate. They were then polished on a silk pad with 1μm diamond mixed with Hyprez polishing oil, which is petroleum Naphtha CAS NO. 64742-48-9. After polishing, the samples were removed from the mount plate and cleaned with Opticlear, which is d-limonene with chemical formula $C_{10}H_{16}$ and CAS NO. 5989-27-5, to remove wax and then with isopropyl alcohol (IPA) to remove the Opticlear residue. The sample thicknesses were checked with a depth micrometer and the surface roughness was measured by an optical surface profilometer, to ensure it meets specifications of roughness and thickness variations less than 10 nm for testing.

After cutting and polishing, the samples are annealed at their annealing temperature, as determined by beam bending viscometry, for 2 hrs. and then cooled at 5°C/min. The annealing removes any internal stresses which were generated during the cutting and polishing process. The annealing temperatures for each of the glass composition is shown in Table 3.1. After annealing the samples were stored in a desiccator to prevent water absorption at the surface of the sample until testing is performed. No crystals were observed in these glasses after annealing.

3.2. Composition and structural characterization

3.2.1. Composition Characterization

The composition of glasses studied in this experiment were measured by Inductively Coupled Plasma-Optical Emission Spectrometry (ICP-OES) chemical analysis. The measured glass compositions and accuracy of each measurement are shown in Table 3.1.

Table 3.1: Measured Compositions of Glasses along with measured accuracy.

Glass	Measured composition in mole%					Annealing Temp. °C	Density g/cm^3
	SiO_2	Al_2O_3	MgO	CaO	Ga_2O_3		
1	39.75 ± 0.4	31.56 ± 0.4	0.00	28.69 ±0.2	0.00	850	2.79
2	45.14 ± 0.4	28.97 ± 0.4	0.00	25.89 ± 0.2	0.00	853	2.76
3	48.51 ± 0.4	25.89 ± 0.4	0.00	25.61 ± 0.2	0.00	853	2.72
4	60.61 ± 0.7	20.09 ± 0.3	0.00	19.30 ± 0.2	0.00	860	2.68
5	72.57 ± 0.7	13.49 ± 0.2	0.00	13.95 ± 0.1	0.00	866	2.67
6	81.51 ± 0.8	9.23 ± 0.1	0.00	9.26 ± 0.08	0.00	882	2.51
7	85.98 ± 0.8	6.63 ± 0.1	0.00	7.40 ± 0.07	0.00	883	2.35
8	89.93 ± 0.9	4.56 ± 0.07	0.00	5.51 ± 0.04	0.00	900	2.30
9	100.00	0.00	0.00	0.00	0.00	1140	2.21
10	45.69 ± 0.4	26.89 ± 0.4	27.42 ± 0.2	0.00	0.00	801	2.72
11	50.34 ± 0.4	24.76 ± 0.4	24.9 ± 0.2	0.00	0.00	804	2.68
12	60.11 ± 0.4	19.73 ± 0.4	20.16 ± 0.2	0.00	0.00	816	2.57
13	69.97 ± 0.7	14.81 ± 0.3	15.22 ± 0.1	0.00	0.00	Not Able to Obtain	2.48
14	80.56 ± 0.8	9.62 ± 0.2	9.82 ± 0.06	0.00	0.00	Not able to Obtain	2.36

15	85.53 ± 0.8	7.38 ± 0.1	7.09 ± 0.05	0.00	0.00	965	2.33
16	90.12 ± 0.9	4.87 ± 0.08	5.01 ± 0.03	0.00	0.00	996	2.28
17	35.25 ± 0.2	0.00	0.00	32.39 ± 0.2	32.35 ± 0.6	728	3.81
18	40.44 ± 0.3	0.00	0.00	29.8 ± 0.2	29.67 ± 0.6	735	3.72
19	45.5 ± 0.3	0.00	0.00	27.4 ± 0.2	27.11 ± 0.5	743	3.62
20	49.69 ± 0.3	0.00	0.00	25.23 ± 0.2	25.08 ± 0.5	748	3.51
21	60.21 ± 0.4	0.00	0.00	20.03 ± 0.1	19.75 ± 0.4	763	3.27

The density of the glass samples was measured by buoyancy in water with an estimated error of ±2%. The density data is shown above in Table 3.1.

3.2.2. Structural Characterization

^{27}Al magic angle spinning (MAS) NMR experiments were conducted at 16.4 T (182.34 MHz resonance frequency) using a commercial spectrometer (VNMRS, Agilent) and a commercial 1.6 mm MAS NMR probe (Agilent). Powdered glasses were packed into 1.6 mm zirconia rotors with sample spinning at 25 kHz. 0.6 μs radio-frequency (RF) pulses, corresponding to a $\pi/12$ tip angle, were used to uniformly excite the ^{27}Al central transitions and thus provide quantitatively accurate Al speciation. The ^{27}Al MAS NMR spectra were processed without additional line broadening and referenced to aqueous aluminum nitrate at 0.0 ppm. ^{27}Al MAS NMR spectra were analyzed using the DMfit program[(1)]. This program simulates second-order quadrupolar lineshapes, and in the case of ^{27}Al NMR spectra, an additional

parameter (Czjzek distribution) to account for distributions in the quadrupolar interaction[1]. Additional ^{27}Al triple quantum MAS (3QMAS) NMR experiments were conducted at 16.4 T using the hypercomplex shifted-echo pulse sequence. RF pulses were optimized to provide best signal-to-noise ratio, resulting in hard pulse widths of 2.1 and 0.8 μs, and a soft z-filter reading pulse of 15 μs. These data were processed with 100 Hz apodization in both time domains and referenced to aqueous aluminum nitrate at 0 ppm.

^{71}Ga (I=3/2; 39.6% natural abundance) magic angle spinning (MAS) NMR spectra were collected at 16.4 T (213.40 MHz resonance frequency) using a 1.6 mm MAS NMR probe with sample spinning of 35 kHz. Powdered glasses were packed into 1.6 mm outer diameter zirconia rotors. Data were acquired using very short radio-frequency pulses of 0.6 ms, corresponding to a $\pi/12$ tip angle. Between 22,000 and 230,000 scans were co-added for each sample to obtain sufficient signal to noise, and the recycle delay was 1s. Spectra were processed without apodization and plotted against the standard shift reference (aqueous gallium nitrate) at 0 ppm.

Processed MAS NMR spectra were deconvoluted using DMFit,[1] incorporating a Czjzek lineshape for the $Ga^{(IV)}$ peak and a small Gaussian peak to account for the presence of $Ga^{(V)}$. Due to the large quadrupole moment of ^{71}Ga, these MAS NMR lineshapes exhibit significant 2nd order quadrupolar coupling and substantial overlap between the resonances.

3.3. Mechanical Properties

3.3.1. Hardness, modulus and indentation size effect

A Hysitron TriboIndenter equipped with a Berkovich diamond tip was used. The indenter was calibrated using a fused silica sample provided by the manufacturer before each test. An example of a typical load/displacement curve for the fused silica calibration is shown below in Figure 3.1. The instrument compliance, indenter geometry and thermal drift were all calibrated using the Oliver and Pharr method.[2]

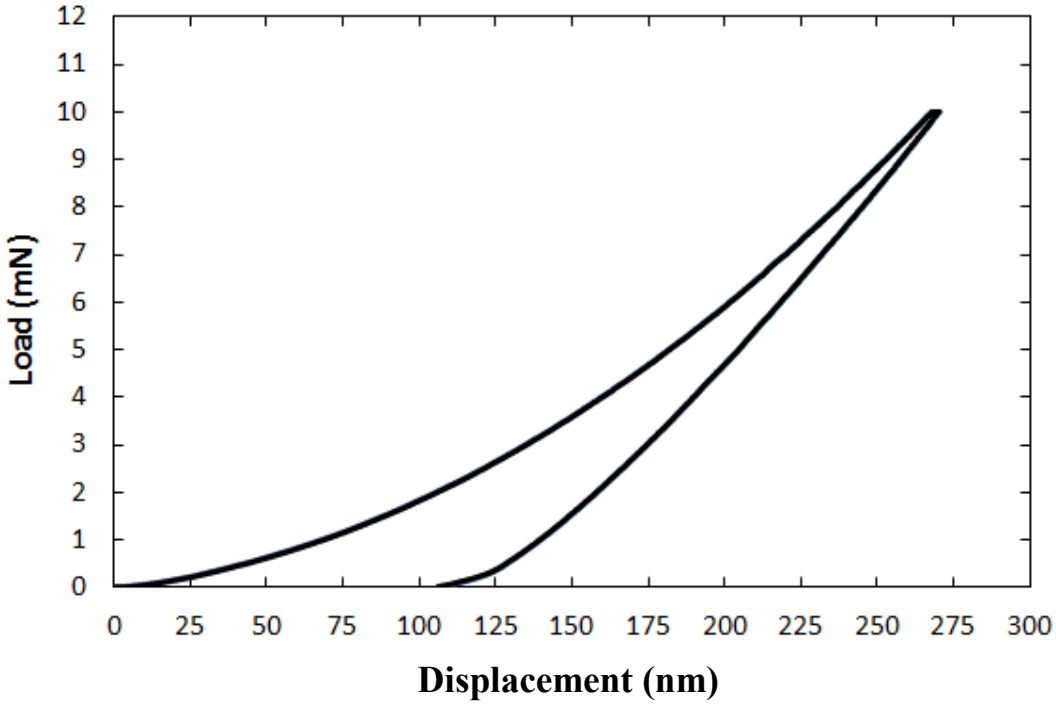

Figure 3.1: Typical Load/Displacement curve for a fused silica calibration sample.

The hardness and modulus of each of the glasses was measured using a maximum load during nanoindentation of 10 mN which produces a maximum depth of about 200 nm. The ramp rate used for these measurements was 1 mN/s and then the

load was held at 10 mN for 10 sec. followed by a ramp down at the same rate. Figure 3.2 below shows the load profile described above.

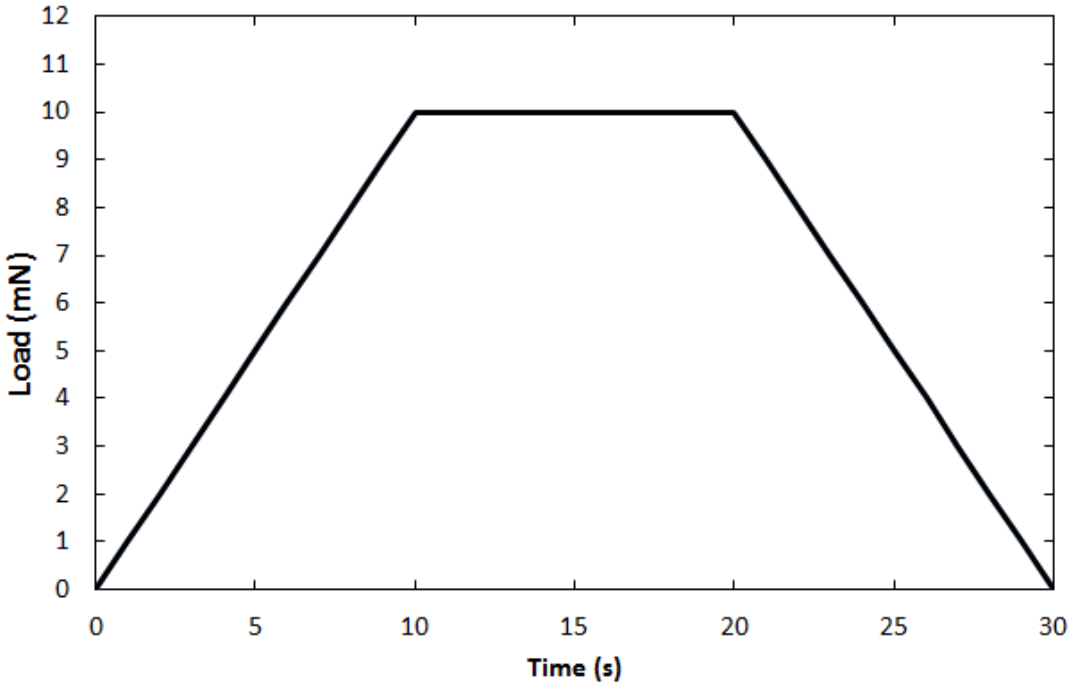

Figure 3.2: Load vs. time profile used for indentation of glasses to determine hardness and indentation modulus.

A 5 X 5 array of indents were performed on each sample with 10 μm between each indentation. The hardness and indentation modulus were calculated for each indentation using the Oliver and Pharr method which was previously described above in section 2.2.2.[2]

The indentation size effect (ISE) results in a decrease in hardness with an increase in indentation load. This has been associated with factors such as water on the surface,[3] and sub-surface cracking.[4] Tadjiev and Hand[3] showed that water absorption at the glass surface can be greater than 80 nm deep in glasses with poor durability and held in water environments for more than 2 hrs. These are extreme conditions and since our samples are only exposed to normal atmospheric

environment for the duration of the testing we do not expect to have large amounts of water adsorption at the glass surface. We can however determine this by measuring the hardness of our samples at several different depths. This was done by varying the peak load for each indentation in a 10 × 10 array with 10 μm between each of the indents from 10 mN to 0.1 mN in 0.1 mN increments. For each indentation, the ramp rate was 1 mN/s and the peak load was held constant for 10 s. The hardness data was analyzed using the O&P method as described previously.[2] The data below 50 nm is not shown as the tip shape calibration is not accurate at depths < 50 nm due to rounding of the tip. Figure 3.3 is an example of what the hardness as a function of depth looked like for all of our glass samples.

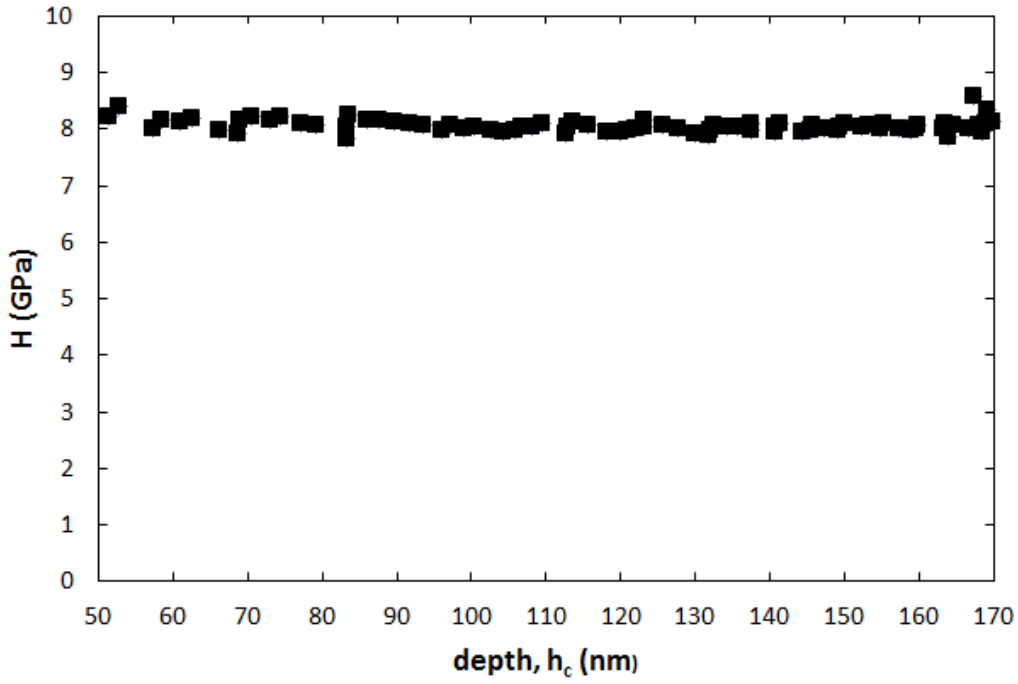

Figure 3.3: Hardness as a function of depth for a 10 Al_2O_3 -10 CaO- 80 SiO_2 glass. Glass composition in mole%.

3.3.2. Pile-Up

Glasses that contain modifiers or plastically deform by shear are known to result in pile-up. Pile-up is material that has moved during indentation from the bulk to the surface of the glass resulting in a buildup of material around the indentation impression. Pile-up in these glasses was measured by conducting scans of the indents after indentation using the indenter tip as the probe. Line scans are taken from the point of one side of indent across to center of other side. Figure 3.4 is a picture of Atomic Force Microscope AFM scan of a nanoindentation impression made with peak load of 10 mN. Lines are drawn across the indentation impression showing how the pile-up was measured.

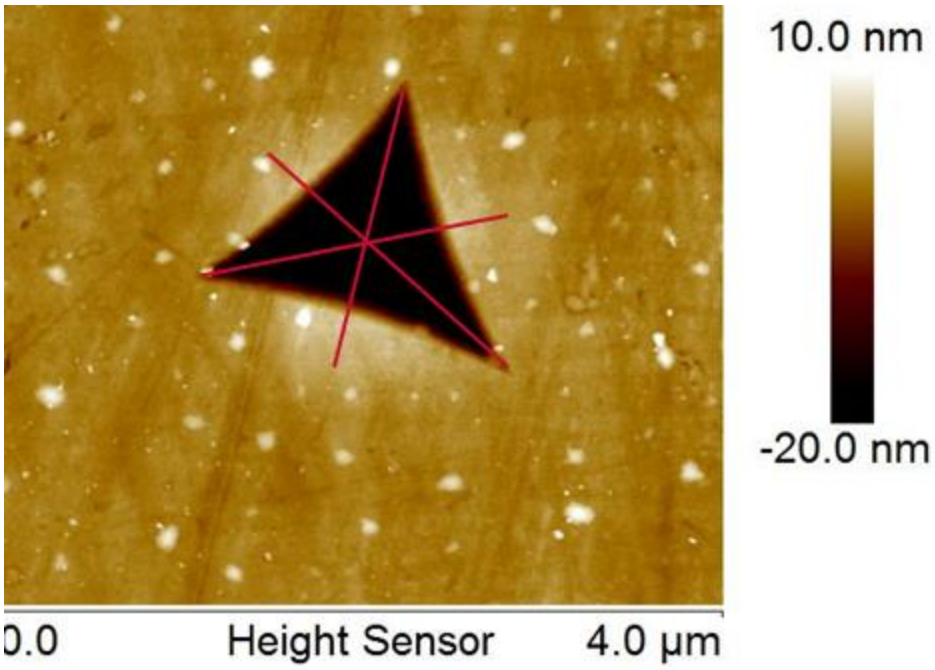

Figure 3.4: AFM image of nanoindentation conducted at peak load of 10 mN on a glass sample. The red lines show where the line scans were taken in order to calculate the pile-up.

From these line scans we can obtain information on the height and width of the pile-up if there is any. The line scans are taken across all 3 sides of the indentation impression and the pile-up height for all three sides is averaged to obtain the total amount of pile-up for each sample. Figure 3.5 is an example of a line scan taken of a nanoindent with a Berkovich tip at 10 mN peak load. The scan is taken from one corner through the center of the opposite side. The pile-up, circled in red, is shown as bumps above the surface of the indentation impression. A black line is drawn across the indentation impression for eye to more easily see the glass sample surface.

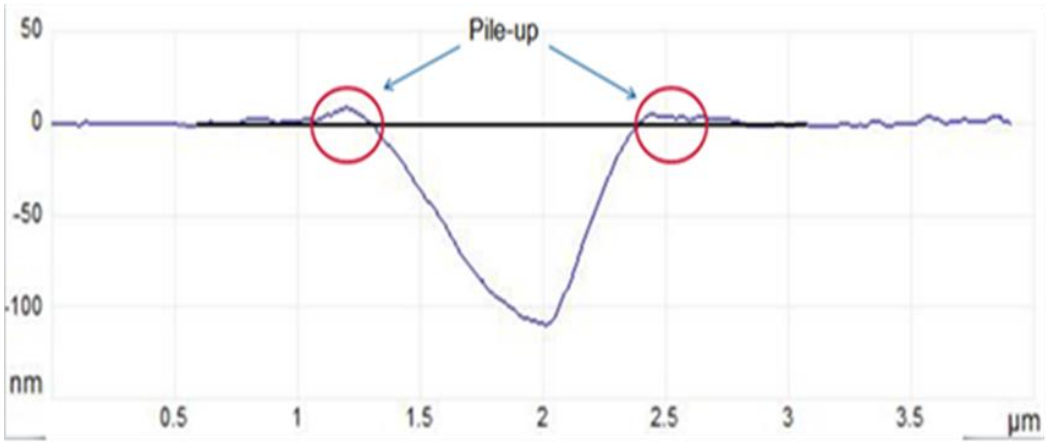

Figure 3.5: Line scan across indentation impression made in glass sample at 10 mN. The red circles show the pile-up along the edge of the indentation impression. The black line is drawn to show the glass sample surface.

REFERENCES

1. D. Massiot, F. Fayon, M. Capron, I. King, S. Le Calve, B. Alonso, J. O. Durand, B. Bujoli, Z. Gan, G. Hoatson, *Magn. Reson. Chem.* **40,** 70 (2002).

2. W.C. Oliver and G.M. Pharr, "Measurement of Hardness and Elastic Modulus by Instrumented Indentation: Advances in Understanding and Refinements to Methodology." *J. Mater. Res.*, **19** [1] 3-20 (2004).

3. D. K. Tadjiev, R. J. Hand. "Surface Hydration and Nanoindentation of Silicate Glasses." *J. of Non-Cryst. Solids,* **356,** 102-108 (2010).

4. M. Smedskjaer, "Indentation Size Effect and the Plastic Compressibility of Glass." *Appl. Phys. Let.* **104,** 251906 (2014)

CHAPTER 4

PLASTIC DEFORMATION MECHANISMS AND THE HARDNESS OF CALCIUM ALUMINOSILICATE GLASSES

4.1. Abstract

In the glass making industry, aluminosilicate glasses are considered a highly important family of glasses due to their use in such products as car windshields, touch screens for cell phones, and tablets among others. However, little is understood about the plastic deformation mechanisms and what effects modifier ions such as Ca have on these mechanisms. In this paper, the hardness and indentation modulus of a series of tectosilicate $(CaO + Al_2O_3)_{1-x} + (SiO_2)_x$ (CAS) glasses determined using nanoindentation are compared with the composition, including aluminum speciation determined using ICP and NMR. The indentation modulus of the tectosilicate CAS glasses was found to increase with glass density. The hardness however, exhibited a non-monotonic behavior as a function of mole% SiO_2. Modeling of this behavior by the topological constraint model was found to be ineffective.

4.2. Introduction

Aluminosilicate glasses have been long sought after because of their environmental friendliness, transparency and durability. For these reasons the aluminosilicate glass family is a prime choice for technologies such as substrate glass for photovoltaics, LCD, cover glass in hand held devices, and car windows. The main key to applying aluminosilicate glasses successfully in these applications is to increase strength and

damage resistance while reducing glass thickness to address weight and energy cost concerns

One way of characterizing the damage resistance of a glass is to measure its hardness. More specifically, hardness reflects the glasses ability to resist permanent deformation under an applied indentation load.[1-4] Permanent deformation in a glass is the result of either shear deformation or densification deformation, resulting in a residual impression.[5-6]

The two most common methods employed for studying plasticity in glasses are microindentation and nanoindentation. In both of these methods, a permanent impression can be left in the glass by the use of a sharp contact under an applied load. Since glass is considered a brittle material, the glass can respond to the applied contact by both plastic deformation and fracture.

Microindentation is currently the more utilized technique for measuring hardness in glasses. This technique, however, usually uses loads of > 980 mN, which commonly results in fracture. When trying to understand plasticity, fracture is not desirable as it will convolute the data and provide artificially low hardness values. One way to prevent fracture from occurring during indentation is to use loads that are well below the crack threshold of the glass system under investigation. However, the crack threshold is not well known or understood in most glass systems, so the safest way to prevent fracture during testing is to use loads of 10 mN or lower. This is achievable with the use of nanoindentation.

Nanoindentations are usually performed at loads on the order of 10's of mN, which is about a factor of 10 X lower than the most commonly used loads in microindentation. These low loads enable the ability of obtaining repeatable data without fracture. For this reason we have chosen to use nanoindentation as the method of choice for investigating plasticity in CaO-Al_2O_3-SiO_2 glasses.

There are two main forms of deformation found in glasses, shear and densification.[1,3,6-8] Shear deformation is thought to be related to the amount of modifier ions in the glass structure. The more modifier ions present the greater the shear deformation and the lower the hardness. Shear deformation is found to be a characteristic mode of deformation in "normal glasses", these are glasses which contain roughly 15 mole% or greater modifier ions in the structure.[8] Shear deformation is commonly identified by the presence of pile-up of material at the surface of the indentation impression.[1] However, it is not necessary to have pile-up in order to have shear deformation as can also be stored as elastic strains beneath the indentation.

The other form of deformation found in glasses is densification. This form of deformation is the result of the contraction of material under the indenter tip during loading which results in bond bending and compaction of the glass structure.[1, 7-8] Densification deformation will not result in any visible pile-up of material around the impression as there is no bond breaking or reforming resulting in the movement of material to the surface. Densification is the characteristic mode of deformation in glasses that have more open structures, lower packing densities and modifier ion concentrations lower than about 15 mole%.[7-8] Glasses that deform mainly by densification, such as fused silica, are considered to be "anomalous" glasses.[8]

There have been several different methods employed to try and predict hardness in glass, however all have been met with minimal success. Of the different methods which have been investigated the topological constraint model is a model which is based upon the glass structure. This model was originally developed by Phillips and Thorpe as a way to measure elastic modulus in glasses.[9-11] It has often been thought that hardness and modulus are linked and therefore, if a glass has a high elastic modulus it will also have a high hardness. Based on this belief the topological

constraint model has gained momentum as a tool for predicting hardness in glasses. The model has been applied to several different glass families, including borate glasses,[3] borosilicate glasses,[12] chalcogenide glasses,[13] and boroaluminosilicate glasses[2] and shown to provide qualitatively accurate calculations of macroscopic properties such as Vickers hardness, however the model has yet to be applied to alkaline-earth aluminosilicate glasses.

This model is based on the premise that each atom in a glass has three translational degrees of freedom in three dimensional space, which can be removed by the presence of rigid bond constraints.[12] There are two body bond constraints which are bond stretching constraints and three body bond bending constraints, which are angular constraints.[2,14] Glassy networks are classified as having internal degrees of freedom when the total number of bond bending and bond stretching constraints per atom (n) is less than the total degrees of freedom (d) per atom. (i.e. 3).[2,14] When n = 3 an isostatic state is achieved and when $n > 3$ the network has a high amount of connectivity and is considered to be "stressed rigid". When $n < 2$ the network is considered to be floppy and cannot hold a hardness impression, so for this reason it has been determined that in most glass systems $n = 2.5$ is the point at which the glass can begin to hold a plastic impression.[2,14]

We have chosen to investigate the tectosilicate CaO-Al_2O_3-SiO_2 glass system due to its technological importance and simplicity of the glass structure. Glasses located on the tectosilicate line have a 1:1 ratio of CaO: Al_2O_3, so according to ideal glass structure, all of the Ca should be acting as a charge balancer for Al, which is in tetrahedral coordination. This would mean that there should not be any higher coordinated Al or non-bridging oxygen (NBO) present in the glass structure. During our investigation of hardness in this glass system we discovered an anomalous behavior with increasing SiO_2 content. When we applied topological constraint theory

to this series of glasses we found that it was insufficient in describing the hardness. We propose that the observed anomalous behavior in hardness of the tectosilicate CaO-Al_2O_3-SiO_2 glass system is the result of a transformation from shear deformation to densification deformation. This transformation is what results in a minimum in hardness at roughly 85 mole% SiO_2. We further show the presence of $Al^{(V)}$ in the glass structure through the use of ^{27}Al 3Q MAS NMR. Our results indicate that the $Al^{(V)}$ may result in an increase in hardness of the glasses. This hardening effect outweighs the effect of increasing NBO in the glass structure.

4.3. Experiments and Results

4.3.1. Specimen preparation

Glasses were made with 99.99% purity SiO_2, 99.98% purity Al_2O_3 and 99.9% purity $CaCO_3$ powders. The glasses were melted in Pt. crucibles at 1650°C for 15 hrs. The melts were poured onto a metal table and then rolled with a metal rolling pin to rapidly cool the glass and crush it into small pieces. The glass remaining in the crucibles was knocked out and added to the crushed glass and re-melted. This method is adopted to aid in mixing of the glass ensuring good homogeneity in the final glass patty. The glasses were annealed at 700°C for 2 hrs to reduce internal stresses generated during pouring and cooling. The glasses were inspected after annealing in a polarized scope to ensure good homogeneity and absence of phase separation. The glasses containing SiO_2 of greater than 80 mole% contained small bubbles of about 0.1 mm in size. However, there were still areas of the glass samples of up to
6 mm x 6 mm that did not contain any bubbles. The bubbles are randomly distributed throughout the glass so large areas without bubbles are easily located.

Glass samples were cut on a precision diamond saw and then mounted on a plate with Unibond 5.0 Adhesive wax. The samples were then lapped with 22 µm alumina powder on a steel plate. The samples were then polished on a silk pad with 1µm diamond mixed with Hyprez polishing oil, which is petroleum naphtha CAS NO. 64742-48-9. After polishing the samples were removed from mount plate and cleaned with Opticlear, which is d-limonene with chemical formula $C_{10}H_{16}$ and CAS NO.

5989-27-5, to remove wax and then with IPA to remove Opticlear residue. The samples thickness was checked with a depth micrometer and the surface roughness was measured using an optical surface profilometer, ensuring the sample meets the specification of roughness and thickness variations less than 10 nm for testing. The final sample dimensions were 10 mm × 10 mm × 1 mm. After cutting and polishing the samples were annealed at their measured annealing temperature, as determined by beam bending viscometry, for 2 hrs. The annealing removes any internal stresses that were generated during the cutting and polishing process. The annealing temperatures for each of the glass compositions are shown in Table 4.1. After annealing, the samples were stored in a dessicator to prevent water absorption at the surface of the sample until testing was performed.

4.3.2. Composition and Density

The compositions of the final glasses were determined using ICP-OES (inductively coupled plasma-optical emission spectrometry). Table 4.1 shows the compositions in mole% for each of the oxides in each of the glasses along with the uncertainty for each element. Density was measured by buoyancy. The accuracy of this measurement is ± 2%. The results for the density measurements are also shown in Table 4.1.

Table 4.1: Measured glass compositions, annealing points and mole% $Al^{(IV)}$ and $Al^{(V)}$.

Glass Code	***Measured composition in Mole%***						
	SiO_2	**Al_2O_3**	**CaO**	Anneal Pt. (°C)	Density (g/cm^3)	$Al^{(IV)}$ (mole%)	$Al^{(V)}$ (mole%)
1	39.75 ± 0.4	31.56 ± 0.4	28.69 ± 0.2	850	2.79	30.27	1.29
2	45.14 ± 0.4	28.97 ± 0.4	25.89 ± 0.2	853	2.76	27.75	1.22
3	48.51 ± 0.4	25.89 ± 0.4	25.61 ± 0.2	853	2.71	25.01	0.88
4	60.61 ± 0.7	20.09 ± 0.3	19.30 ± 0.2	860.3	2.68	19.65	0.44
5	72.57 ± 0.7	13.49 ± 0.2	13.95 ± 0.1	865.7	2.67	13.31	0.18
6	81.51 ± 0.8	9.23 ± 0.1	9.26 ± 0.08	882.1	2.50	9.11	0.12
7	85.98 ± 0.8	6.63 ± 0.1	7.40 ± 0.07	883	2.34	6.52	0.11
8	89.93 ± 0.9	4.56 ± 0.07	5.51 ± 0.04	900	2.29	4.43	0.13
9	100.00	0.00	0.00	1140	2.20	0	0

4.3.3. Mechanical Properties

A Hysitron TriboIndenter equipped with a Berkovich diamond tip was used. The indenter was calibrated using a fused silica sample provided by the manufacturer before each test. The instrument compliance, indenter geometry and thermal drift were all calibrated using the Oliver and Pharr method.[15]

4.3.3.1. Hardness and Modulus

The hardness and modulus of each of the glasses was measured using a maximum load during nanoindentation of 10 mN which produces a maximum depth of about 200 nm. The ramp rate used for these measurements was 1 mN/s and then the load was held at

10 mN for 10 sec. followed by a ramp down at the same rate. A 5 X 5 array of indents were performed on each sample with 10 µm between each indentation. The hardness and indentation modulus were calculated for each indentation using the Oliver and Pharr method.[15]

Figure 4.1 shows hardness and indentation modulus as a function of mole% SiO_2. From Figure 4.1 one can see that the hardness exhibits a non-monotonic behavior with increasing SiO_2 content. At roughly 85 mole% SiO_2, the hardness reaches a minimum. In contrast, the indentation modulus decreases monotonically with increasing SiO_2 content across the entire composition range.

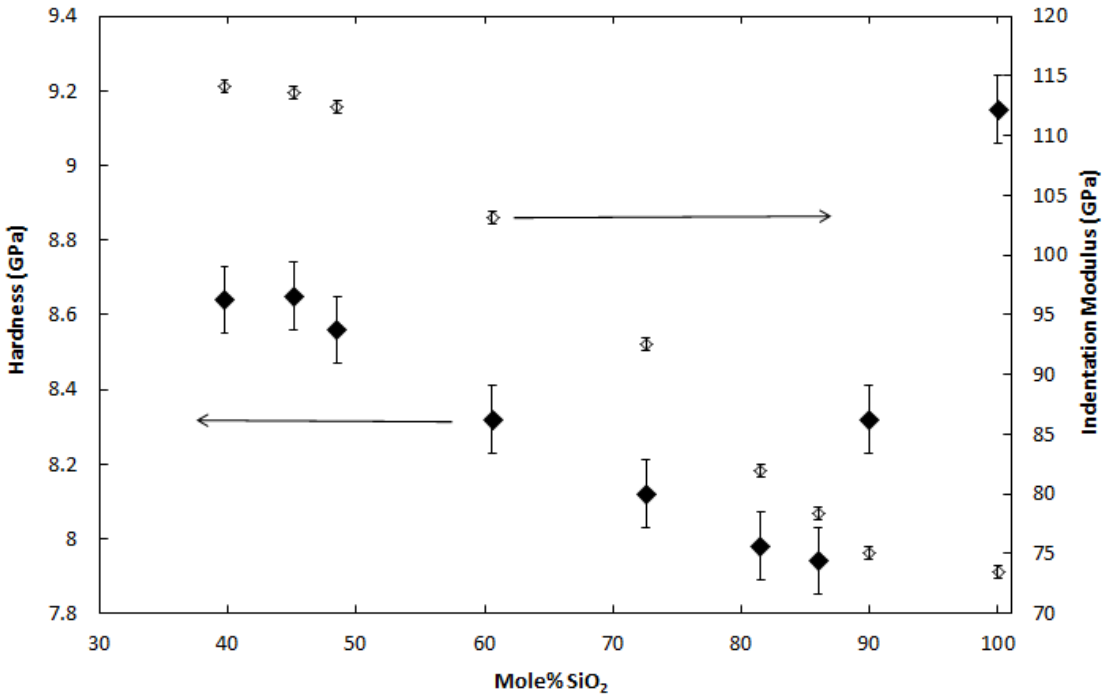

Figure 4.1: Hardness and indentation modulus as a function of mole% SiO_2 in calciumaluminosilicate glasses with Al_2O_3:CaO = 1.0

4.3.3.2. Pile-Up

Glasses that contain modifiers or plastically deform by shear are known to result in pile-up. Pile-up is material that has moved during indentation from the bulk to the surface of the glass resulting in a buildup of material around the indentation impression.

Pile-up in these glasses was measured by conducting scans of the indents after indentation using the indenter tip as the probe. Line scans are taken from the point of one side of indent across to center of other side. From these line scans we can obtain information on the height and width of the pile-up if there is any. The line scans are taken across all 3 sides of the indentation impression and the pile-up height for all three sides is averaged to obtain the total amount of pile-up for each sample. Figure 4.2 shows the height of the indentation pile-up as a function of mole% SiO_2. This plot clearly shows that glasses have a decreasing amount of pile up as the mole% SiO_2 is increased until about 80 mole% SiO_2 is reached and then no more pile-up is observed around the indentations.

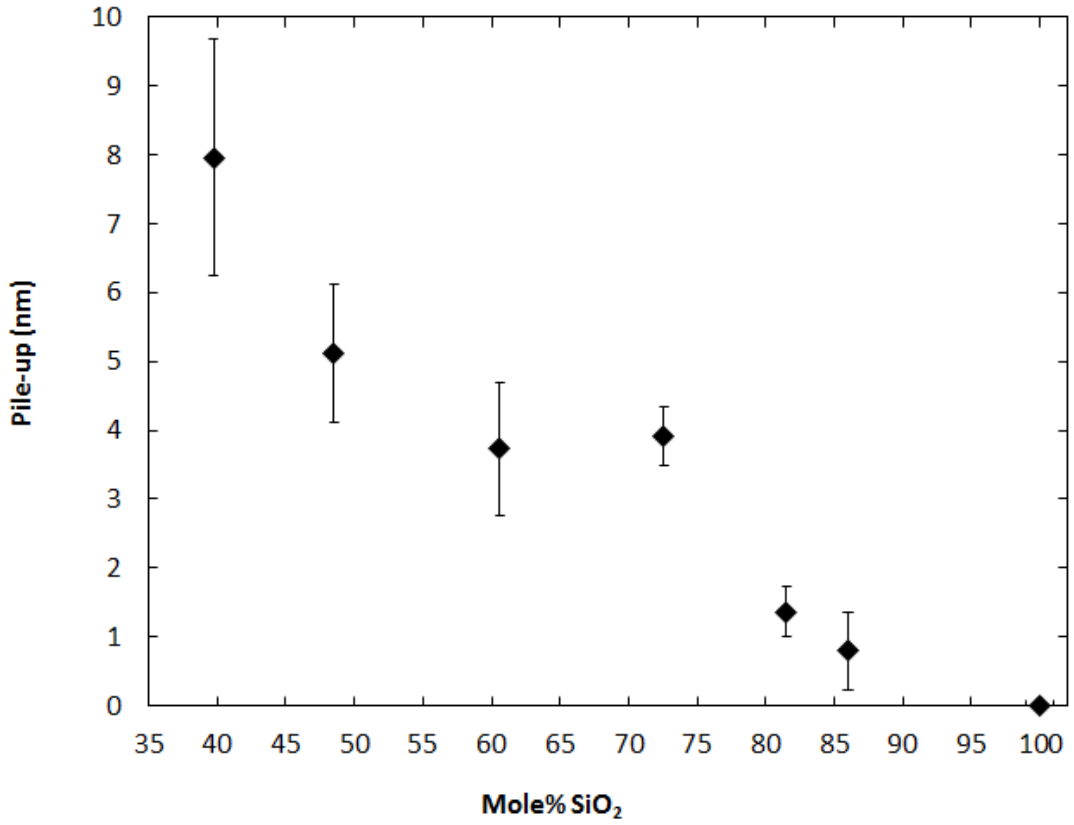

Figure 4.2: Indentation pile-up in nm as a function of mole% SiO_2 in tectosilicate CaO-Al_2O_3-SiO_2 glasses.

4.3.3.3.Indentation Size Effect

Another factor which could impact the hardness results is known as indentation size effect (ISE). ISE results in a decrease in hardness with an increase in indentation load. This has been associated with factors such as water on the surface,[16] and sub-surface cracking.[17] Tadjiev and Hand[16] showed that water absorption at the glass surface can be greater than 80 nm deep in glasses with poor durability and held in water environments for more than 2hrs. These are extreme conditions and since our samples are only exposed to normal atmospheric environment for the duration of the testing we do not expect to have large amounts of water adsorption at the glass surface. We can

however determine this by measuring the hardness of our samples at several different depths. This was done by varying the peak load for each indentation in a 10 × 10 array with 10 μm between each of the indents from 10 mN to 0.1 mN in 0.1 mN increments. For each indentation, the ramp rate was 1 mN/s and the peak load was held constant for 10 s. The hardness data was analyzed using the Oliver &Pharr method as described previously.

ISE was measured for all of the glass samples in the study and no variation in hardness was observed. Figure 4.3 shows results for the 45 mole% SiO_2 glass, which is representative of what the data looked like for all of the glasses in this study. Data at depths below 50 nm are not shown as the tip shape calibration is not accurate in this range. These results suggest that for our samples, neither water absorption near the surface, nor surface damage, nor onset of cracking affects results.

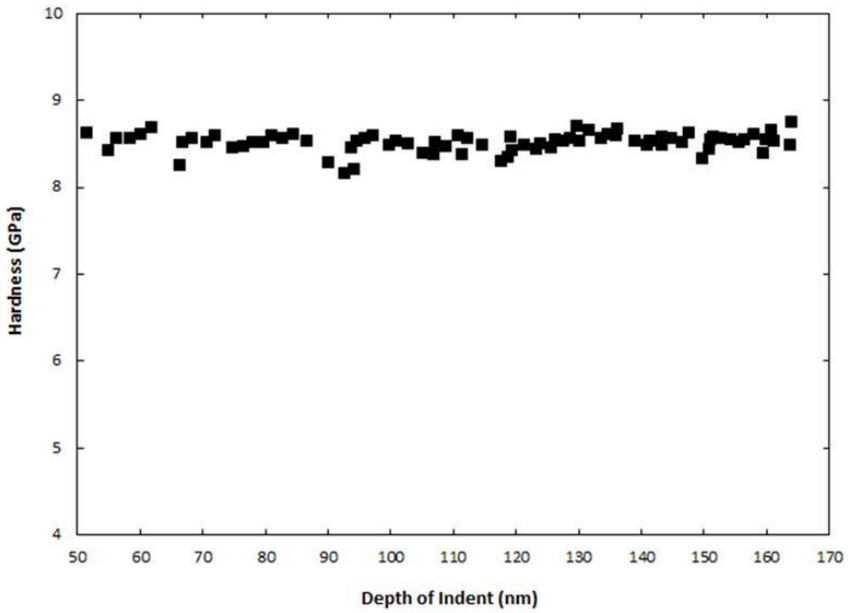

Figure 4.3: Hardness as a function of indent depth. This plot shows no evidence of indentation size effect as measured on the 45 mole% SiO_2 tectosilicate CaO-Al_2O_3-SiO_2 glass. All of the other glasses showed the same result of no variation in hardness with depth.

4.3.4. Al Speciation

^{27}Al magic angle spinning (MAS) NMR[se] experiments were conducted at 16.4 T (182.34 MHz resonance frequency) using a commercial spectrometer (VNMRS, Agilent) and a commercial 1.6 mm MAS NMR probe (Agilent). Powdered glasses were packed into 1.6 mm zirconia rotors with sample spinning at 25 kHz. 0.6 μs radio-frequency (RF) pulses, corresponding to a $\pi/12$ tip angle, were used to uniformly excite the ^{27}Al central transitions and thus provide quantitatively accurate Al speciation. The ^{27}Al MAS NMR spectra were processed without additional line broadening and referenced to aqueous aluminum nitrate at 0.0 ppm. ^{27}Al MAS NMR spectra were analyzed using the DMfit program[18]. This program provides a means by which to simulate second-order quadrupolar lineshapes, and in the case of ^{27}Al NMR spectra, an additional parameter (Czjzek distribution) to account for distributions in the quadrupolar interaction[18]. Additional ^{27}Al triple quantum MAS (3QMAS) NMR experiments were conducted at 16.4 T using the hypercomplex shifted-echo pulse sequence. RF pulses were optimized to provide best signal-to-noise ratio, resulting in hard pulse widths of 2.1 and 0.8 μs, and a soft z-filter reading pulse of 15 μs. These data were processed with 100 Hz apodization in both time domains and referenced to aqueous aluminum nitrate at 0 ppm.

^{27}Al MAS NMR and 3Q MAS NMR spectra are shown below in Figures 4.4 and 4.5 respectively.

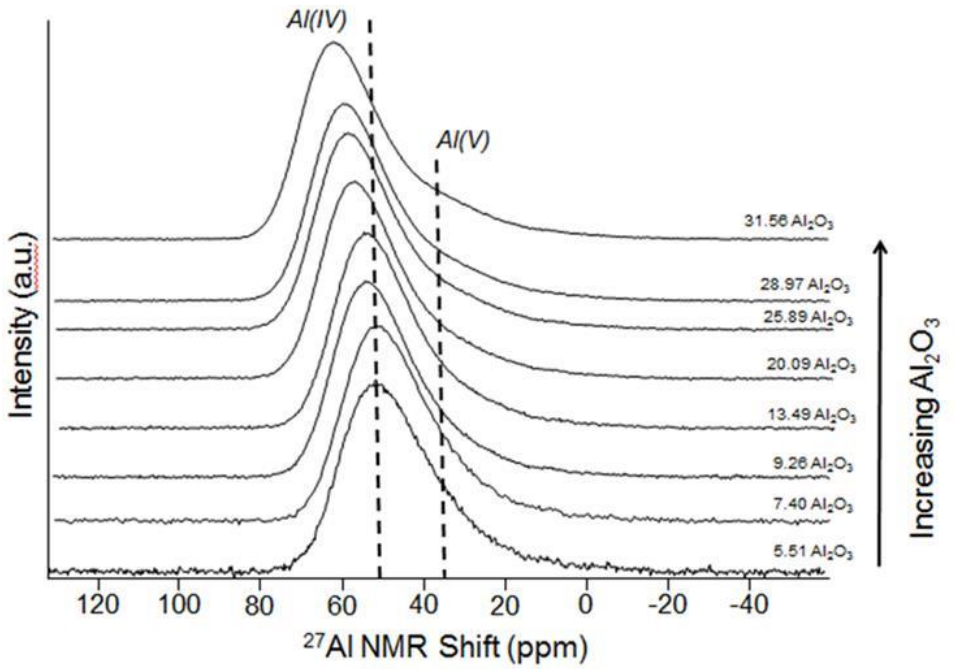

Figure 4.4: ^{27}Al MAS NMR spectra for annealed calcium aluminosilicate glasses with Al_2O_3:CaO = 1.

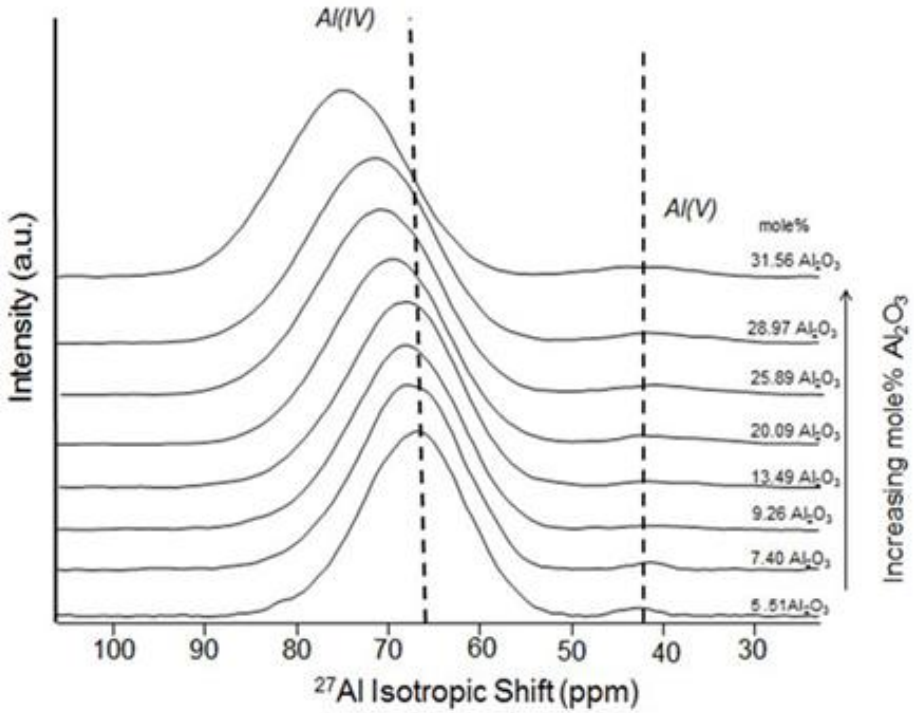

Figure 4.5: ^{27}Al 3QMAS NMR spectra for annealed calcium aluminosilicate glasses with Al_2O_3:CaO = 1.

The presence of a peak at roughly 50 ppm and 65 ppm in Figures 4.4 and 4.5 respectively, for the sample with 5.51 mol% Al_2O_3, is indicative of $Al^{(IV)}$. From Figures 4.4 and 4.5, it can be seen that the $Al^{(IV)}$ peak shifts towards higher values as the amount of Al_2O_3 in the glass increases. The shift in the peak position is known as the chemical shift. The chemical shift is a result of the bonds around Al changing from Al-O-Si to Al-O-Al or from a change in the Q^n species of Al , Where Q represents the atom of interest and n is the number of bridging oxygen attached to the atom of interest, as the amount of Al_2O_3 in the glass increases. Since Al does not commonly form NBO[19-21] then the chemical shift is most likely due to a change in second nearest neighbor

Table 4.2 lists the Al site parameters of δ_{iso} and P_Q for these glasses. These numbers clearly show a uniform change in the chemical shift which would indicate that there is good mixing between the Si and Al atoms in the lattice. Also the higher the P_Q number the more distorted the shape of the Al species.

Table 4.2: Average Al site parameters from ^{27}Al 3QMAS NMR

SiO_2 (mole%)	Al_2O_3 (mole%)	$Al^{(IV)}$		$Al^{(V)}$	
		δ_{iso}(ppm)	P_Q(MHz)	δ_{iso}(ppm)	P_Q(MHz)
39.75	31.56	69	7.47	37.2	7.01
45.14	28.97	66.3	7.28	36.1	6.58
48.51	25.89	64.4	7.21	35.7	6.60
49.70	20.09	62.9	7.63	35.8	6.81
60.61	13.49	62.1	7.81	35.1	7.23
72.57	9.23	60.9	8.23	38.3	5.60
85.98	6.63	59.9	8.40	40.1	4.91
89.93	4.56	59.7	8.66	38.7	5.76

From the 3Q data shown in Figure 4.5 specifically we can quantify the mole% of $Al^{(IV)}$ and $Al^{(V)}$ species in these glasses. The peak at around 45 ppm in Figure 4.5 is indicative of $Al^{(V)}$ presence in the glass structure. Relative amounts of $Al^{(IV)}$ and $Al^{(V)}$ are calculated from peak fitting analysis of the 3Q MAS NMR spectra for each of the glasses and are shown in Table 4.1. Stebbins, et. al, and Neuville, et. al. have shown similar results in the amount of $Al^{(V)}$ present in tectosilicate glasses across a similar range of SiO_2 content.[21-24]

4.4. Discussion

The indentation modulus and hardness of tectosilicate CaO-Al_2O_3-SiO_2 (CAS) glasses follow similar trends until about 85 mole% SiO_2, where the hardness reaches a minimum and begins to increase and the modulus continues to decrease with increasing SiO^2 mole%, as shown in Figure 4.1. This behavior is unexpected considering many people believe that hardness and modulus should follow similar trends.[25-27] Both hardness and indentation modulus are impacted by the density of the glass in that the more dense a glass is the higher the indentation modulus and hardness should be. This can be demonstrated very nicely in the tectosilicate CAS glasses in Figure 4.6 shown below. However, as shown in Figure 4.1 the hardness does not follow the same trend as indentation modulus across the entire tectosilicate series. This is an example of how, for hardness, not only the density of atoms in the glass matters but also the types of bonds present in the glass. The types of bonds present in the glass structure are important, because in order for a material to exhibit plastic deformation by shear bonds must be broken and re-formed with new neighbors.

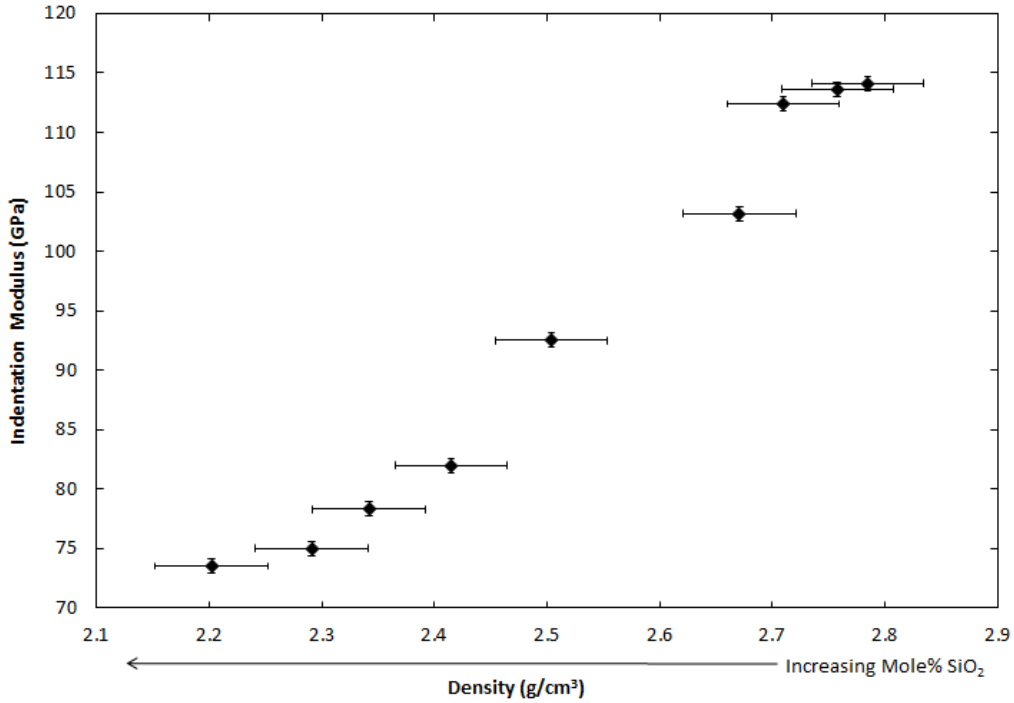

Figure 4.6: Indentation modulus as a function of glass density in the tectosilicate $CaO\text{-}Al_2O_3\text{-}SiO_2$ glasses.

In order to understand our observed hardness anomaly and how plastic deformation works in the tectosilicate CAS glass system, we are going to take a closer look at a variety of things such as the plastic to fracture threshold, the topological constraint model, and the differing mechanisms, shear and densification, of plastic deformation which exist in glasses. It is well known in glasses that hardness will decrease with increasing indentation load.[17] This effect is known as the indentation size effect, (ISE). The origin of the ISE has been attributed to several different things such as surface energy, friction, cracking and dislocations.[17] In order to study only plasticity we must make sure that we are forming a permanent deformation in the glasses without causing fracture. The presence of fracture will convolute our understanding of plasticity as well as cause a decrease in the measured hardness. In order to ensure we do not have fracture in our samples after indentation we have used

a very low load,10 mN, for our indentations. This load is well below the 1000 mN load that Gross and Tomozawa needed to induce fracture in similar CaO-Al_2O_3-SiO_2 glasses.[28] We have also scanned the indentation impressions left in our glasses by atomic force microscopy and they show no evidence of cracking. The last test we conducted to ensure the absence of fracture in our data is we measured the hardness of our glasses as a function of indentation load and show, in a representative sample, that there is no change in the glasses hardness with indentation depth. These two tests confirm that we do not have any fracture or ISE in our samples, at the loads we are using, that would impact our results.

Now that we are sure our anomalous behavior in hardness in not related to fracture we are going to look at modeling the hardness for the tectosilicate CaO-Al_2O_3-SiO_2 glasses using the topological constraint model (TC) developed for predicting indentation modulus in glasses by Phillip and Thorpe.[9-11] This model has been applied to several glass families with good success.[2-3, 12-13] The TC model is based on the premise that glasses, even though they have random networks, still have specifically defined constraints associated with the network atoms. Network atoms are atoms which participate in the glass network such as Si, Al and O in the CaO-Al_2O_3-SiO_2 glasses. These constraints are bond bending and bond stretching constraints associated with individual atoms. For example Si-O has a specific bond length and angles needed to keep the preferred tetrahedral shape in the glass structure.[12] In glasses atoms can act as either charge compensators or as network modifiers in the structure and as such are treated differently according the TC model.

For example atoms such as Ca, which act mainly as charge compensators for $(AlO_4)^-$ in the tectosilicate $CaO\text{-}Al_2O_3\text{-}SiO_2$ glasses, are not accounted for in the TC model.[12] Each network atom has a defined set of constraints based upon the coordination number of that particular atom. For example Si in tetrahedral form has five Si-O-Si bond bending constraints, called β constraints, which are the angles necessary to keep the Si atom in tetrahedral coordination. Oxygen atoms have two bond stretching constraints, called α constraints, as the oxygen are bonded to two other atoms, and one bond bending constraint, called a γ constraint, associated with the Si-O-Si bond angle.[12] In total, each O then would have $1\gamma + 2\alpha$ for a total of three constraints.

There are three steps involved in applying the TC model. The first step requires knowing what atom species are present in our glasses. This is determined from the ICP data on each of the glasses along with results of the ^{27}Al 3Q MAS NMR data for each of the glasses. The chemistry data along with the ^{27}Al 3Q MAS NMR data are used to calculate the atom% of each of the species in our glasses. This is done by converting the chemistry data, from mole% to atom% and then subtracting out the amount of $Al^{(V)}$ atom% determined from the ^{27}Al 3Q MAS NMR data from the total Al atom% calculated previously. Lastly we consider that for every $Al^{(V)}$ atom there is 1 NBO created in order to maintain charge balance. Then we subtract the amount of NBO from the calculated atom % O to obtain the atom % that is BO and NBO. Results for the atom% of every species in each of these glasses is shown in Figure 4.7 as a function of the mole% SiO2 in the glass.

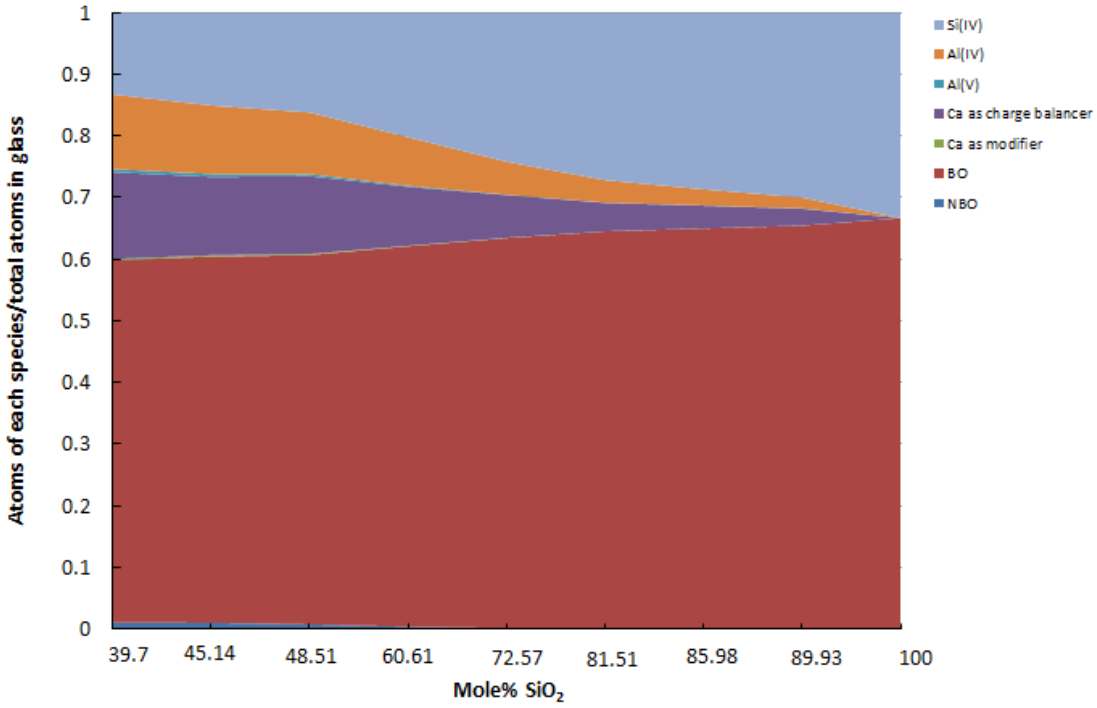

Figure 4.7: Fraction of atoms of each species in the glass as a function of mole% SiO_2 for tectosilicate CaO-Al_2O_3-SiO_2 glasses.

The second step is to identify the number of bond bending and stretching constraints for each atom.[12] The number of bond stretching constraints (BS) is given by $r_i/2$, where (r_i) is the coordination number of the atom being considered, as each α constraint is shared by two atoms and the number of bond bending (BB) constraints is given by $2r_i$-3, which is the number of independent angles needed to define the 3D shape the coordination requires, for example the Si bond structure is tetrahedral.[12] The constraints as defined above for these glasses are then:

- α: Al-O, Si-O and M^{NB}-O BS constraints. There are two α constraints at each oxygen. M^{NB} stands for network modifiers that create non bridging oxygen.

- β_{Si}: O-Si-O BB constraints. 5 β_{Si} constraints are required per Si to form rigid Si tetrahedra.
- β_{Al}: O-Al-O BB constraints. Similarly, there are 5 β_{Al} constraints per $Al^{(IV)}$ and 7 β_{Al} constraints per $Al^{(V)}$
- γ: Al-O-Al, Si-O-Si, Al-O-Si, Si-O-M^{NB} and Al-O-M^{NB} BB constraints. There is one γ at each oxygen.

Step 3 is to calculate the number of constraints (n) per atom for each glass The number of constraints per atom (n) for the glass $(CaO + Al_2O_3)_{1-x} + (SiO_2)_x$ can be calculated from the above analysis based on the atom fraction (N) of each network forming species identified in these glasses. For example $Si^{(IV)}$ has 5 BB or β constraints only, while the O atoms have two α BS constraints and one γ BB constraint for a total of 3 constraints. The rest of the atoms constraints are tallied up from the above analysis in the same way to obtain the constraints per atom listed in equation 1 below.

$$n_{(x)} = 5N_{(Si^{IV})} + 5N_{(Al^{IV})} + 7N_{(Al^{V})} + 3N_{(O)} \quad (1)$$

Figure 4.8 shows the calculated n for each of the glasses as a function of mole% SiO_2. From Figure 4.8 we can see that the total number of constraints per atom in the glass increases linearly with increasing mole% SiO_2.

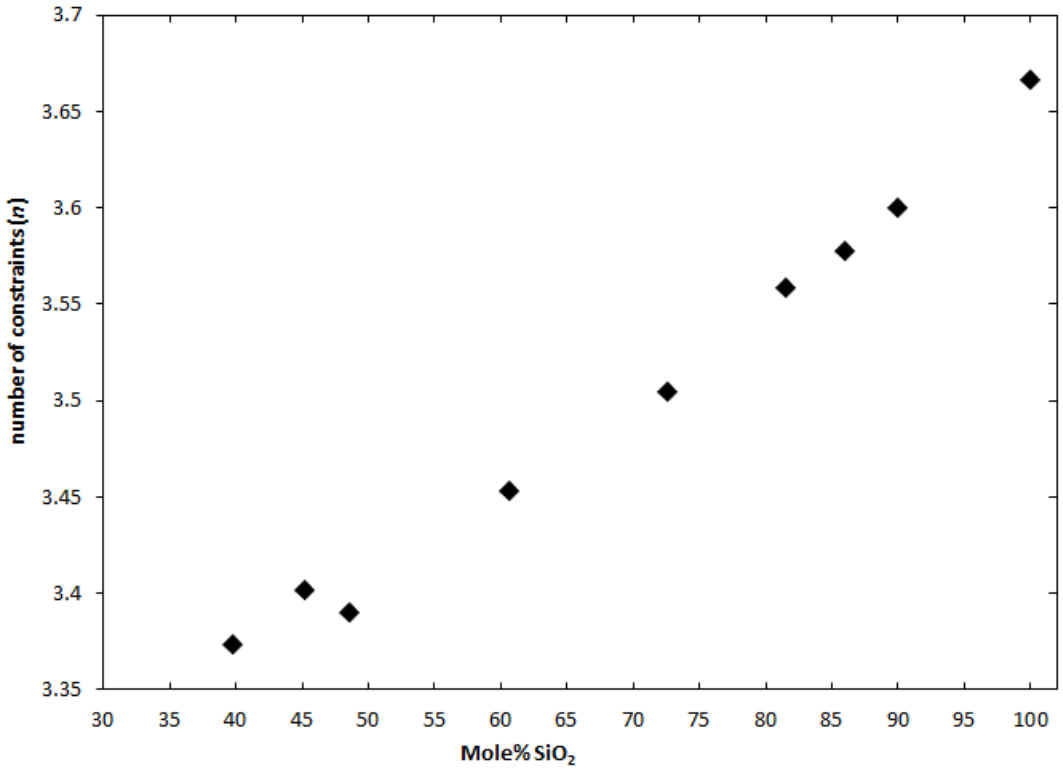

Figure 4.8: The total number of constraints in the tectosilicate CaO-Al_2O_3-SiO_2 glasses as a function of mole% SiO_2.

In principle, the indentation hardness should now be calculated as:

$$H_{(x)} = \left(\frac{dH}{dn}\right)[n_{(x,y)} - n_{crit}] \quad (2)$$

$$= \left(\frac{dH}{dn}\right)[n_{(x)} - 2.5] \quad (3)$$

Where x is the composition variable, and $\frac{dH}{dn}$ is a proportionality constant that is determined empirically and found to be dependent on load of indenter and possibly on composition. Lastly n_{crit} is the critical number of constraints which must be present in the glass structure in order to have a connected network which is a requirement for a material to display mechanical resistance.[12-14] n_{crit} is set at 2.5 based on the idea that 3.0 is considered to be a bond structure which is rigid, has no degrees of motion, and

2.0 is considered to be a bond structure which is floppy therefore 2.5 gives a network bond structure which can deform enough to exhibit plastic deformation.[2] Results of the model along with experimental data are shown in Figure 4.9, which is a plot of experimentally measured hardness and the model predicted hardness, which is obtained from equation three using $\frac{dH}{dn}$ as a fitting parameter, as a function of mole% SiO_2.

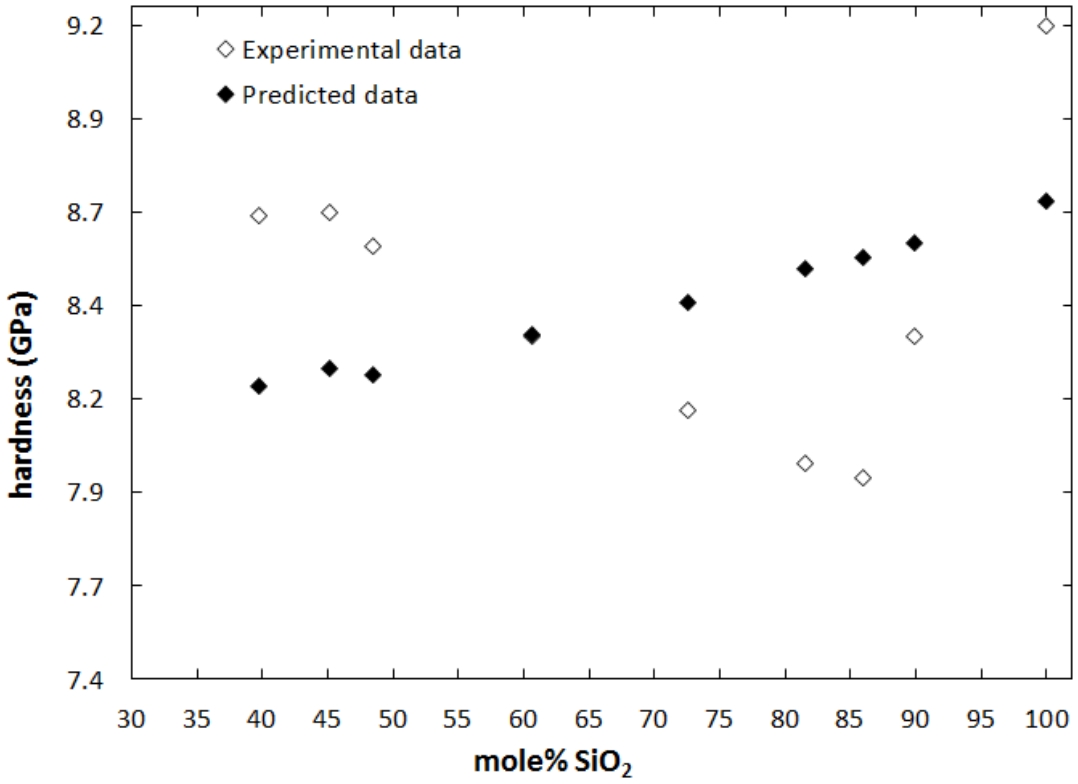

Figure 4.9: Experimental and predicted hardness as a function of mole% SiO_2 for tectosilicate CaO-Al_2O_3-SiO_2 glasses.

As can be seen from Figure 4.9 the TC model in its original form does not work for predicting hardness in these glasses. However, if we look at constraints per volume calculated as below:

$$\frac{N_c \times N_A \times 6.022E^{23} \times \rho}{(mole\%\ SiO_2 \times M.W.SiO_2)+(Mole\%Al_2O_3 \times M.W.Al_2O_3)+(mole\%\ MgO \times M.W.MgO)}, \quad (4)$$

Where N_c is the constraints per atom, N_a is the total atoms in glass, ρ is the glass density, and M.W. is the molecular weight of the oxide. We can see from Figure 4.10 that this produces a better fit to the hardness data however it still does not fit the entire range of our hardness data.

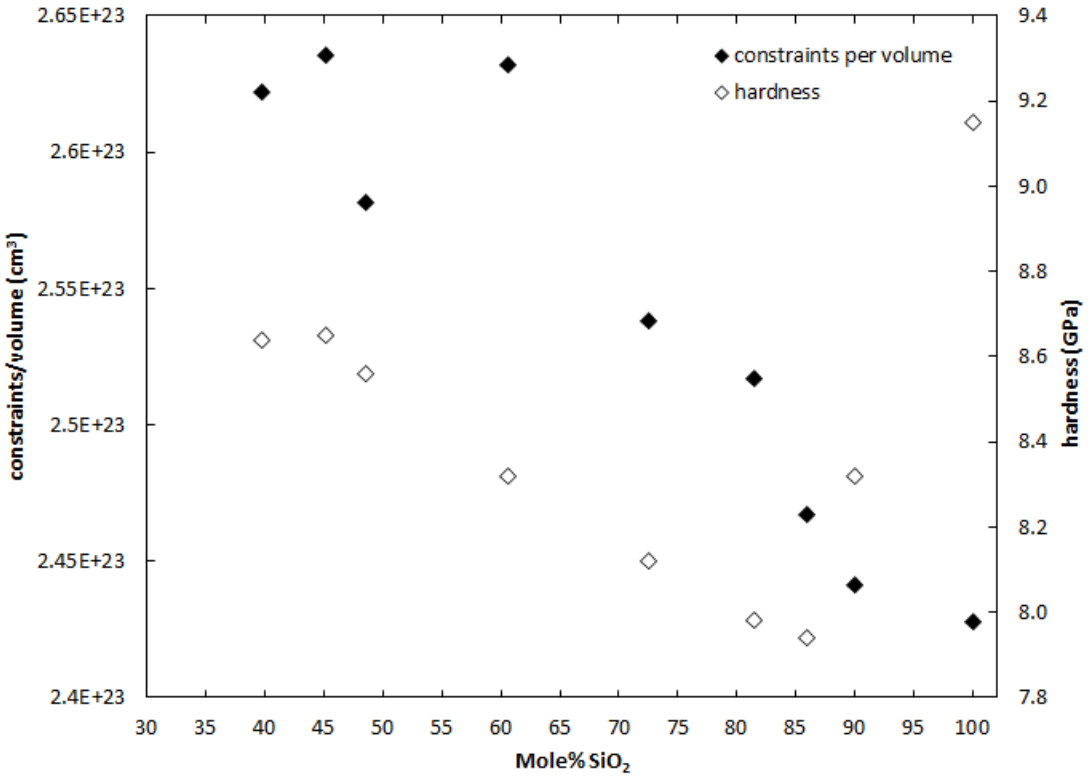

Figure 4.10: constraints per volume and hardness as a function of mole% SiO_2 in tectosilicate CaO-Al_2O_3-SiO_2 glasses.

In order to gain further understanding about the plastic behavior of this series of tectosilicate CaO-Al_2O_3-SiO_2 glasses we will look beyond the constraint model to the actual deformation modes known in glasses. There are two known plastic deformation modes in glasses and they are shear and densification. Shear deformation

is the result of bonds breaking and re-forming. Shear deformation is the dominant form of plastic deformation in "normal" glasses, glasses which have greater than about 15 mole% network modifiers in the structure.[29-30] Shear deformation is often identified in glasses by the observation of pile-up around the indentation impression. Pile-up is the result of movement of material during indentation to the surface around the indentation impression. Pile-up does not have to be an indication of shear deformation though as shear deformation can also occur without pile-up, as the strains can also be stored elastically beneath the indentation impression. In our glasses we have shear deformation for those glasses that contain less than 85 mole% SiO_2. This is shown in Figure 4.2 by the measured pile-up in our samples after indentation. The measured pile-up is less than 1 nm when 85 mole% SiO_2 is reached, however this does not mean that the glass at 85 mole% SiO_2 still does not deform by shear as mentioned above. The absence of pile-up in glasses with > 85 mole% SiO_2 along with an increase in the hardness of these glasses indicates that another deformation process such as densification deformation must be taking place.

We know that silica predominantly deforms by densification[29-30], which is the other mode of deformation found in glasses. Densification is the result of compaction of the material structure, and in glasses this is believed to occur by the change in the Si-O-Si bond angles to smaller ones.[8] Densification is the dominant form of plastic deformation in "anomalous" glasses, glasses that contain few to no modifiers and have open structures such as fused silica.[29-30] Glasses which densify will also show little to no pile-up around the indentation impression.[31] Based on Figure 4.2 we know that in our glasses we have pile-up until about 85 mole% SiO_2 where we no longer have

evidence of it. This lack of pile-up could be further evidence that glasses below 85 mole% SiO_2 deform by shear and glasses above 85 mole% SiO_2 deform by densification.

A mechanism shift from shear to densification at around 80 mole% SiO_2 has previously been shown for silicate glasses.[,32] The mechanism shift from shear to densification was evidenced by the use of fracture analysis[8,32] as well as residual stress observations.[218 Another factor indicating a mechanism shift in our glasses is that the hardness of fused silica in Figure 4.1 is greater than the hardness of calcium-aluminosilicate glasses, therefore it must be true that, rather than suppressing densification as previously believed [29] NBO and Ca must be facilitating shear. Densification is a more difficult process as compared to shear but less difficult than breaking the stronger more covalent bonds of Si-O resulting in a higher hardness for glasses which deform by densification.

For now we are going to focus on the shear deformation in glasses. It is true that plastic deformation is not as well understood in glasses as it is in crystals. For instance, in crystals, defects such as dislocations are able to move through the crystal structure creating the plastic deformation observed. However, in glasses, shear plastic deformation is not as easily understood as there are no crystal dislocations in glasses. However, glasses do have "defects" in their structure. In glasses "defects" refer to over or under coordinated species and NBO's, which may be able to move similarly to dislocations in a crystal. These species are considered defects as the under and over-coordinated species are less energetically favorable, in that Si and Al would prefer to be in four fold coordination, allowing for easier transitions from the over or

under-coordinated state to the preferred state of $Si^{(IV)}$ or $Al^{(IV)}$. Also the NBO are weaker ionic bonds as compared to the more covalent bonds of Si-O and Al-O allowing for ease of breaking and reforming bonds. NBO and their effects on plasticity and shear deformation in glasses have widely been discussed in the literature. [5,30,33-34] It has been clearly shown that as NBO content increases in a glass the hardness decreases.[30, 35-36] Therefore, NBO's help or encourage glasses to plastically deform by shear.[29-30, 35-36] The effect of under or over-coordinated species throughout the glass structure on plastic deformation, however, has not been extensively investigated. Ken-ichi Nomura et. al.[5] looked at over-coordinated and under-coordinated species in fused silica using molecular dynamic simulations. They looked at these under and over coordinated species to determine how they participate in shear plastic deformation. What they found were that defects such as over-coordinated oxygen and Si present under the indenter during loading can migrate by a bond-switching mechanism[5] Ken-ichi Nomura et. al.[5] describe this by showing how a bond will break between Si-O causing the Si to become under-coordinated and then the Si atom will re-bond to a nearby NBO becoming fully coordinated again. This leaves the original O that the Si atom was attached to as a NBO.[5] This mechanism resembles that of dislocation motion in a crystal.

Since we know we have shear deformation in some of our glasses we investigated what types of defects are found in our glasses that could be aiding in or preventing shear deformation. As discussed previously, the types of defects we will be looking for are NBO and under and over-coordinated network species. NMR data shown in Table 4.2 clearly shows that our tectosilicate $CaO\text{-}Al_2O_3\text{-}SiO_2$ glasses do

have over-coordinated Al. This is no surprise as the presence of higher coordinated Al has been observed for similar glasses by Stebbins.[23-24] The presence of over-coordinated Al would require the presence of NBO in order to maintain charge balance. In the ideal glass structure we would assume one NBO for every $Al^{(V)}$, however O NMR work by Stebbins in similar glasses shows a greater abundance of NBO than would be needed for charge balancing purposes.[23-24] For this reason it is safe for us to assume we have at least one NBO for every $Al^{(V)}$ identified by NMR in our glasses. Further, it is determined that the NBO will be found predominantly associated with Si and not Al, depolymerizing the glass network.[19-21]

Since we know that our glasses must contain NBO's and we know that NBO's decrease hardness in glasses [30, 35-36] we can compare this to what we observe in the hardness for our glasses as shown in Figure 4.1. Since we consider one NBO for every $Al^{(V)}$ in our glasses, we can see from Table 4.2 that the NBO content will be the highest at 35-50 mole% SiO_2, where $Al^{(V)}$ was found to be most abundant, and decrease to below 1 mole% at around 80-85 mole% SiO_2. If NBO's were controlling hardness, we would expect to see the hardness increase with increasing SiO_2 mole% or decreasing NBO mole% until 85 mole% SiO_2 where the NBO's fall to below 1 mole% in the glass and the glass switches from shear to densification deformation. According to the data plotted in Figure 4.1 we see just the opposite. We observe a decrease in hardness with increasing mole% SiO_2 until about 85 mole% SiO_2 where the deformation mode changes. This would seem to indicate that some other species in the glass must have a more dominant effect on hardness than the NBO's do.

The only other species found in our glass which could be causing the observed decrease in hardness with decrease in NBO would be $Al^{(IV)}$ or $Al^{(V)}$, however we know from bond dissociation energies that Al-O, with a dissociation energy of 501.9 KJ/mol, is a weaker bond than that of Si-O, with a dissociation energy of 799.6 KJ/mol, therefor our observed trend in hardness must be due to $Al^{(V)}$.[37] This is important as we have already shown that the NBO are the species most likely responsible for shear deformation in our glasses. Therefore, it appears that the $Al^{(V)}$ presence in the glass structure is able to slow down or to a certain extent prevent the shear deformation from occurring. It could be that the $Al^{(V)}$ helps the glass to resist shear deformation by preventing the Ca from breaking with the NBO's and reforming with another O creating an NBO in a different location . $Al^{(V)}$ also edge shares as opposed to corner sharing like $Al^{(IV)}$ and $Si^{(IV)}$ do giving it a stronger bond with its neighboring tetrahedra. If in fact the $Al^{(V)}$ prevents Ca from being able to break and re-form bonds with neighboring atoms, moving the NBO, then this would result in a inhibition of plastic deformation and subsequent increase in hardness.

Our data is not the first time an increase in hardness with an increase in Al coordination has been observed. Shahriar Iftekhar, et. al.[27] have observed this in Re_2O_3-Al_2O_3-SiO_2 glasses previously. Shahriar Iftekhar, et. al. believed that the higher amount of $Al^{(V)}$ species aids in crosslinking network fragments thereby increasing the hardness.[27] However, It is more likely that $Al^{(V)}$ has a stronger hold on NBO associated with it, thereby preventing the NBO from moving in the structure and creating shear deformation.

4.5. Summary and Conclusion

Tectosilicate CaO-Al_2O_3-SiO_2 glasses show a decrease in indentation modulus with a decrease in glass density. Hardness, on the other hand, for these same glasses shows an "anomalous" behavior as indicated by a minimum in the hardness at 85 mole% SiO_2. The minimum in hardness was shown to be a change from shear deformation to densification deformation.

Shear deformation requires "defects" which can move by breaking and reforming of bonds. We have identified three sources of defects in our glasses from ^{27}Al 3Q MAS NMR. The three types of defects are $Al^{(V)}$, NBO, and Ca^{+2} acting as a modifier. The $Al^{(V)}$ was shown to increase with increasing hardness in these glasses. The $Al^{(V)}$ also results in the creation of one NBO based on charge balancing rules and the ideal structure of CaO-Al_2O_3-SiO_2 glasses. This means that the amount of NBO in the glass structure will increase with the amount of $Al^{(V)}$ present in the glass structure. According to our hardness data the hardness of the tectosilicate CaO-Al_2O_3-SiO_2 glasses increases with increasing NBO, which is contrary to what has been reported in the literature, of a decrease in hardness with an increase in NBO. For this reason we believe that $Al^{(V)}$ has the dominant role in controlling the shear deformation and hardness of tectosilicate CaO-Al_2O_3-SiO_2 glasses with < 85 mole% SiO_2. It is reasonable to imagine that the $Al^{(V)}$ would aid in increasing the cross-linking of the glass network and prohibit the Ca^{2+} ions from being able to move and create shear bands through the glass structure.

Densification deformation, a higher energy deformation mechanism, occurs when a glass can no longer deform by shear. We know this based on the fact that fused silica deforms by purely densification and our data shows that this glass has the highest hardness of all the glasses investigated in this experiment. Therefore modifying ions do not prevent densification, as has been previously thought, but rather they promote shear deformation.

Attempts at modeling the observed hardness by topological constraint theory has proved to be ineffective. However, it was found that rather than using constraints per atom using constraints per volume provides an improved fit to the hardness data of those glasses that deform by a shear mechanism. The main reason the TC model is unsuccessful at modeling hardness for these glasses is that it only considers the amount of constraints in the glass structure rather than also considering the strength of those constraints.

It is clear from this work that a deeper and more thorough understanding of what "defects" exist or can be created under contact load in the glass structure is needed. There is also a strong need to gain a better understanding of how these defects can move through the glass structure during contact loading. These two pieces of information will be crucial to understanding and predicting hardness in glasses.

REFERENCES

1. T. Rouxel, H. Ji, J.P. Guin, F. Augereau, B. Ruffle. “Indentation deformation mechanisms in Glass: Densification vs. Shear Flow.” *J. App. Phys.* **107** 094903 (2010).

2. M. M. Smedskjaer. “Topological Model for Boroaluminosilicate Glass Hardness.” *Frontiers in Mater.*,**1** [23] 1-6 (2014).

3. K.W. Peter. “Densification and Flow Phenomena of Glass in Indentation Experiments.” *J. Non-Cryst Solids,* **5**, 103-115 (1970).

4. T.M. Gross, “Glasses with Fictive Temperature-Independent Properties: Minimization of Indentation Size Effect and Maximization of Crack Resistance.” PhD Thesis, Rensselaer Polytechnic Institute, April 2008.

5. K.Nomura, Y. Chen, R. K. Kalia, A. Nakano, P. Vashishta, “Defect Migration and Recombination in Nanoindentation of Silica Glass.” *Appl. Phys. Lett.* **99**, 111906 (2011).

6. M. Yamane and J.D. Mackenzie.”Vicker’s Hardness of Glass.” *J. Non-Cryst. Solids,* **15,** 153-164 (1974).

7. A. Faivre, F. Despetis, F. Guillaume, P. Solignac.”Role of Movile Cations on Microplasticity in Alumino-Phosphate Glasses.” *J. Am. Ceram. Soc.,* **93** [10] 2986-2989 (2010).

8. M., Bertoldi, V. M. Sglavo, “Soda-Borosilicate Glass: Normal or Anomalous Behavior Under Vickers Indentation?” *J. Non-Cryst. Solids* **344,** 51-59 (2004).

9. J.C. Phillips. “Topology of Covalent Non-Crystalline Solids I: Short-range Order in Chalcogenide Alloys.” *J. Non-Cryst. Solids*, **34,** 153-181 (1979).

10. H. He and M.F. Thorpe. “Elastic Properties of Glasses.” *Phys. Rev. Lett.* **54** [19] 2107-2110 (1985).

11. J. C. Phillips and M. F. Thorpe, “Constraint Theory, Vector Percolation and Glass Formation.” *Solid state communications*., **53** [8] 699-702 (1985).

12. M. M. Smedskjaer, J. C. Mauro, R. E. Youngman, C. L. Hogue, M. Potuzak and Y. Yue. "Topological Principles of Borosilicate Glass Chemistry." *J. Phys. Chem. B* **115**, 12930-12946 (2011).

13. D.R. Swiler, A.K. Varshneya and R.M. Callahan. "Microhardness, Surface Toughness and Average Coordination Number in Chalcogenide Glasses." *J. Non-Cryst. Solids* **125**, 250-257 (1990).

14. M.M. Smedskjaer, J. C. Mauro, Y.Yue. "Prediction of Glass Hardness Using Temperature Dependent Constraint Theory." *Phys. Rev. Lett.* **105,** 1115503 (2010).

15. W.C. Oliver and G.M. Pharr, "Measurement of Hardness and Elastic Modulus by Instrumented Indentation: Advances in Understanding and Refinements to Methodology." *J. Mater. Res.,* **19,** [1] 3-20 (2004).

16. D. K. Tadjiev, R. J. Hand. "Surface Hydration and Nanoindentation of Silicate Glasses." *J. of Non-Cryst. Solids,* **356,** 102-108 (2010).

17. M. Smedskjaer, "Indentation Size Effect and the Plastic Compressibility of Glass." *Appl. Phys. Let.* **104,** 251906 (2014)

18. D. Massiot, F. Fayon, M. Capron, I. King, S. Le Calve, B. Alonso, J. O. Durand, B. Bujoli, Z. Gan, G. Hoatson, *Magn. Reson. Chem.* **40,** 70 (2002).

19. V. Petkov, S.J.L. Bilinge, S.D. Shastri and B. Himmel, "Polyhedral Units and Network Connectivity in Calcium Aluminosilicate Glasses From High Energy X-Ray Diffraction." *Phys. Rev. Lett.,* **85** [16] 3436-3439 (2000).

20. C. I. Merzbacher, B. L. Sherriff, J. S. Hartman and W. B. White, "A High Resolution 29Si and 27Al NMR Study of Alkaline Earth Aluminosilicate Glasses." *J. Non-Cryst. Solids*, **124**, 194-206 (1990).

21. L. M. Thompson and J. F. Stebbins."Non-Bridging Oxygen and High-Coordinated Aluminum in Metaluminous and Peraluminous Calcium and Potassium Aluminosilicate Glasses: High Resolution 17O and 27Al MAS NMR Results." *American Minerologist*, **96,** 841-853 (2011).

22. D. R. Neuville, L. Cormier and D. Massiot."Al Coordination and Speciation in Calcium Aluminosilicate Glasses: Effects of Composition Determined by 27Al MQ-MAS NMR and Raman Spectroscopy." *Chemical Geology*, **229**, 173-185 (2006).

23. J.F. Stebbins and Z. Xu. "NMR evidence for excess non-bridging oxygen in an Aluminosilicate Glass." *Nature,* **390**, 60-62 (1997)

24. J.F. Stebbins, E.V. Dubinsky, K. Kanehashi, K.E. Kelsey. “Temperature Effects on Non-Bridging Oxygen and Al Coordination Number in Calcium Aluminosilicate Glasses and Melts.” *Geochim. Cosmochim. Acta,* **72**, 910-925 (2008).

25. D. M. Teter, “Computational Alchemy: The Search for New Superhard Materials.” *Mater. Res. Bull.,* **23**, 22-27 (1998).

26. A. Y. Liu and M. L. Cohen.” Prediction of New Low Compressibility Solids.” *Science*, **245** [4920] 841-842 (1989).

27. S. Iftekhar, B. Pahari, K. Okhotnikov, A. Jaworski, B. Stevensson, J. Grins, M. Eden. “Properties and Structures of RE2O3-Al2O3-SiO2 (RE = Y, Lu) Glasses Probed by Molecular Dynamics Simulations and Solid State NMR: The Roles of Aluminum and Rare-Earth Ions for Dictating the Microhardness.” *J. Phys. Chem. C*, **116,** 18394-18406 (2012).

28. T.M.Gross and M. Tomozawa,”Fictive Temperature-Independent Density and Minimum Indentation Size Effect In Calcium Aluminosilicate Glass.” *J. Appl. Phys.*, **104** [6] 63529-1 (2008).

29. A. Arora, D.B. Marshall and B.R. Lawn, “Indentation, Deformation/Fracture of Normal and Anomalous Glasses.” *J. Non-Cryst. Solids*, **31** [3] 415-428 (1979).

30. D.A. Kilymis and J.M. Delaye. “Deformation Mechanisms during Nanoindentation of Sodium Borosilicate Glasses of Nuclear Interest.” *J. Chem. Phys.* **141,** 014504 (2014).

31. A. Shorey, K. Xin, K.Chen, and J. C. Lambropoulos,”Deformation of Fused Silica: Nanoindentation and Densification.” *SPIE* **3424,** 72-81 (1998).

32. T.M. Gross, M. Tomozawa, A. Koike, “A glass with high crack initiation load: Role of fictive temperature-independent mechanical properties.” *J. non-cryst. Sol.* **355**, 563-568 (2009).

33. J.J. Gilman, “Flow Via Dislocations in Ideal Glasses.” *J. of Appl. Phys.,* **44**, 675-679 (1973).

34. A. Tandia, N. T. Timofeev, J. C. Mauro, K. D.Vargheese, “ Defect Mediated Self-Diffusion in Calcium Aluminosilicate Glasses: A Molecular Modeling Study.” *J. of Non-Cryst. Sol.* **357**, 1780-1786 (2011).

35. T.M. Gross, ”Deformation and Cracking Behavior of Glasses Indented with Diamond Tips of Various Sharpness.” *J.Non-Cryst. Solids* **358** [24] 3445-3452 (2012).

36. M. Smedskjaer, M. Jensen, Y.Yue,”Effect of Thermal History and Chemical Composition on Hardness of Silicate Glasses.” *J. non-cryst. Sol.* 3**56**, 893-897 (2010).

37. Y.R. Lou, *Comprehensive Handbook of Chemical bond Energies,* CRC Press, Boca Raton, Fl 2007.

CHAPTER 5

EFFECT OF MG REPLACEMENT FOR CA ON HARDNESS OF ALUMINOSILICATE GLASSES

5.1. Abstract

In the glass making industry, aluminosilicate glasses are considered a highly important family of glasses due to their use in such products as car windshields, touch screens for cell phones, and tablets among others. However, little is understood about the plastic deformation mechanisms and what effects modifier ions such as Ca and Mg have on these mechanisms. In this paper the hardness and indentation modulus of a series of tectosilicate $(MgO + Al_2O_3)_{1-x} + (SiO_2)_x$ (MAS) glasses determined using nanoindentation are compared with the composition, including aluminum speciation determined using ICP and NMR. The results are compared with previously reported data for tectosilicate $(CaO + Al_2O_3)_{1-x} + (SiO_2)_x$ (CAS) glasses. It was found that the Mg atom in MAS glasses creates larger quantities of higher coordinated Al resulting in an increase in hardness over CAS glasses. The increase in indentation modulus of MAS glasses compared to CAS glasses was a result of an increase in constraints per volume for the MgO containing glasses. A transformation in hardness from shear to densification deformation was also observed in the MAS glasses just as it was previously in the CAS glasses.

5.2. Introduction

Aluminosilicate glasses are a highly important family of glasses in the glass making industry. Of the Aluminosilicate glasses, the calcium Aluminosilicate (CAS) glasses are one of the most significant systems because of their excellent chemical durability,

and mechanical and optical properties. Even with their high importance, the exact mechanisms of shear and densification deformation are poorly understood. A previous study on tectosilicate CAS glasses showed a non-monotonic behavior in hardness with increasing mole% SiO_2.[3] It was previously proposed that this behavior results from a change in deformation mechanism from shear in glasses < 80 mole% SiO_2 to densification in glasses with > 80 mole% SiO_2.[1-3] This transition from shear to densification is presumed to be related to an insufficient amount of species which can easily be sheared, such as NBO, left in the glass structure and therefore the glass must use another mode of deformation, densification.[3] It was further shown that inclusion of higher coordinated Al species, such as $Al^{(V)}$ and $Al^{(VI)}$, can also act to increase the hardness of glasses by creating better crosslinking in the glass structure and thereby increasing the difficulty of shear deformation or even preventing shear deformation.[3-4] In order to better understand how shear plasticity works in aluminosilicate glasses, and especially in alkaline-earth aluminosilicate glasses one could substitute another alkaline-earth, i.e. Mg, for Ca to determine what effect this has on the hardness and the deformation mechanisms involved in plastic deformation.

Currently, little is known about the effect Mg will have on the plastic deformation properties of aluminosilicate glasses, however, based upon available structural information one can make speculations about how swapping Ca for Mg may impact the hardness and the plastic deformation mechanisms. It is known that Mg has a higher field strength, where field strength = net charge/square of average bond distance to O = Z/d^2, as compared to Ca.[5] This increased field strength results in Mg having a stronger ionic bond with O, as compared to Ca.[5-6] Further, it was shown by NMR data from Thompson and Stebbins[7] that higher field strength atoms, such as Mg, preferentially bond with non-bridging oxygen (NBO), whereas lower field strength atoms, such as Ca, are preferentially associated with the charged bridging

oxygen (BO). Therefore, this may mean that Mg will have a stronger bond than Ca with NBO in the glass structure thereby preventing the NBO from partaking in shear deformation. It was further shown by Guignard[5] and Thompson[7] that glasses containing Mg tend to have more $Al^{(V)}$ and $Al^{(VI)}$ species present in the glass structure as compared to their Ca counterparts. If the increase in higher coordinated Al, which has been discussed only a few times in the literature,[3-4] is in fact able to prevent shear deformation by increased crosslinking of the glass structure, and the Mg does in fact have a stronger bond with NBO over that of Ca, then we should see an increase in hardness for MAS glasses over CAS glasses. We also know that Mg is a smaller atom compared to Ca, therefore we might expect this to result in a more open glass structure. We know that glasses which deform mainly by densification have more open structures, such as fused silica glass,[8] therefore one could assume that creating a more open glass structure along with increasing the difficulty for shear deformation would make densification deformation easier. This would result in the previously observed minimum in H for CAS glasses[3] to move to lower SiO_2 content for MAS glasses. In other words, the transition from shear deformation to densification deformation would occur at lower SiO_2 content in the MAS glasses as opposed to the CAS glasses.

The present paper reports on the effect of substituting Mg for Ca in tectosilicate CAS glasses on the hardness and plastic deformation mechanisms previously observed for the tectosilicate CAS glass system by Lamberson et. al.[3] The intent of this paper is to further increase understanding of the unit deformation mechanisms involved in shear deformation and densification deformation of RO-aluminosilicate glasses through the use of nanoindentation, to determine harness and indentation modulus, and ^{27}Al 3Q MAS NMR, to obtain structural information. More specifically we hope to 1) confirm higher coordinated Al results in strengthening of

glasses by preventing or making shear deformation more difficult, 2) Determine if NBO are the predominant atom species involved in shear deformation and 3) gain a better understanding of why and how glasses change deformation modes from shear to densification. Increased knowledge in these three areas would help us to develop improved models for predicting glass hardness, which will ultimately aid in the development of glasses with improved mechanical properties such as hardness and scratch resistance.

5.3. Experiments and Results

5.3.1. Specimen Preparation

Glasses were made with 99.99% purity SiO_2, 99.98% purity Al_2O_3 and 99.992% purity MgO powders. The glasses were melted in Pt crucibles at 1650°C for 15 hrs. The melts were poured onto a metal table and then rolled with a metal rolling pin to rapidly cool the glass and crush it into small pieces. The glass remaining in the crucibles was knocked out and added to the crushed glass and re-melted. This method is adopted to aid in mixing of the glass ensuring good homogeneity in the final glass patty. The glasses were annealed at 700°C for 2 hrs to reduce internal stresses generated during pouring and cooling. The glasses were inspected after annealing in a polarized scope to ensure good homogeneity and absence of phase separation. The glasses containing SiO_2 of greater than 80 mole% contained small bubbles of about 0.1 mm in size. However, there were still areas of the glass samples of up to 6 mm x 6 mm which did not contain any bubbles. The bubbles are randomly distributed throughout the glass so large areas without bubbles are easily located.

Glass samples were cut on a precision diamond saw and then mounted on a plate with Unibond 5.0 Adhesive wax. The samples were then lapped with 22 µm alumina powder on a steel plate. The samples were then polished on a silk pad with 1µm diamond mixed with Hyprez polishing oil, which is petroleum naphtha CAS NO. 64742-48-9. After polishing the samples were removed from the mount plate and cleaned with Opticlear, which is d-limonene with chemical formula $C_{10}H_{16}$ and CAS NO. 5989-27-5, to remove wax and then with IPA to remove Opticlear residue. The samples thickness was checked with a depth micrometer and the surface roughness was measured using an optical surface profilometer, ensuring the sample meets the specification of roughness and thickness variations less than 10 nm for testing. The final sample dimensions are 10 mm × 10 mm × 1 mm.

After cutting and polishing the samples were annealed at their measured annealing temperature, as determined by beam bending viscometry, for 2 hrs. The annealing removes any internal stresses which were generated during the cutting and polishing process. The annealing temperatures for each of the glass compositions is shown in Table 1. After annealing the samples are stored in a dessicator to prevent water absorption at the surface of the sample until testing is performed.

5.3.2. Composition and Density

The composition of glasses studied in this experiment were measured by Inductively Coupled Plasma-Optical Emission Spectrometry (ICP-OES) chemical analysis. The measured glass compositions and accuracy of each

measurement are shown in Table 5.1**.** The density of the glass samples was measured by buoyancy in water with an estimated error of ±2%. The density data is also provided in Table 5.1.

Table 5.1: glass compositions as measured by ICP-OES along with annealing point and density for Mg and Ca containing Aluminosilicate glasses.

Glass	Measured composition in mole%					
	SiO_2	Al_2O_3	MgO	CaO	Anneal Pt. (°C)	Density g/cm^3
1	39.75 ± 0.4	31.56 ± 0.4	0.00	28.69 ± 0.2	850	2.79
2	45.14 ± 0.4	28.97 ± 0.4	0.00	25.89 ± 0.2	853	2.76
3	48.51 ± 0.4	25.89 ± 0.4	0.00	25.61 ± 0.2	853	2.72
4	60.61 ± 0.7	20.09 ± 0.3	0.00	19.30 ± 0.2	860.3	2.68
5	72.57 ± 0.7	13.49 ± 0.2	0.00	13.95 ± 0.1	865.7	2.67
6	81.51 ± 0.8	9.23 ± 0.1	0.00	9.26 ± 0.08	882.1	2.51
7	85.98 ± 0.8	6.63 ± 0.1	0.00	7.40 ± 0.07	883	2.35
8	89.93 ± 0.9	4.56 ± 0.07	0.00	5.51 ± 0.04	900	2.30
9	100.00	0.00	0.00	0.00	1140	2.21
10	45.69 ± 0.4	26.89 ± 0.4	27.42 ± 0.2	0.00	801.4	2.72
11	50.34 ± 0.4	24.76 ± 0.4	24.9 ± 0.2	0.00	804.2	2.68
12	60.11 ± 0.4	19.73 ± 0.4	20.16 ± 0.2	0.00	815.6	2.57
13	69.97 ± 0.7	14.81 ± 0.3	15.22 ± 0.1	0.00	Not able to obtain	2.48
14	80.56 ± 0.8	9.62 ± 0.2	9.82 ± 0.06	0.00	Not able to obtain	2.36
15	85.53 ± 0.8	7.38 ± 0.1	7.09 ± 0.05	0.00	964.9	2.33
16	90.12 ± 0.9	4.87 ± 0.08	5.01 ± 0.03	0.00	996.1	2.28

5.3.3. Mechanical Properties

A Hysitron TriboIndenter equipped with a Berkovich diamond tip was used. The indenter was calibrated using a fused silica sample provided by the manufacturer before each test. The instrument compliance, indenter geometry and thermal drift were all calibrated using the method developed by Oliver and Pharr.[9-10]

5.3.3.1. Hardness and Modulus

The hardness and modulus of each of the glasses was measured using a maximum load during nanoindentation of 10 mN which produces a maximum depth of about 200 nm. The ramp rate used for these measurements was 1 mN/s and then the load was held at 10 mN for 10 sec. followed by a ramp down at the same rate. A 5 X 5 array of indents were performed on each sample with 10 μm between each indentation. The hardness and indentation modulus were calculated for each indentation using the Oliver and Pharr method[9-10]

Figures 5.1 and 5.2 show hardness and indentation modulus as a function of mole% SiO_2 respectively.

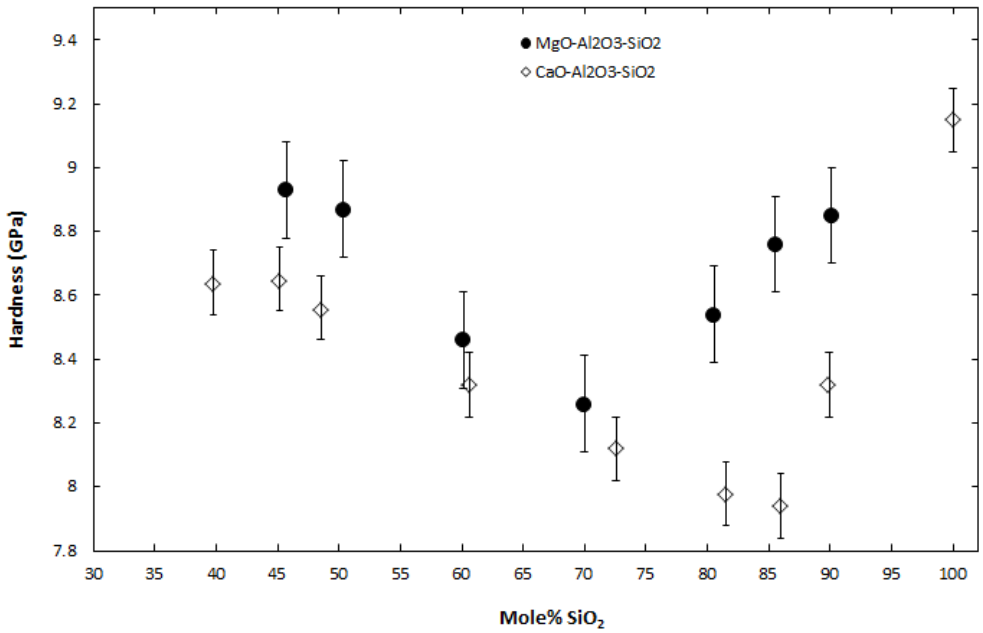

Figure 5.1: Hardness as a function of mole% SiO_2 for tectosilicate CaO-Al_2O_3-SiO_2 and MgO-Al_2O_3-SiO_2 glasses. MgO glasses have a higher overall H and the minimum is shifted to lower SiO_2 containing glass as compared to comparable CaO containing glass.

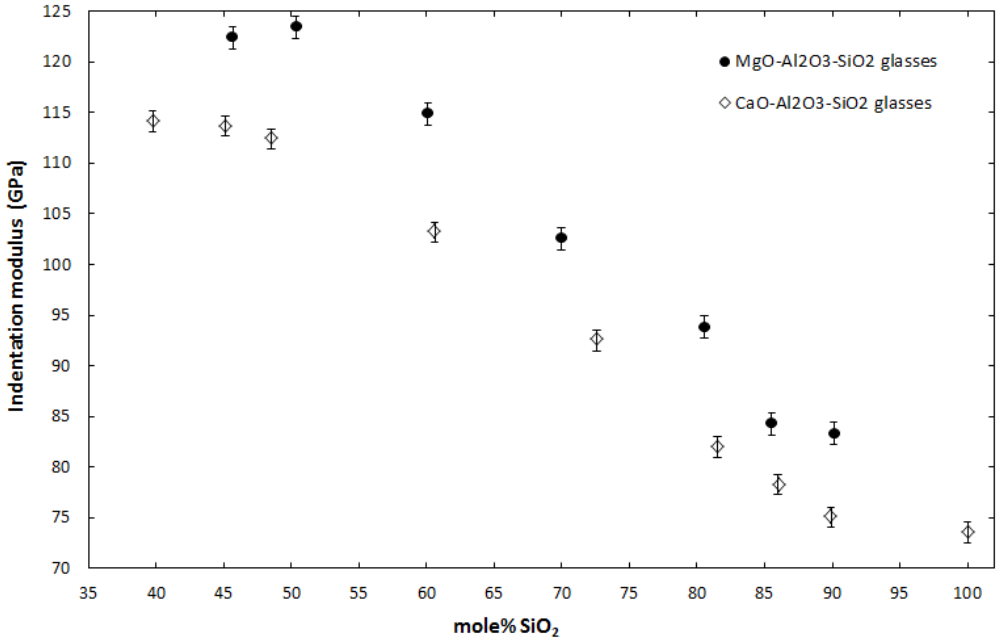

Figure 5.2: Indentation modulus as a function of mole% SiO_2 for tectosilicate CaO-Al_2O_3-SiO_2 and MgO-Al_2O_3-SiO_2 glasses.

From Figure 5.1 one can see that the hardness exhibits a non-monotonic behavior with increasing SiO_2 content for both the MgO and CaO containing glasses. At roughly 85 mole% SiO_2, the hardness reaches a minimum in the CaO containing glasses however for the MgO containing glasses the minimum is at 70 mole% SiO_2. The hardness values for the MgO containing glasses are also all larger than their CaO counterparts. In contrast, the indentation modulus, as seen in Figure 5.2, decreases with increasing SiO_2 content for both the CaO and MgO containing glasses.

5.3.4. Al Speciation

^{27}Al magic angle spinning (MAS) NMR[se] experiments were conducted at 16.4 T (182.34 MHz resonance frequency) using a commercial spectrometer (VNMRS, Agilent) and a commercial 1.6 mm MAS NMR probe (Agilent). Powdered glasses

were packed into 1.6 mm zirconia rotors with sample spinning at 25 kHz. 0.6 μs radio-frequency (RF) pulses, corresponding to a π/12 tip angle, were used to uniformly excite the ^{27}Al central transitions and thus provide quantitatively accurate Al speciation. The ^{27}Al MAS NMR spectra were processed without additional line broadening and referenced to aqueous aluminum nitrate at 0.0 ppm. ^{27}Al MAS NMR spectra were analyzed using the DMfit program[11]. This program provides a means by which to simulate second-order quadrupolar lineshapes, and in the case of ^{27}Al NMR spectra, an additional parameter (Czjzek distribution) to account for distributions in the quadrupolar interaction[11]. Additional ^{27}Al triple quantum MAS (3QMAS) NMR experiments were conducted at 16.4 T using the hypercomplex shifted-echo pulse sequence. RF pulses were optimized to provide best signal-to-noise ratio, resulting in hard pulse widths of 2.1 and 0.8 μs, and a soft z-filter reading pulse of 15 μs. These data were processed with 100 Hz apodization in both time domains and referenced to aqueous aluminum nitrate at 0 ppm.

^{27}Al MAS NMR and 3Q MAS NMR spectra are shown below in Figures 5.3 and 5.4 respectively.

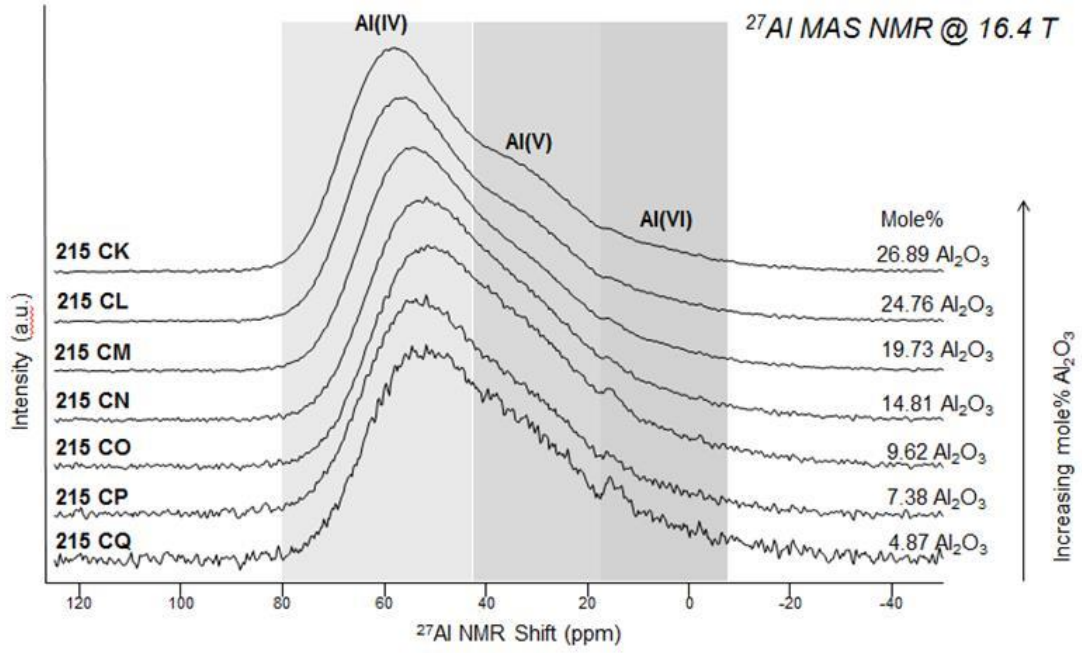

Figure 5.3: ^{27}Al MAS NMR plot showing the peak shift and shape change of the $Al^{(IV)}$, $Al^{(V)}$ and $Al^{(VI)}$ peaks as move from low Al_2O_3 to high Al_2O_3 in the tectosilicate MgO-Al_2O_3-SiO_2 glasses.

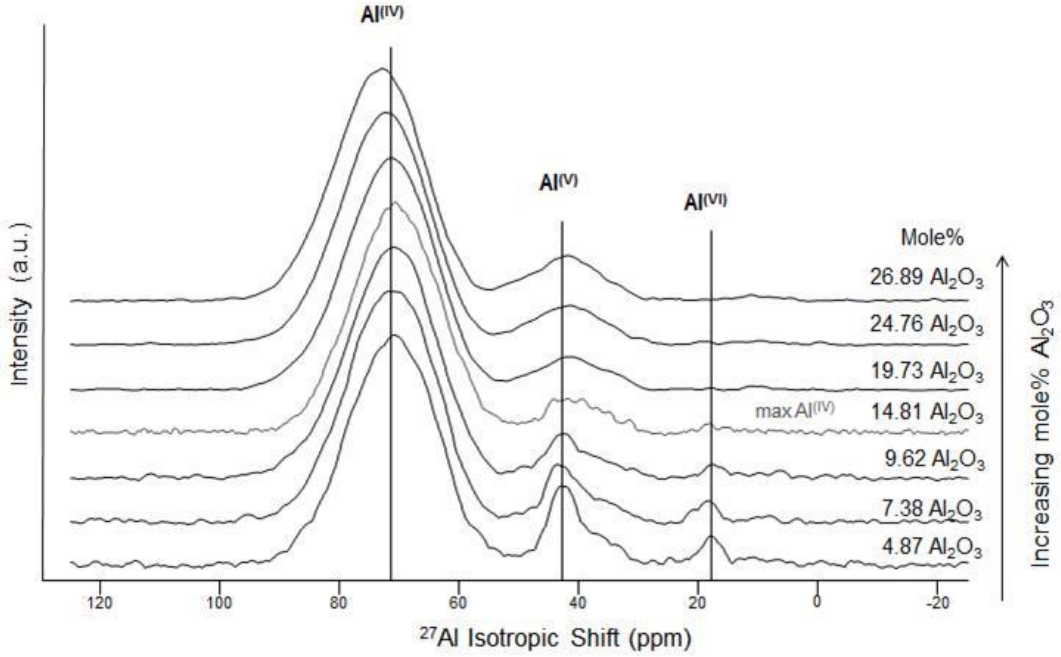

Figure 5.4: ^{27}Al 3QMAS NMR isotropic projections plot showing the chemical shift and peak shape change of the $Al^{(IV)}$, $Al^{(V)}$ and $Al^{(VI)}$ peaks in tectosilicate MgO-Al_2O_3-SiO_2 glasses.

One can see the uniform peak shift of $Al^{(IV)}$ indicating the uniform change of second nearest neighbor from Al-O-Si to Al-O-Al as the mole% Al_2O_3 in the glass increases. In Figure 5.4 one can notice the change in the peak shape of the $Al^{(V)}$ and $Al^{(VI)}$ peaks. Table 5.2 shows the % $Al^{(IV)}$, $Al^{(V)}$ and $Al^{(VI)}$ in both the tectosilicate $CaO-Al_2O_3-SiO_2$ glasses and the $MgO-Al_2O_3-SiO_2$ glasses for comparison. As one can see the MgO containing glasses have more $Al^{(V)}$ and $Al^{(VI)}$ species in the structure than the glasses containing CaO.

Table 5.2: The mole% $Al^{(IV)}$, $Al^{(V)}$ and $Al^{(VI)}$ found in each of the glasses from table 5.1 by ^{27}Al 3Q MAS NMR. Glasses 1-8 are $CaO-Al_2O_3-SiO_2$ glasses and 10-16 are $MgO-Al_2O_3-SiO_2$ glasses. Glass 9 is fused silica

Glass	mole% $Al^{(IV)}$	mole% $Al^{(V)}$	mole% $Al^{(VI)}$
1	30.27	1.29	0.00
2	27.75	1.22	0.00
3	25.01	0.88	0.00
4	19.65	0.44	0.00
5	13.31	0.18	0.00
6	9.11	0.12	0.00
7	6.52	0.11	0.00
8	4.43	0.13	0.00
9	0.00	0.00	0.00
10	23.13	3.52	0.24
11	21.62	3.00	0.15
12	17.74	1.91	0.08
13	13.37	1.32	0.12
14	8.64	0.87	0.12
15	6.46	0.79	0.13
16	4.26	0.52	0.09

5.4. Discussion

The indentation modulus and hardness of MAS glasses follow similar trends to the CAS glasses. In Figure 5.2 one can see that both MAS and CAS glasses have a decrease in indentation modulus with increase in mole% SiO_2 in the glass. As is shown in Figure 5.5 for both series of glasses, MAS and CAS, the indentation modulus has a linear relationship with density. That is, as the density of the glass increases so does the indentation modulus.

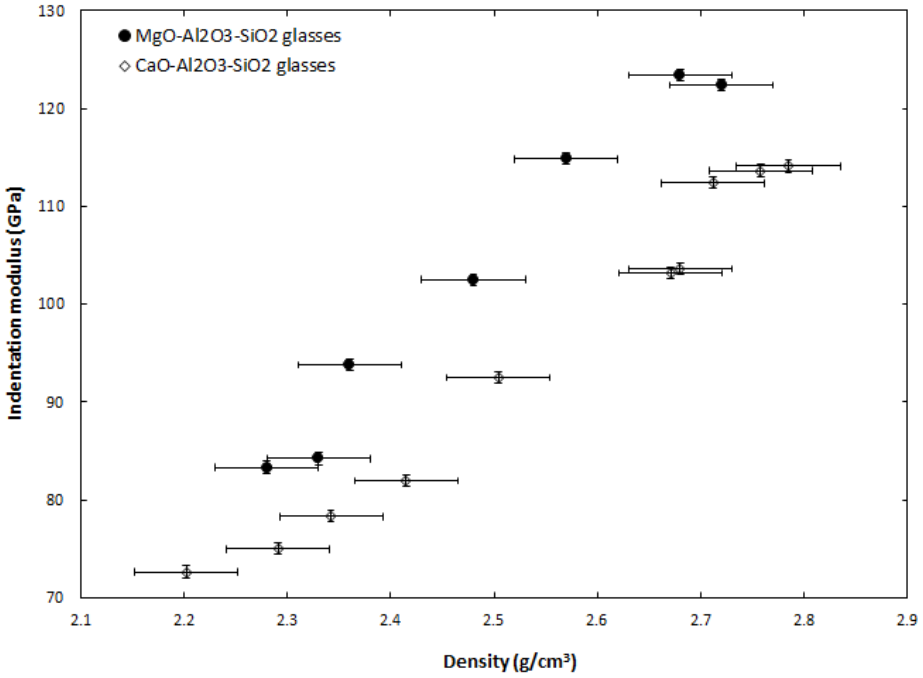

Figure 5.5: Indentation modulus as a function of density for tectosilicate $CaO\text{-}Al_2O_3\text{-}SiO_2$ and $MgO\text{-}Al_2O_3\text{-}SiO_2$ glasses. For both the Mg and Ca containing glasses the modulus is linear with respect to density of the glasses.

However, the reason for the increase in indentation modulus of MAS glasses over CAS glasses is not related to the glass density but rather the amount of atom constraints per unit volume in the glass. The way in which the constraints in the glasses are counted has previously been described for the $CaO\text{-}Al_2O_3\text{-}SiO_2$ glasses and

published in reported in a paper by Lamberson, et. al.[3] After the constraints per atom in the glass are determined the number of atom constraints per unit volume in the glass can be calculated by the following formula:

$$\frac{N_c \times N_A \times 6.022E^{23} \times \rho}{(mole\%\ SiO_2 \times M.W.SiO_2)+(Mole\%Al_2O_3 \times M.W.Al_2O_3)+(mole\%\ MgO \times M.W.MgO)}, \quad (1)$$

Where N_c is the constraints per atom, N_a is the total atoms in glass, ρ is the glass density, and M.W. is the molecular weight of the oxide.

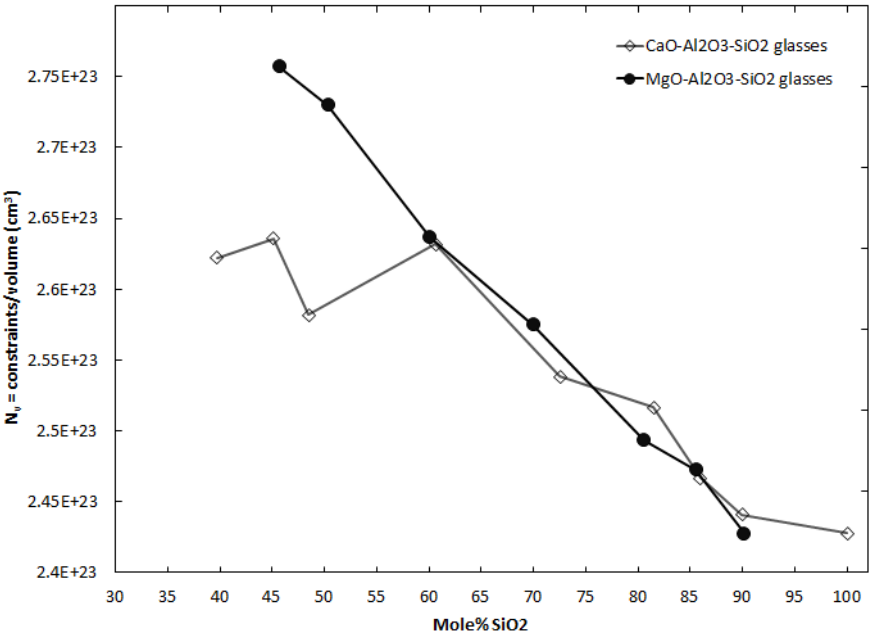

Figure 5.6. constraints/cm^3 as a function of mole% SiO_2 in tectosilicate $CaO\text{-}Al_2O_3\text{-}SiO_2$ and $MgO\text{-}Al_2O_3\text{-}SiO_2$ glasses.

As can be seen in Figure 5.6, MAS glasses have more constraints per unit volume as compared to CAS glasses. So, even though MAS glasses are slightly less dense than CAS glasses, as is shown in Table 5.1, the increase in constraints per unit volume for MAS glasses over CAS glasses enables MAS glasses to better resist elastic deformation, resulting in the higher indentation modulus over CAS glasses. The

increase in bonds per unit volume for MAS glasses is related to a substantial increase in higher coordinated Al over CAS glasses, shown below in Figure 5.7.

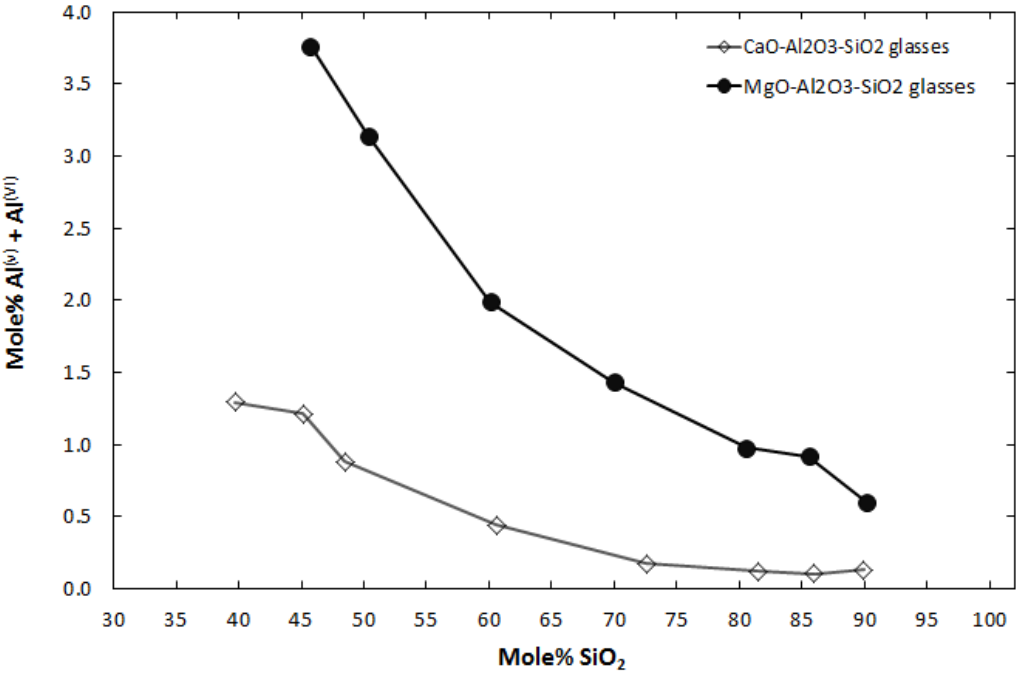

Figure 5.7: Mole% $Al^{(V)}$ + $Al^{(VI)}$ as a function of mole% SiO_2 in CAS and MAS glasses

The hardness of MAS glasses exhibits a similar trend to that of CAS glasses however, there are noticeable differences between the two as can be seen in Figure 5.1. The MAS glasses have a higher hardness overall as compared to CAS glasses. The overall increase in hardness for MAS glasses with < 70 mole% SiO_2 over CAS glasses with < 85 mole% SiO_2 is related to the increased amount of higher coordinated Al, as shown in Figure 5.7, along with the stronger Mg-NBO bond.[5-7] Higher coordinated Al is able to prevent shear deformation by creating more network connections and preventing the atoms which can easily shear from moving.[3-4] Based upon ^{27}Al 3Q MAS NMR data collected for the MAS and CAS glasses in this study and what was previously known about the structures of similar glasses, the species

which must be facilitating shear in both types of glasses are NBO. As the higher coordinated Al decreases in both MAS and CAS glass systems, shown in Figure 5.7, with increasing SiO_2 mole% the NBO become less restricted and can begin to move by breaking and reforming bonds resulting in the decrease in hardness with increase in mole% SiO_2 up to 70 mole% SiO_2 for MAS glasses and 85 mole% SiO_2 for CAS glasses as shown in Figure 5.1. This is shown more clearly in Figure 5.8 below, which shows a plot of hardness and mole% $Al^{(V)}$ and $Al^{(VI)}$ as a function of mole% SiO_2. From this plot one can see that as the mole% $Al^{(V)}$ and $Al^{(VI)}$ decreases so too does the hardness. Also Figure 5.9 shows how the hardness increases linearly with the mole fraction of $Al^{(V)}$ + $Al^{(VI)}$ in the tectosilicate CAS and MAS glasses.

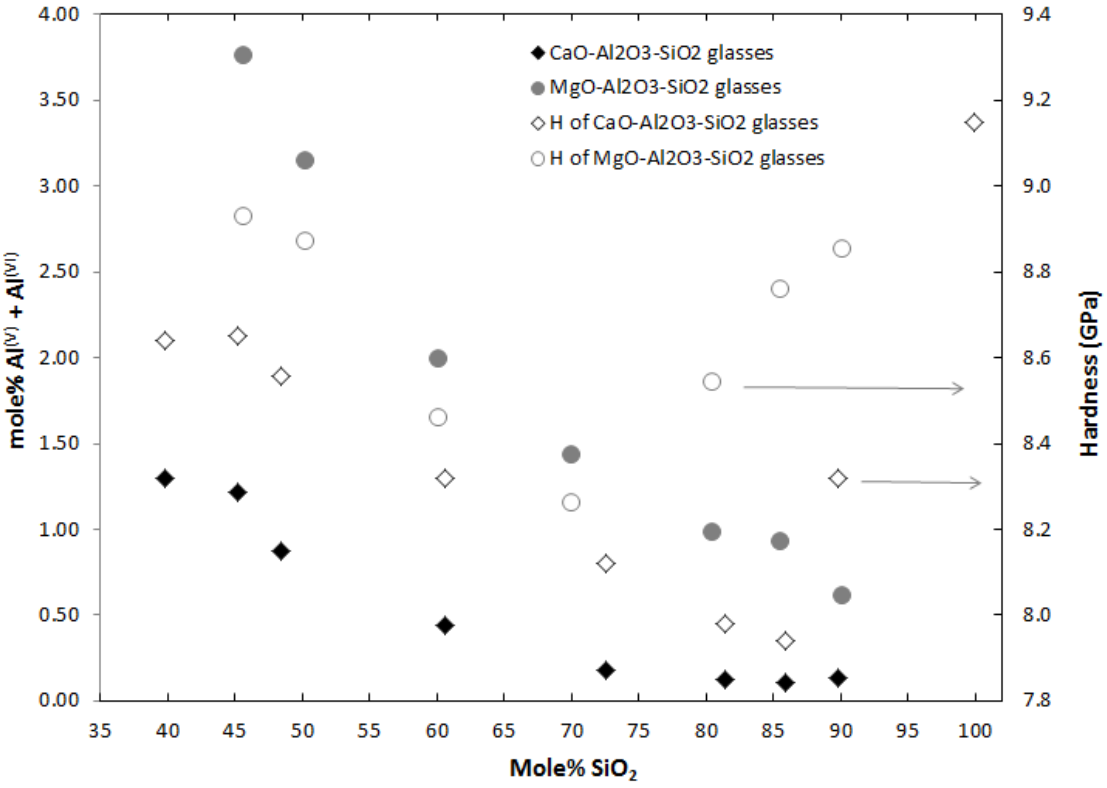

Figure 5.8: Mole% $Al^{(V)}$ + $Al^{(VI)}$ and hardness as a function of mole% SiO_2 in tectosilicate CAS and MAS glasses.

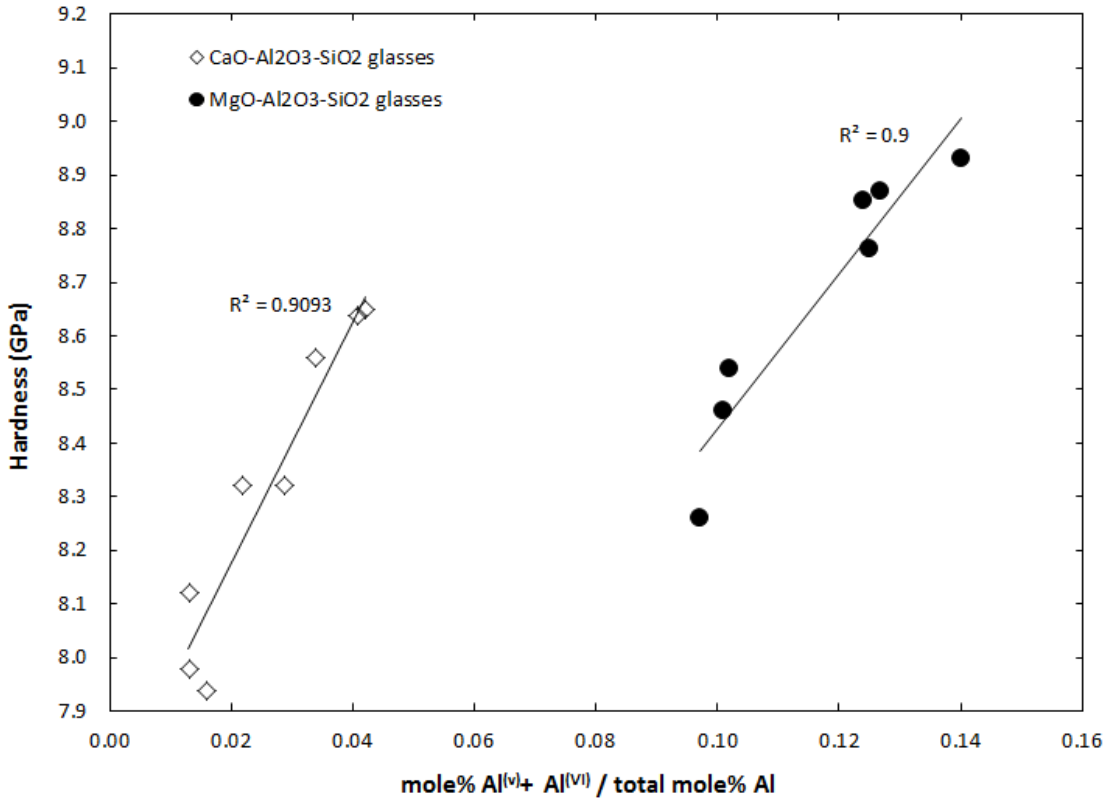

Figure 5.9: Hardness as a function of mole fraction $Al^{(V)} + Al^{(VI)}$ in tectosilicate CAS and MAS glasses.

MAS glasses along with having a larger amount of higher coordinated Al in their structures also have the added benefit of the stronger Mg-NBO bond over the Ca-NBO bond. This increased bond strength makes it more difficult to shear, so even though the NBO are becoming less entangled in the structure by the higher coordinated Al they still cannot break and reform as easily as Ca-NBO bonds because of the higher bond strength between Mg and the NBO. Hence, the increase in H of MAS glasses with up to 70 mole% SiO_2 over CAS glasses with up to 85 mole% SiO_2 is related to both the increase in higher coordinated Al and the stronger Mg-NBO bond.

The shift in the hardness minimum with mole% SiO_2 to lower mole% SiO_2 for MAS glasses over CAS glasses, shown in Figure 5.1, is a result of 2 factors. First the MAS glasses have a more open structure as compared to CAS glasses, which is observed in density data shown in Table 5.1. The smaller Mg atom takes up less space in the glass structure, therefore, leaving more open volume for densification. This results in a decrease in the energy required to densify MAS glasses over CAS glasses. Secondly, the increase in the resistance to shear in MAS glasses will also play a role in causing the shift from shear to densification. It is the combination of these two processes which causes the shift from shear deformation to densification deformation to occur at lower mole% SiO_2 in MAS glasses over CAS glasses.

5.5. Summary and Conclusions

MAS glasses were found to exhibit the same behavior as CAS glasses in indentation modulus. The indentation modulus for both series of glasses increases with increasing density. In MAS glasses, however the indentation modulus is at larger values than it is for CAS glasses. This is related to the higher density of bonds per unit volume in MAS glasses over CAS glasses. MAS glasses have a larger amount of higher coordinated Al species than CAS glasses therefore increasing the density of bonds per unit volume in MAS glasses over CAS glasses.

MAS glasses exhibit the same non-monotonic behavior in hardness with increasing SiO_2 content that is observed in CAS glasses. The two main differences between the hardness behavior for each glass system is an overall increase in hardness with MAS glasses over CAS glasses and a shift of the minimum in hardness to lower

SiO_2 mole% for MAS glasses. The minimum was shown in both glass systems to be a result of a change in the deformation mechanism from shear to densification.

The overall increase in hardness for MAS glasses over CAS glasses is shown to be related to the stronger Mg-NBO bond along with the presence of substantially more higher coordinated Al in the glass structure. The higher coordinated Al ties up the structure preventing NBO from being involved in shear. Also the increased strength of the Mg-NBO bond over the Ca-NBO bond increases the difficulty of shear even when the NBO are available to move.

The shift from shear to densification at lower SiO_2 content in the MAS glasses is shown to be a combination of two effects. First, the increase in difficulty for the glass to shear by stronger Mg-NBO bonds and an increased amount of higher coordinated Al. Secondly, the more open glass structure in MAS glasses as a result of the smaller Mg atom allows for easier densification. It is both the increased difficulty in shearing along with the easier densification which results in the shift from shear to densification at lower SiO_2 mole% for MAS glasses over CAS glasses.

In conclusion, this study on MAS glasses was able to show further evidence for the unit deformation mechanism of NBO movement by breaking and reforming bonds with the modifying ions, which results in shear deformation. We also provided further evidence that the minimum observed in hardness as a function of mole% SiO_2 is in fact a transition from shear to densification which is controlled mainly by the openness of the glass structure and the difficulty of the shearing process.

REFERENCES

1. C. Hermansen, J. Matsuoka, S. Yoshida, H. Yamazaki, Y. Kato, Y.Z. Yue. "Densification and Plastic Deformation under Microindentation in Silicate Glasses and the Relation to Hardness and Crack Resistance." *J. of Non-Cryst. Sol.* **364**, 40-43 (2013).

2. P. Sellappan, T. Rouxel, F. Celarie, E. Becker, P. Houizot, R. Conradt, "Composition Dependence of Indentation Deformation and Indentation Cracking in Glass." *Acta Materialia* **61**, 5949-5965 (2013).

3. L.A. Lamberson, R.E. Youngman, S.P. Baker, "Plastic Deformation Mechanisms and the Hardness of CaO-Al_2O_3-SiO_2 Glasses." *In process*

4. S. Iftekhar, B. Pahari, K. Okhotnikov, A. Jaworski, B. Stevensson, J. Grins, M. Eden. "Properties and Structures of RE_2O_3-Al_2O_3-SiO_2 (RE = Y, Lu) Glasses Probed by Molecular Dynamics Simulations and Solid State NMR: The Roles of Aluminum and Rare-Earth Ions for Dictating the Microhardness." *J. Phys. Chem. C*, **116,** 18394-18406 (2012).

5. M. Guignard, L. Cormier,"Environments of Mg and Al in MgO-Al_2O_3-SiO_2 glasses: A study Coupling Neutron and X-Ray Diffraction and Reverse Monte Carlo Modeling." *Chem. Geo.*, **256**, 111-118 (2008).

6. S. Kroeker, J. F. Stebbins. "Magnesium Coordination Environment in Glasses and Minerals: New Insight From High-field Magnesium-25 MAS-NMR." *American Minerologist*, **85**, 1459-1464 (2000).

7. L. M. Thompson, J. F. Stebbins."Non-Stoichiometric Non-Bridging Oxygens and five-Coordinated Aluminum in Alkaline Earth Aluminosilicate Glasses: Effect of Modifier Cation Size." *J. Non-Cryst. Solids*, **358**, 1783-1789 (2012).

8. A. Arora, D.B. Marshall and B.R. Lawn, "Indentation, Deformation/Fracture of Normal and Anomalous Glasses." *J. Non-Cryst. Solids*, **31,** [3] 415-428 (1979).

9. W.C. Oliver and G.M. Pharr, "Measurement of Hardness and Elastic Modulus by Instrumented Indentation: Advances in Understanding and Refinements to Methodology." *J. Mater. Res.,* **19,** [1] 3-20 (2004).

10. W.C. Oliver and G.M. Pharr, "An Improved Technique for Determining Hardness and Elastic Modulus Using Load and Displacement Sensing Indentation Experiments." *J. Mater. Res.,* **7,** [6] 1564-1583 (1992).

11. D. Massiot, F. Fayon, M. Capron, I. King, S. Le Calve, B. Alonso, J. O. Durand, B. Bujoli, Z. Gan, G. Hoatson, *Magn. Reson. Chem.* **40**, 70 (2002).

CHAPTER 6

EFFECT OF GA REPLACEMENT FOR AL ON HARDNESS OF ALUMINOSILICATE GLASSES

6.1. Abstract

Among the most widely used commercial glasses are aluminosilicates. Calcium aluminosilicates (CAS) glasses are the most significant due to their great mechanical properties, optical properties, and chemical durability. However, much still needs to be understood about their plastic deformation mechanisms. Gallosilicate glasses have been thought to be easier to melt analogs of aluminosilicate glasses, exhibiting similar structures and property trends. This paper looks at a series of tectosilicate $(CaO + Ga_2O_3)_{1-x} + (SiO_2)_x$ (CGS) glasses and compares the results of hardness and indentation modulus to the composition and structure as determined by ICP and NMR. These results are compared with previously reported data on tectosilicate $(CaO + Ca_2O_3)_{1-x} + (SiO_2)_x$ (CAS) and $(MgO + Al_2O_3)_{1-x} + (SiO_2)_x$ (MAS) glasses. The indentation modulus for all three series of glasses was found to increase with increasing density. The hardness of CGS glasses was found to behave non-monotonically with SiO_2 content just like was reported previously for tectosilicate CAS and MAS glasses. However, the minimum in hardness for CGS glasses was found to be unrelated to the transformation from shear to densification.

6.2. Introduction

Aluminosilicate glasses are among the most widely used commercial glasses. Of the aluminosilicate glasses, calcium aluminosilicate (CAS), are the most significant as

they have excellent chemical durability, mechanical and optical properties. Even with their high importance the exact mechanisms of shear and densification deformation are poorly understood. This is surprising considering the importance of increased hardness and scratch resistance needed for glasses used in today's technologies such as touch screens and hand held devices.

Two previously reported studies on CAS and magnesium aluminosilicate (MAS) glasses showed a non-monotonic behavior in hardness with increasing mole% SiO_2.[1-2] It was shown that this non-monotonic behavior in hardness with increasing mole% SiO_2 is a result of a transformation from shear deformation to densification deformation.[1] Silicate glasses containing a substantial amount of modifying ions, glasses with less than 80 mole% SiO_2, are considered to be "normal" glasses and will deform by mainly a shear mechanism.[3] On the other hand, glasses with greater than 80 mole% SiO_2 are considered "anomalous" and will deform mainly by a densification mechanism.[3] It was shown in the earlier studies on CAS and MAS glasses, that by changing the modifying ion, one can impact the glass structure enough to move the transition point from shear to densification to a lower or higher mole% SiO_2 content.[2] These studies on CAS and MAS glasses also showed that the predominant mode of shear deformation in CAS and MAS glasses to be the breaking and reforming of bonds with non-bridging oxygen (NBO).[1-2] The other key factor involved in increasing the difficulty of shear deformation in these previous CAS and MAS glass systems is the presence of higher-coordinated Al species. In the CAS, MAS and rare earth aluminosilicate glass systems the presence of higher coordinated Al has resulted in an increase in hardness.[1-2, 4] The increase in hardness is believed to be a result of the higher coordinated Al being able to tie up the NBO or other shearable species, preventing them from either breaking or reforming with new neighbors.[1-2, 4]

In order to further understand the role that Al plays, specifically higher coordinated Al, we can swap out the Al species from the CAS system and replace it with Ga. It has been found in crystals that Ga and Al ions have the same oxidation state and typically the same coordination number.[5] However, Al and Ga differ in their field strengths, with Ga having a lower field strength than Al due to the larger mass and diameter of the Ga atom compared to Al atom.[5] The lower field strength of Ga results in weaker Ga-O bonds, which is evidenced in the decrease in melting temperature for alkaline-earth gallosilicate glasses over that of alkaline-earth aluminosilicate glasses.[5] Despite the weaker Ga-O bonds, property trends in things such as density, refractive index, thermal expansion, viscosity and glass transition temperature are similar to those of aluminosilicates.[6]

Structurally, NMR studies using ^{17}O have shown that gallium ions mostly occupy tetrahedral sites just as aluminum ions do.[6] However, silicate glasses containing Ga were shown to have a higher quantity of NBO over aluminosilicate systems[6-7] along with a larger quantity of higher coordinated Ga, up to 7% over what is found in aluminosilicate glasses.[6] These structural differences between gallosilicate and aluminosilicate glasses are most likely related to two things. First, the electronegativity differences of Al (1.61) being smaller than that of Ga (1.81) and Si (1.90) which are similar, resulting in longer Ga-O bond distances compared to Al-O bond distances. Secondly, the difference in cation radius of Ga^{3+} compared to Al^{3+} (0.047 vs. 0.039 nm) when in tetrahedral coordination leads to the greater tendency of Ga to shift to higher coordination numbers.[6] The longer bond distance of Ga-O over Al-O may also lead to more Ga-O-Ga linkages in gallosilicate glasses over Al-O-Al linkages in aluminosilicate glasses due to the reduction in cation/cation repulsion and reduction of steric hindrance to charge balancing by multiple alkali or alkaline earth

cations.[6] The increase in Ga-O-Ga linkages will lead to a more disordered glass as compared to aluminosilicate glasses.

All of these structural differences between Ga containing silicate glasses and Al containing silicate glasses should result in a change in the glass hardness resulting from a change in plastic deformation mechanisms in the two types of glasses. The weaker Ga-O bond over Al-O bond could result in the shearing mechanisms in calcium gallosilicate glasses (CGS) to not only be from NBO but also from Ga-O bonds breaking and reforming. However, the increased amount of higher coordinated Ga over Al could result in a more connected network which prevents shear. The only published hardness data for CGS glasses by Angel, et al. showed a decrease in hardness with increase in SiO_2 mole% in glasses containing up to 15 mole% Ga_2O_3 and up to 65 mole% SiO_2 with the remainder of the compositions being made up of CaO.[8] They hypothesized that the higher coordinated Ga resulted in higher hardness despite Si-O having a higher bond strength.[8] Also, the longer Ga-O bond could create a more open structure; however the larger size of Ga vs. Al could negate the effect of the longer bond length.

This present paper looks at what the effect of substituting Ga for Al in tectosilicate CAS glasses will have on the hardness and plastic deformation mechanisms of these glasses. The intent of this paper is to further increase understanding of the unit deformation mechanisms involved in shear deformation and densification deformation of RO-aluminosilicate glasses by looking at CGS glasses. This will be accomplished through the use of nanoindentation, to determine hardness and indentation modulus, and ^{71}Ga MAS NMR to obtain structural information on the particular glasses used in this study. More specifically, we hope to add more evidence to the previously reported findings of increased Al or Ga higher coordinated species in the glass structure results in strengthening of glasses by inhibiting shear

deformation.[1-2, 4, 8] We would also like to determine if shear can be made easier by having more weakly bonded atoms other than NBO in the glass structure. Lastly, we would like to further understand what structural aspects of the glass control the transformation from shear to densification deformation. Increased knowledge in these three areas would aid in the development of improved models for predicting glass hardness, which will ultimately aid in the development of glasses with improved mechanical properties such as hardness and scratch resistance.

6.3. Experiments and Results

6.3.1. Specimen Preparation

Glasses were made with 99.99% purity SiO_2, 99.99% purity Ga_2O_3 and 99.9% purity $CaCO_3$ powders. The glasses were melted in Pt. crucibles at 1650°C for 15 hrs. The melts were poured onto a metal table and then rolled with a metal rolling pin to rapidly cool the glass and crush it into small pieces. The glass remaining in the crucibles was knocked out and added to the crushed glass and re-melted. This method is adopted to aid in mixing of the glass ensuring good homogeneity in the final glass patty. The glasses were annealed at 700°C for 2 hrs to reduce internal stresses generated during pouring and cooling. The glasses were inspected after annealing in a polarized scope to ensure good homogeneity and absence of phase separation. The glasses containing SiO_2 of greater than 80 mole% contained small bubbles of about 0.1 mm in size. However, there were still areas of the glass samples of up to 6 mm x 6 mm which did not contain any bubbles. The bubbles are randomly distributed throughout the glass so large areas without bubbles are easily located.

Glass samples were cut on a precision diamond saw and then mounted on a plate with Unibond 5.0 Adhesive wax. The samples were then lapped with 22 µm alumina powder on a steel plate. The samples were then polished on a silk pad with 1µm diamond mixed with Hyprez polishing oil, which is petroleum naphtha CAS NO. 64742-48-9. After polishing the samples were removed from mount plate and cleaned with Opticlear, which is d-limonene with chemical formula $C_{10}H_{16}$ and CAS NO. 5989-27-5, to remove wax and then with IPA to remove Opticlear residue. The samples thickness was checked with a depth micrometer and the surface roughness was measured using an optical surface profilometer, ensuring the sample meets the specification of roughness and thickness variations less than 10 nm for testing. The final sample dimensions are 10 mm × 10 mm × 1 mm.

After cutting and polishing the samples were annealed at their measured annealing temperature, as determined by beam bending viscometry, for 2 hrs. The annealing removes any internal stresses which were generated during the cutting and polishing process. The annealing temperatures for each of the glass compositions is shown in Table 1. After annealing the samples are stored in a desiccator to prevent water absorption at the surface of the sample until testing is performed.

6.3.2. Compositional and Density

The composition of glasses studied in this experiment were measured by Inductively Coupled Plasma-Optical Emission Spectrometry (ICP-OES) chemical analysis. The measured glass compositions and accuracy of each measurement are shown in Table

6.1. The density of the glass samples was measured by buoyancy in water with an estimated error of ±2%. The density data is also provided in Table 6.1.

Table 6.1: glass compositions as measured by ICP-OES along with annealing point and density for CAS, MAS and CGS tectosilicate glasses.

Glass	Measured composition in mole%					Anneal Pt. (°C)	Density g/cm^3
	SiO_2	Al_2O_3	MgO	CaO	Ga_2O_3		
1	39.75 ± 0.4	31.56 ± 0.4	0.00	28.69 ± 0.2	0.00	850	2.79
2	45.14 ± 0.4	28.97 ± 0.4	0.00	25.89 ± 0.2	0.00	853	2.76
3	48.51 ± 0.4	25.89 ± 0.4	0.00	25.61 ± 0.2	0.00	853	2.72
4	60.61 ± 0.7	20.09 ± 0.3	0.00	19.30 ± 0.2	0.00	860	2.68
5	72.57 ± 0.7	13.49 ± 0.2	0.00	13.95 ± 0.1	0.00	866	2.67
6	81.51 ± 0.8	9.23 ± 0.1	0.00	9.26 ± 0.08	0.00	882	2.51
7	85.98 ± 0.8	6.63 ± 0.1	0.00	7.40 ± 0.07	0.00	883	2.35
8	89.93 ± 0.9	4.56 ± 0.07	0.00	5.51 ± 0.04	0.00	900	2.30
9	100.00	0.00	0.00	0.00	0.00	1140	2.21
10	45.69 ± 0.4	26.89 ± 0.4	27.42 ± 0.2	0.00	0.00	801	2.72
11	50.34 ± 0.4	24.76 ± 0.4	24.9 ± 0.2	0.00	0.00	804	2.68
12	60.11 ± 0.4	19.73 ± 0.4	20.16 ± 0.2	0.00	0.00	816	2.57
13	69.97 ± 0.7	14.81 ± 0.3	15.22 ± 0.1	0.00	0.00	Not able to obtain	2.48
14	80.56 ± 0.8	9.62 ± 0.2	9.82 ± 0.06	0.00	0.00	Not able to obtain	2.36
15	85.53	7.38	7.09	0.00	0.00	965	2.33

	± 0.8	± 0.1	± 0.05				
16	90.12 ± 0.9	4.87 ± 0.08	5.01 ± 0.03	0.00	0.00	996	2.28
17	35.25 ± 0.2	0.00	0.00	32.39 ± 0.2	32.35 ± 0.6	728	3.81
18	40.00 ± 0.3	0.00	0.00	29.8 ± 0.2	29.67 ± 0.6	735	3.72
19	45.5 ± 0.3	0.00	0.00	27.4 ± 0.2	27.11 ± 0.5	743	3.62
20	49.69 ± 0.3	0.00	0.00	25.23 ± 0.2	25.08 ± 0.5	749	3.51
21	60.21 ± 0.4	0.00	0.00	20.03 ± 0.1	19.75 ± 0.4	763	3.27
22	71.22 ± 0.7	0.00	0.00	14.19 ± 0.1	14.59 ± 0.2	770	3.02
23	80.13 ± 0.8	0.00	0.00	9.91 ± 0.08	9.96 ± 0.2	782	2.70

6.3.3. Mechanical Properties

A Hysitron TriboIndenter equipped with a Berkovich diamond tip was used. The indenter was calibrated using a fused silica sample provided by the manufacturer before each test. The instrument compliance, indenter geometry and thermal drift were all calibrated using the Oliver & Pharr method.[9-10]

6.3.3.1. Hardness and Modulus

The hardness and indentation modulus of each of the glasses was measured using a maximum load during nanoindentation of 10 mN which produces a maximum depth of about 200 nm. The ramp rate used for these measurements was 1 mN/s and then the load was held at 10 mN for 10 sec. followed by a ramp down at the same rate. A 5 X 5

array of indents were performed on each sample with 10 μm between each indentation. The hardness and indentation modulus were calculated for each indentation using the Oliver and Pharr method[9-10] Figures 6.1 and 6.2 show hardness and indentation modulus as a function of mole% SiO_2 respectively.

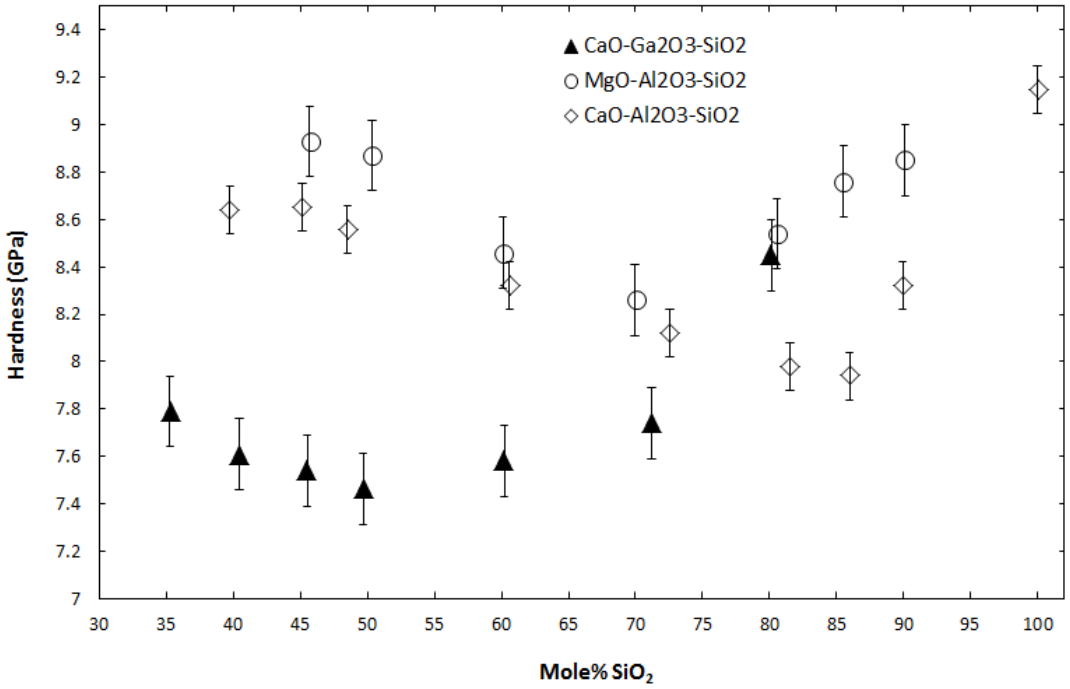

Figure 6.1: Hardness as a function of mole% SiO_2 for tectosilicate CAS, MAS and CGS glasses.

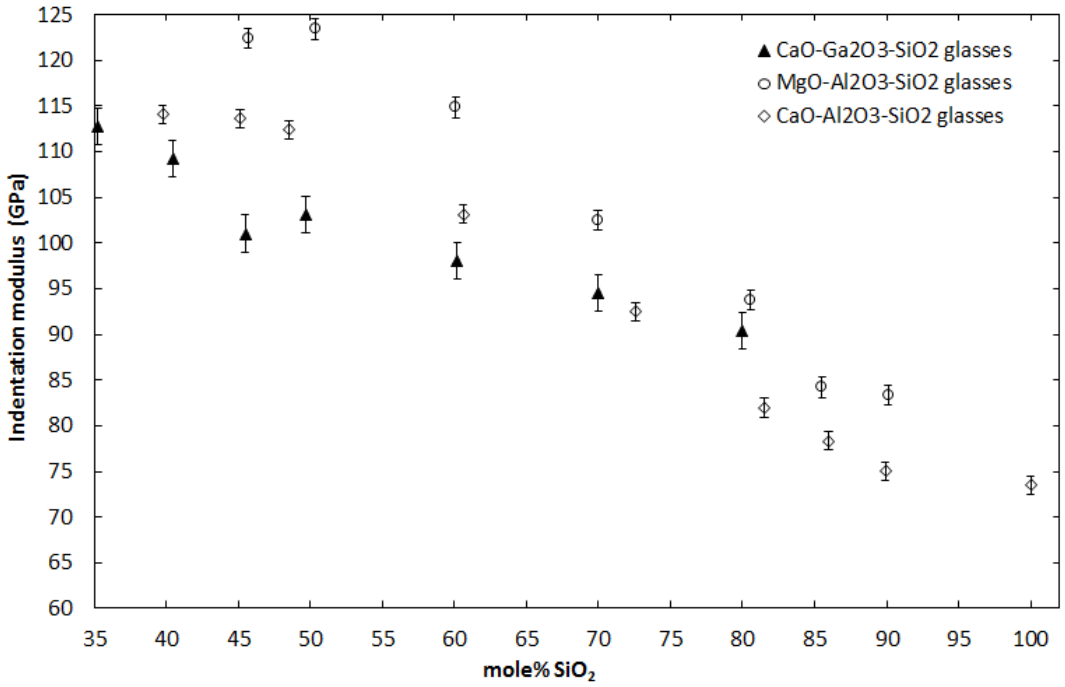

Figure 6.2: Indentation modulus as a function of mole% SiO_2 for tectosilicate CAS, MAS, and CGS glasses.

From Figure 6.1, one can see that the hardness exhibits a non-monotonic behavior with increasing SiO_2 content for the tectosilicate CAS, MAS and CGS glasses. At roughly 85 mole% SiO_2 the hardness reaches a minimum in the CAS glasses however, for the MAS containing glasses the minimum is at 70 mole% SiO_2 and for CGS glasses the minimum is at an even lower silica content of between 50 and 60 mole%. The hardness values for the MAS glasses are all higher than the CAS glasses while the CGS glasses have lower hardness values than both CAS and MAS glasses until about 80 mole% SiO_2 where the hardness value becomes comparable to that of the equivalent MAS glass. In contrast, the indentation modulus, as seen in Figure 6.2, decreases with increasing SiO_2 content for all three, CAS, MAS and CGS, series of glasses.

6.3.4. Ga Speciation

^{71}Ga (I=3/2; 39.6% natural abundance) magic angle spinning (MAS) NMR spectra were collected at 16.4 T (213.40 MHz resonance frequency) using a 1.6 mm MAS NMR probe with sample spinning of 35 kHz. Powdered glasses were packed into 1.6 mm outer diameter zirconia rotors. Data were acquired using very short radio-frequency pulses of 0.6 μs, corresponding to a $\pi/12$ tip angle. Between 22,000 and 230,000 scans were co-added for each sample to obtain sufficient signal to noise, and the recycle delay was 1s. Spectra were processed without apodization and plotted against the standard shift reference (aqueous gallium nitrate) at 0 ppm.

Processed MAS NMR spectra were deconvoluted using DMFit[11], incorporating a Czjzek lineshape for the $Ga^{(IV)}$ peak and a small Gaussian peak to account for the presence of $Ga^{(V)}$. Due to the large quadrupole moment of ^{71}Ga, these MAS NMR lineshapes exhibit significant 2nd order quadrupolar coupling and substantial overlap between the resonances. The data in Figure 6.3 clearly show a shoulder due to some amount of $Ga^{(V)}$, and there is no evidence for $Ga^{(VI)}$ in any of these glasses. The mole fraction of $Ga^{(V)}$, calculated from the MAS NMR data, as a function of mole% SiO_2 is shown in Figure 6.4. The data in Figure 6.4 shows an increase in $Ga^{(V)}$ up to 70 mole% SiO_2, where the maximum is, and then the amount of $Ga^{(V)}$ decreases in the glass.

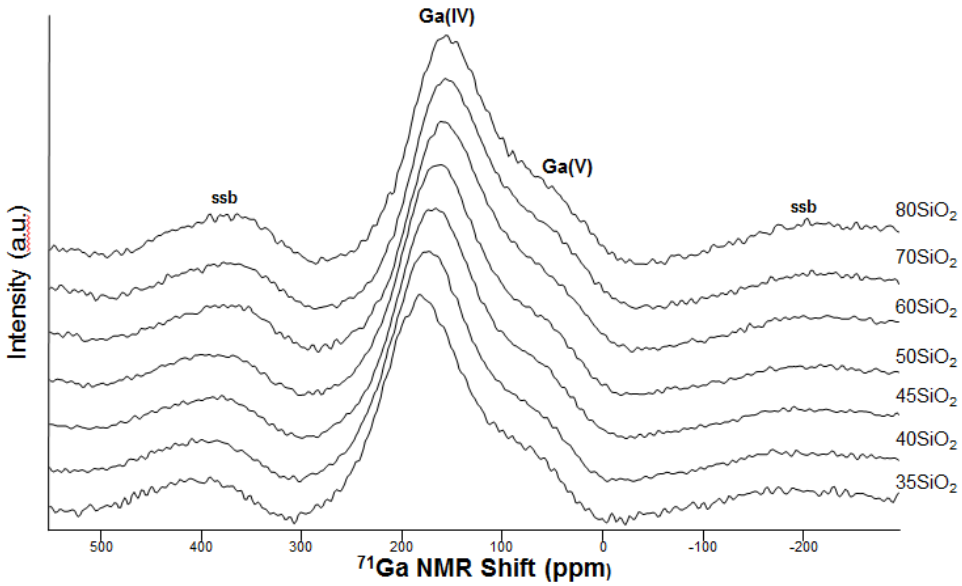

Figure 6.3: ^{71}Ga MAS NMR isotropic projections plot showing the chemical shift and peak shape change of the $Ga^{(IV),}$ and $Ga^{(V)}$ peaks in tectosilicate $CaO\text{-}Ga_2O_3\text{-}SiO_2$ glasses. (ssb stands for spinning side band)

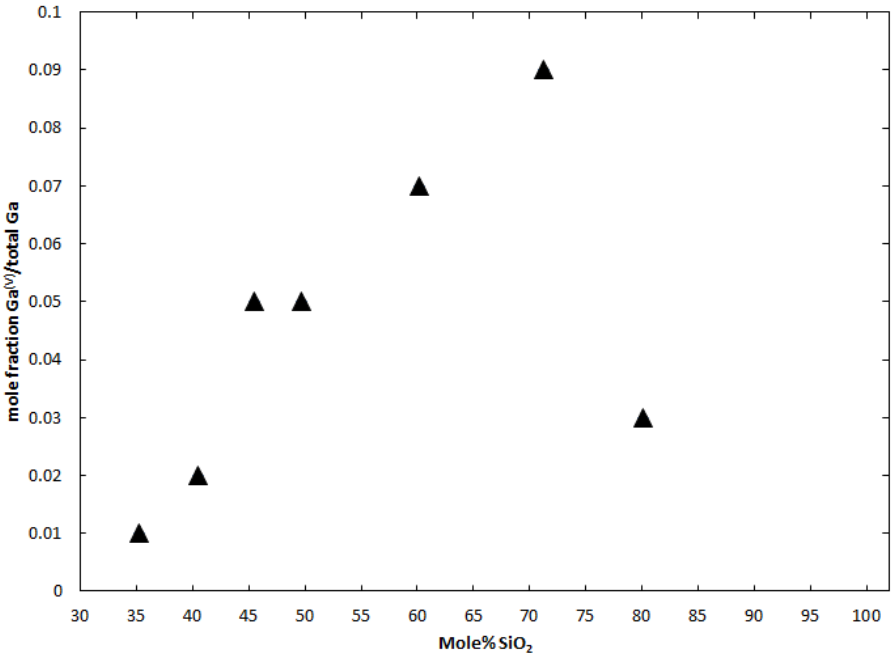

Figure 6.4: mole fraction $Ga^{(V)}$, as determined from MAS NMR, as a function of mole% SiO_2 in tectosilicate $CaO\text{-}Ga_2O_3\text{-}SiO_2$ glasses.

The chemical shift of $Ga^{(IV)}$ as compared to that of $Ca^{(IV)}$ as a function of mole% SiO_2, in the tectosilicate $CaO\text{-}Ga_2O_3\text{-}SiO_2$ and $CaO\text{-}Al_2O_3\text{-}SiO_2$ glasses respectively, is

shown in Figure 6.5. As can be seen in Figure 6.5 the chemical shift of $Al^{(IV)}$ is slightly more linear than that of $Ga^{(IV)}$. This indicates that the mixing of $Al^{(IV)}$ and $Si^{(IV)}$ tetrahedral is more uniform than that of $Ga^{(IV)}$ and $Si^{(IV)}$. In other words, there is a higher frequency of Ga-O-Ga linkages as compared to Al-O-Al linkages in the respective glasses.

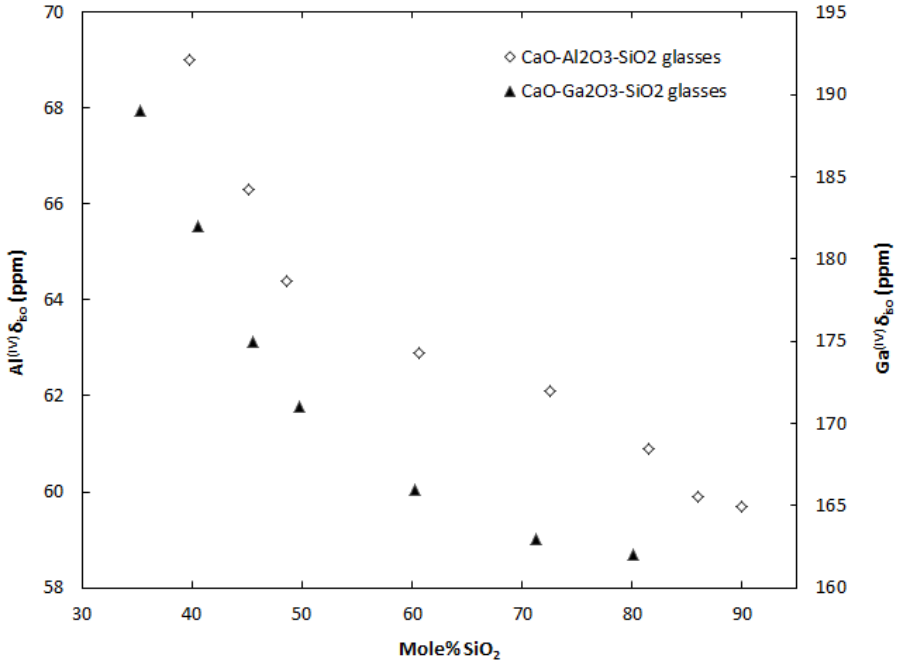

Figure 6.5: $Al^{(IV)}$ and $Ga^{(IV)}$ chemical shift (δ_{iso}) as a function of mole% SiO_2 in tectosilicate CaO-Al_2O_3-SiO_2 and CaO-Ga_2O_3-SiO_2 glasses.

6.4. Discussion

Gallosilicate glasses show a similar behavior of decreasing indentation modulus with increasing silica content as shown in Figure 6.2. Figure 6.6 also shows that the indentation modulus of the gallosilicate glasses increases with increasing density as it does for the aluminoslicate glasses. However, from Figure 6.6 it can be seen that the increase in indentation modulus for the gallosilicate glasses is much more gradual with density as compared to the aluminosilicate glasses.

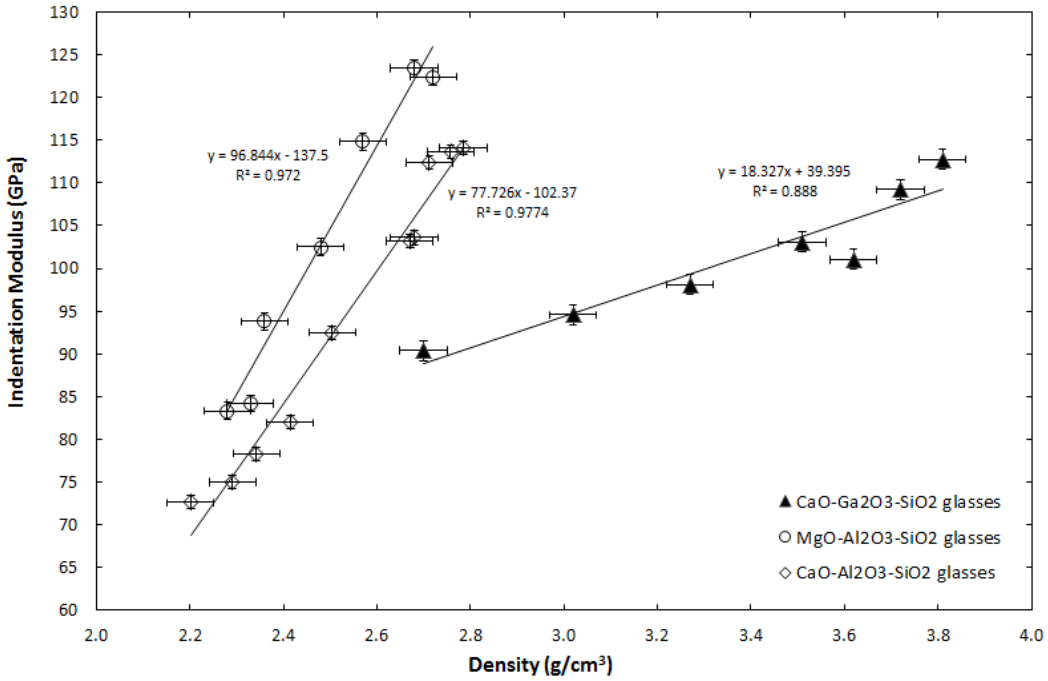

Figure 6.6. Indentation modulus as a function of density for tectosilicate $CaAl_2O_4SiO_2$, $MgAl_2O_4SiO_2$, and $CaGa_2O_4SiO_2$ glasses.

This more gradual increase in modulus with density is related to the heavier Ga atom as compared to Al atom. The heavier atom will result in larger changes in density while the amount of constraints per unit volume does not change as much because there is less higher coordinated Gain the glass structure as compared to higher coordinated Al in the structure of the other glasses. The constraints per volume was calculated using the same method as was previously used for CaO and MgO containing Al_2O_3-SiO_2 glasses reported previously by Lamberson et. al.[1-2] This results in the gallium containing glasses having fewer constraints per unit volume compared to the aluminosilicate glasses studied previously, as is shown in Figure 6.7.

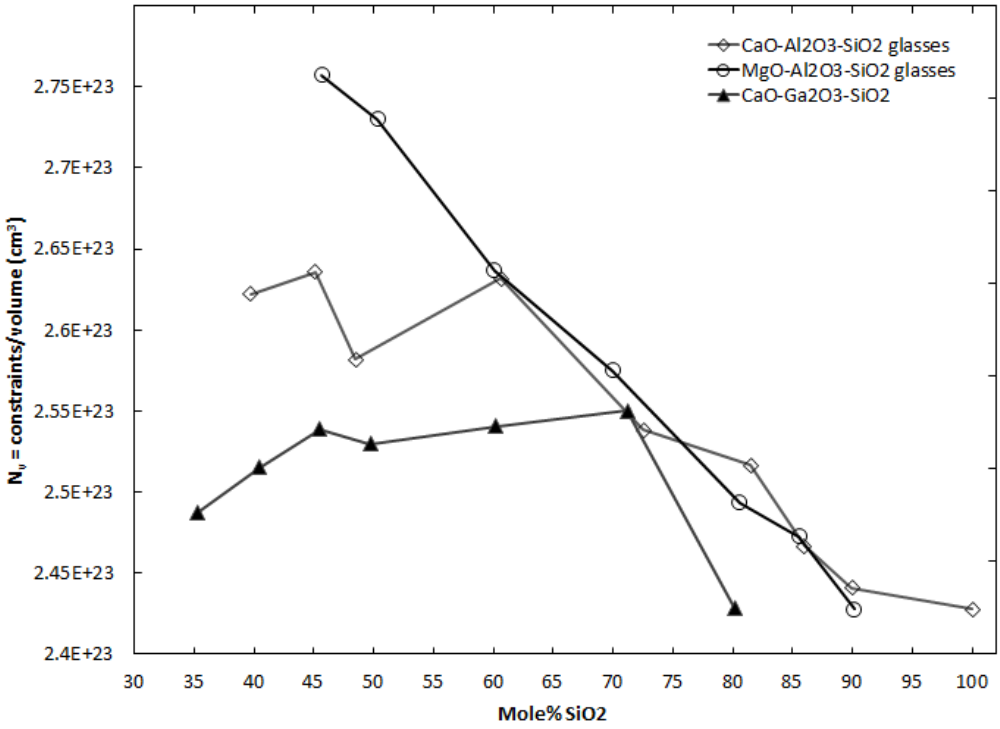

Figure 6.7: Constraints per unit volume as a function of Mole% SiO_2 for tectosilicate $CaO\text{-}Al_2O_3\text{-}SiO_2$, $MgO\text{-}Al_2O_3\text{-}SiO_2$, and $CaO\text{-}Ga_2O_3\text{-}SiO_2$ glasses.

Even the presence of a larger quantity of $Ga^{(V)}$ in calcium-gallosilicate glasses over $Al^{(V)}$ and $Al^{(VI)}$ found in the comparable calcium-alumniosilicate glasses, as is shown in Figure 6.8, is still not enough to overcome the effect of the longer Ga-O bond length. This is evidenced in Figure 6.8 by the fact that the gallosilicate glasses with greater than 50 mole% SiO_2 have a larger mole% of $Ga^{(V)}$ present in their structure than the comparable calcium-aluminosilicate glasses have $Al^{(V)}$ and $Al^{(VI)}$ in their structure. However, as can be observed in Figure 6.7, the gallosilicate glasses still have fewer constraints per unit volume than the aluminosilicate glasses do with the exception of the glass at about 70 mole% SiO_2. The gallosilicate glass at 70 mole% SiO_2 also has a slightly higher indentation modulus as compared to the calcium-aluminosilicate counterpart, as is shown in Figure 6.2, which provides further evidence that indentation modulus is very closely linked to the constraints per unit volume of the material.

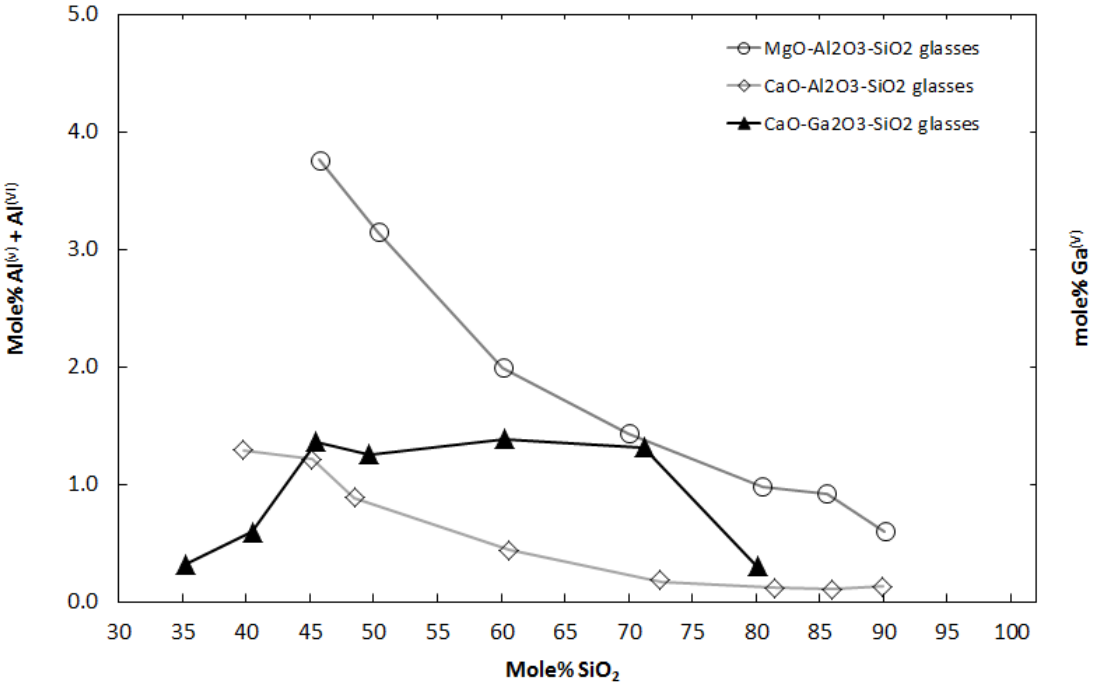

Figure 6.8. Mole% $Al^{(V)}$ + $Al^{(VI)}$ or mole% $Ga^{(V)}$ as a function of mole% SiO_2 in tectosilicate CaO-Al_2O_3-SiO_2, MgO-Al_2O_3-SiO_2, and CaO-Ga_2O_3-SiO_2 glasses.

The hardness of the Ga containing glasses exhibits a similar trend as does the hardness for the Ca and Mg aluminosilicate glasses, as is shown in Figure 6.1. The Ga containing glasses however, have a lower hardness as compared to the aluminosilicate glasses until 80 mole% SiO_2 is reached in the Ga containing glasses and then the hardness of this glass exceeds that of the equivalent calcium-aluminosilicate glass and is about equal to that of the equivalent magnesium-aluminosilicate glass. The lower hardness of gallosilicate glasses over aluminosilicate glasses is a result of the weaker Ga-O bond compared to the Al-O bond.

The other major difference between the curve for Ga containing glasses and Al containing glasses shown in Figure 6.1 is the position of the minimum in hardness. The minimum in hardness for the gallosilicate glasses is at 50 mole% SiO_2 which is at

a lower SiO_2 mole% than both Ca and Mg. Unlike in Ca and Mg where the minimum in hardness as a function of mole% SiO_2 was shown to be related to the transition from shear deformation to densification deformation,[1-2] the minimum in hardness for the Ga containing glasses is not believed to be related to this transition.

In order to understand what the minimum in hardness as a function of mole% SiO_2 for the Ga containing glasses is a result of, we must first understand what the structure of our Ga glasses looks like and how that might impact the hardness data. It is known that Ga has a higher electronegativity as compared to Al, 1.81 vs. 1.61 respectively. The higher electronegativity of Ga results in a longer Ga-O bond as compared to an Al-O bond.[6] The longer bond distance of Ga-O over Al-O results in a reduction of the cation-cation repulsion and a reduction of steric hinderance to charge balancing by multiple alkaline-earth atoms, which leads to more Ga-O-Ga linkages and a more disordered glass.[6] Figure 6.3 is ^{71}Ga MAS NMR spectra for all of the tectosilicate $CaGa_2O_4SiO_2$ glasses in this study and one can clearly see the chemical shift of the $Ga^{(IV)}$ peak as we move from low SiO_2 to high SiO_2 containing glasses. Figure 6.5 is a plot of the chemical shift of the $Ga^{(IV)}$ and $Al^{(IV)}$ peak as a function of mole% SiO_2 in the Ca containing glasses. As one can see the chemical shift of the $Ga^{(IV)}$ peak has a steeper slope than the chemical shift of the $Al^{(IV)}$ peak indicating that the Ga containing glasses do in fact have more Ga-O-Ga linkages than the Al glasses have Al-O-Al linkages as move towards glasses with lower mole% SiO_2. The increase in Ga-O-Ga linkages will result in a more disordered glass,[6] and potentially lead to weaker bonds which would aid in making shear easier.

Another factor is the cation radius of Ga^{+3}, 0.047nm, compared to the radius of Al^{+3},0.039nm, which results in Ga shifting to higher coordination numbers[6], as is shown in Figure 6.8. In Figure 6.8 it is clear from NMR results that the mole% $Ga^{(V)}$ in tectosilicate $CaGa_2O_4SiO_2$ glasses is in most cases greater than the mole% $Al^{(V)}$ + $Al^{(VI)}$ in tectosilicate $CaAl_2O_4SiO_2$ glasses. From previous studies [1-2,4] it was determined that higher coordinated Al leads to higher hardness, however according to Figure 6.1 the hardness of the tectosilicate $CaO\text{-}Ga_2O_3\text{-}SiO_2$ glasses is lower than the hardness of the tectosilicate $CaO\text{-}Al_2O_3\text{-}SiO_2$ glasses until 80 mole% SiO_2 is reached. This would seem to indicate that the weaker Ga-O bond plays a more dominant role on hardness than the higher coordinated Ga species does.

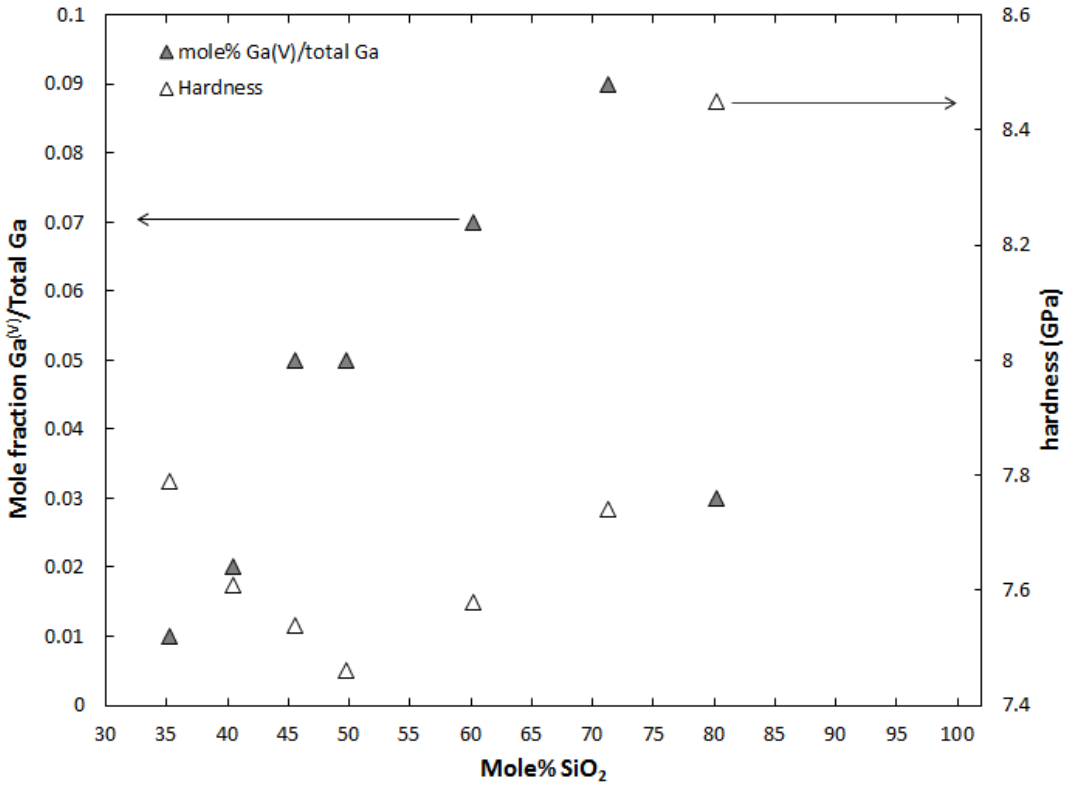

Figure 6.9. Mole fraction $Ga^{(V)}$/Ga and hardness as a function of mole% SiO_2 for tectosilicate $CaO\text{-}Ga_2O_3\text{-}SiO_2$ glasses.

If we now look at Figure 6.9 which is a plot of mole fraction $Ga^{(V)/}$total Ga and hardness as a function of mole% SiO_2 we can see that the hardness decreases until a mole fraction $Ga^{(V)}$/total Ga of 0.05 is reached. At this point a minimum in the hardness occurs. Up to this point it seems that the weaker Ga-O bond has a greater influence on the hardness, making shear easier by adding additional weak bonds other than NBO for breaking and reforming, as compared to the higher coordinated Ga species. Once the mole fraction $Ga^{(V)}$/total Ga increases above 0.05 the hardness begins to increase. It is at this point that the ratio of $Ga^{(V)}$/total Ga is large enough to overcome the weaker bonding of Ga-O and begin to see the increase in hardness from the higher coordinated Ga species, which was previously observed by Angel et. al. in calcium gallosilicate glasses containing up to 15 mole% Ga_2O_3 and up to 65 mole% SiO_2, and in aluminosiliicate glasses.[1-2,4] Once the Ga containing glasses reach 80 mole% SiO_2 we see a large drop in the amount mole fraction of $Ga^{(V)}$/total Ga, however the hardness continues to increase. It is at this point in the glasses where the transition from shear to densification must happen. This has to be the case if we consider that at mole fractions of $Ga^{(V)}$/total Ga below 0.05 we have easier shear and in glasses with mole fraction of $Ga^{(V)}$/total Ga greater than 0.05 we have increase in hardness due to the effect of the higher coordinated Ga species interlocking the glass structure. At 80 mole% SiO_2, according to Figure 6.9 we have a glass that has a mole fraction of $Ga^{(V)}$/total Ga below 0.05 yet we still have an increase in hardness, indicating that the deformation mechanism must have changed to densification as that is the only thing which could cause the hardness to continue to increase. The other thing to remember is that the $CaAl_2O_4SiO_2$ glasses looked at previously [1] showed a

transition from shear to densification at 80 mole% SiO_2 as well. Considering that Ga and Al behave similarly in silicate glasses,[6] one might expect that Ga and Al containing glasses with the same modifier ion may exhibit similar property trends,[6] and there for have a transition from shear to densification at nominally the same mole% SiO_2.

6.5. Summary and Conclusions

The indentation modulus of CGS glasses was found to increase with increasing glass density as it does for CAS and MAS glasses. However, the slope of the indentation modulus vs. density for CGS glasses was found to be much shallower compared to that of the CAS and MAS glasses. This was found to be related to the density of bonds per unit volume in the glass. CGS glasses have a larger glass density compared to MAS and CAS glasses, due to the larger mass of the Ga atom, however the Ga-O bond length is longer than the Al-O bond length resulting in a lower density of bonds per unit volume as compared to the MAS and CAS glasses. It was found that the indentation modulus is not only linked to the overall glass density but that it is also highly dependent on the density of bonds per unit volume in the glass structure.

CGS glasses exhibit a similar non-monotonic behavior in hardness with increasing mole% SiO_2 as CAS and MAS glasses. The main differences between the hardness of aluminosilicate and gallosilicate glasses is 1) the gallosilicate glasses have a lower overall hardness compared to the aluminosilicate glasses and 2) the minimum point in the hardness as a function of mole% SiO_2 for the gallosilicate glasses was found to be unrelated to the transition from shear to densification unlike what was found in the aluminosilicate glasses.

The overall hardness was found to be lower in CGS glasses as opposed to CAS and MAS glasses because of the weaker Ga-O bond over the Al-O bond. The weakness of the Ga-O bond allows it to participate in shear along with any NBO that may be present. This provides more opportunities for the glass to shear which in turn lowers the hardness of the CGS glasses.

The minimum in hardness as a function of mole% SiO_2 in CGS glasses was found to be related to the effect of higher coordinated Ga rather than a transformation in deformation mechanism from shear to densification. It was determined that for CGS glasses initially when the ratio of $Ga^{(V)}$ to total Ga in the glass is low then the Ga-O bonds are still able to participate in shear causing the decrease in hardness with increase in mole% SiO_2. However, when the ratio of $Ga^{(V)}$ to total Ga in the glass is greater than 0.05 then the $Ga^{(V)}$ is able to tie up the structure enough to now inhibit the movement of the Ga-O bonds and possibly even prevent some of the NBO that may be present from participating in shear, resulting in an increase in hardness. At 80 mole% SiO_2 in CGS glasses the ratio of $Ga^{(V)}$ to total Ga in the glass decreases substantially, however the hardness continues to increase. This mole% SiO_2 in CGS glasses is where the transition from shear to densification must occur, which is at about the same mole% SiO_2 as it is found to occur in CAS glasses.

In conclusion the CGS glasses provide more evidence to support the idea that NBO and weaker bonds, such as Ga-O, in glass structure are what participate in shear deformation. This study also provided further evidence that higher coordinated species, be it Ga or Al, when in large enough quantity in the glass structure will cause the hardness to increase by slowing down or preventing shear deformation from occurring. The transition from shear to densification deformation in CGS glasses was found to occur at approximately the same mole% SiO_2 as it was found to occur in CAS glasses.

REFERENCES

1. L.A. Lamberson, R.E. Youngman, S.P. Baker, "Plastic Deformation Mechanisms and the Hardness of CaO-Al_2O_3-SiO_2 Glasses." *In process*

2. L. A. Lamberson, R.E. Youngman, S.P. Baker, "Effect of Mg Replacement for Ca on Hardness of Aluminosilicate Glasses." *In process*

3. A. Arora, D.B. Marshall and B.R. Lawn, "Indentation, Deformation/Fracture of Normal and Anomalous Glasses." *J. Non-Cryst. Solids*, **31,** [3] 415-428 (1979).

4. S. Iftekhar, B. Pahari, K. Okhotnikov, A. Jaworski, B. Stevensson, J. Grins, M. Eden. "Properties and Structures of RE2O3-Al2O3-SiO2 (RE = Y, Lu) Glasses Probed by Molecular Dynamics Simulations and Solid State NMR: The Roles of Aluminum and Rare-Earth Ions for Dictating the Microhardness." *J. Phys. Chem. C*, **116,** 18394-18406 (2012).

5. L.Balewick and J. E. Shelby. "Properties of Calcium, Strontium, and Barium Galliosilicate Glasses." *J. Am. Ceram. Soc.*, **73** [2] 213-216 (1990).

6. L. Peng and J.F. Stebbins. "High Resolution 17O MAS and Triple-Quantum MAS NMR Studies of Gallosilicate Glasses." *J. of Non-Cryst. Sol.*, **354**, 3120-3128 (2008).

7. H. Doweidar, "Optical Properties and Structure of R_2O-Ga_2O_3-SiO_2 and RO-Ga_2O_3-SiO_2 Glasses." *J. Mater. Sci.*, **44**, 2899-2906 (2009).

8. P. W. Angel, C. S. Ray, D. E. Day. "Glass formation and Properties in the System Calcium-Gallia-silica." *J. of Am. Ceram. Soc.*, **73** [10] 2965-69 (1990).

9. W.C. Oliver and G.M. Pharr, "Measurement of Hardness and Elastic Modulus by Instrumented Indentation: Advances in Understanding and Refinements to Methodology." *J. Mater. Res.,* **19,** [1] 3-20 (2004).

10. W.C. Oliver and G.M. Pharr, "An Improved Technique for Determining Hardness and Elastic Modulus Using Load and Displacement Sensing Indentation Experiments." *J. Mater. Res.,* **7,** [6] 1564-1583 (1992).

11. D. Massiot, F. Fayon, M. Capron, I. King, S. Le Calve, B. Alonso, J. O. Durand, B. Bujoli, Z. Gan, G. Hoatson, *Magn. Reson. Chem.* **40**, 70 (2002).

CHAPTER 7

CONCLUSIONS AND FUTURE OUTLOOK

7.1. Conclusions

Tectosilicate calcium-aluminosilicate (CAS) glasses with < 80 mole% SiO_2 and magnesium-aluminosilicate (MAS) glasses with < 70 mole% SiO_2 were found to deform by a shear deformation process. This process was found to be a result of the breaking and reforming of non-bridging oxygen (NBO) with the aid of a modifying ion, in this case Mg or Ca. It was also determined that shear deformation is a lower activation energy process as the hardness for pure SiO_2, which is known to deform by purely densification, is higher than all of the other CAS and MAS glasses, with a hardness = 9.15 GPa, which deform by shear or a combination of shear and densification. It was determined that the shear deformation process can be made easier resulting in a lower hardness or more difficult resulting in a higher H by manipulating the availability of weak bonds for shearing. For instance, we found that the presence of higher coordinated Al can counteract the effect on hardness of NBO. The higher coordinated Al is able to tie up the NBO in a way which prevents them from being able to break or reform. We also found that by substituting Mg, which is a higher field strength atom and has a stronger

Mg-NBO bond than the Ca-NBO bond, for Ca in the tectosilicate CAS glasses we could increase the hardness by making shear more difficult. Since Mg prefers to bond with NBO over charge compensated tetrahedral Al there is a substantial increase in

higher coordinated Al in MAS glasses over CAS glasses. It was found that the increased $Al^{(V)}$ and $Al^{(VI)}$ and the stronger Mg-NBO bond both aided in making shear more difficult. On the other hand, if we substitute Ga, a larger mass and diameter atom with a weaker Ga-O bond, for Al we can increase the ease with which the glass can deform by shear. This is a result of adding another shearable species, Ga-O, besides NBO to the structure. However, it does appear once again that a higher coordinated species, whether it be $Al^{(V)}$ or $Ga^{(V)}$, does result in a strengthening of the glass network in such a way as to prevent or inhibit shear deformation. The data clearly shows however, that Al with the stronger Al-O bond is better at prohibiting shear than Ga with its weaker Ga-O bond.

We further showed that the transformation from shear to densification in CAS glasses can be altered by either making the densification process easier through the creation of a more open network or by making shear more difficult or by a combination of both. The substitution of Mg for Ca in CAS glasses moved the transition from shear to densification to lower mole% SiO_2 because of a combination of more difficult shearing and easier densification. Mg is a smaller atom which takes up less space making a more open structure and Mg also has a preference to bond with NBO resulting in a stronger Mg-NBO bond, while creating more $Al^{(V)}$ and $Al^{(VI)}$ species making shear more difficult. Ga on the other hand, is a larger atom with weaker Ga-O bonds and longer bond lengths over Al. Therefore, the perceived shift from shear to densification to lower mole% SiO_2 in calcium-gallosilicate (CGS) glasses is not actually a shift between the two types of deformation at all. Rather, the observed minimum in hardness for CGS glasses is a result of the higher coordinated

Ga species overcoming the weaker Ga-O bonds. In the CGS system initially the Ga-O bonds along with NBO allow for easier shear, however as the amount of $Ga^{(V)}$ in the structure continues to increase the strengthening effects of the higher coordinated species are able to overtake the effects of the weaker Ga-O bond resulting in an increase in hardness.

In conclusion it was found that shear deformation can be made easier by increasing the amount of NBO available for shearing or by increasing the number of weakly bonded species in the glass structure. On the other hand, shear can be made more difficult by eliminating the presence of NBO in the glass structure or by preventing the NBO, which are already in the structure, from being able to break or reform with new neighbors. Densification can be made easier by creating a more open structure by either using smaller atoms, modifying atoms in this case, or by having longer bond distances. Densification can be made more difficult by having a more compact structure from the use of larger atoms or by having shorter bond distances between atoms.

7.2. Future Outlook

There are several other experiments that would add to the already gained knowledge and help to further flush out what the exact unit deformation mechanisms are in silicate glasses. These additional experiments would aid in the development of a model to predict glass hardness. Below is a list of these experiments and how I think

they would be helpful in furthering our understanding of the modes of plastic deformation in silicate glasses.

7.2.1. Effect on hardness of CAS glasses with substitution of Ba or Sr for Ca

Replacing Ca in CAS glasses with a larger, lower field strength atom should result in glasses that are more difficult to densify and easier to shear. If this is the case, the combination of these two things would result in shifting the transition from shear to densification to higher mole% SiO_2. At the same time the overall hardness of the glasses would decrease as a result of the easier shear process.

7.2.2. Investigate the hardness of Binary CaO-SiO_2 glasses

Binary glasses in the CaO-SiO_2 system should have a lot of NBO without the presence of any higher coordinated species such as $Al^{(V)}$ to prevent them from shearing. The NBO in this case should be available to shear thereby decreasing the glass H and potentially removing the minimum in H due to the transition from shear to densification. The minimum in hardness from a transition in deformation modes should disappear because in the case of pure SiO_2 the deformation process would be densification which would have the highest hardness and as the Ca is added to the SiO_2 structure it will create NBO which will systematically decrease the hardness through the activation of the shear process. In this case I would expect to see a linear decrease in hardness with increase in Ca.

7.2.3. Investigate the hardness of binary Al_2O_3-SiO_2 glasses

The binary Al_2O_3-SiO_2 glass system should not contain any NBO. This system should also have a substantial amount of higher coordinated Al as there is no modifying ion in the structure to charge compensate the Al and keep it in tetrahedral conformation. I think in this instance it would be interesting to know if the higher coordinated Al still has a beneficial effect on hardness by preventing or making shear deformation more difficult. It may be however, that when the higher coordinated Al is present in a purely aluminosilicate structure it acts as a modifier and aids in shear deformation thereby reducing the glass hardness.

7.2.4. Investigate the effect on hardness going from per-calcic to per-aluminous in the CAS glass family

This series of glasses would be interesting as on the per-calcic side of the ternary there will be excess NBO in the glass structure and on the per-aluminous side there should be additional $Al^{(V)}$ and possible $Al^{(VI)}$. In this case I would expect to see hardness increase as Al increases in glass at expense of Ca until a certain level of Al is reached where the $Al^{(V)}$ and $Al^{(VI)}$ would no longer by tying up NBO but could potentially be acting as modifiers and aiding in shearing. These structural changes would result in a maximum in hardness as a function of Al content, if the higher coordinated Al did act as an aid in shearing when NBO are no longer present in the glass structure. It would be interesting to know if a maximum in hardness did occur and if so did it fall at the same content of Al that the maximum in viscosity occurs at, which was found to be on the per-aluminous side of the CAS ternary instead of on the tectosilicate line as would

be expected considering the glass should be fully polymerized when on the tectosilicate line.

7.2.5. Effect on hardness of densifying CAS glasses under pressure

It would be interesting to know in the CAS glass system if densifying the glasses under high pressure removes or makes the densification deformation mechanism more difficult resulting in higher hardness. Also, it would be interesting to know if forcing all of the atoms closer together through pressurizing the glass results in increasing the difficulty of shear deformation. If in fact glass densification by pressurization results in increasing the difficulty of shear and potentially removing a portion or all of the glasses ability to deform by densification then hardness should increase for all glasses no matter what mechanism of deformation they use. I would be interesting to know what effect this would have on the minimum in hardness found for CAS glasses as a function of mole% SiO_2.

7.2.6. Observation of glass structure during Nanoindentation through Raman or IR Spectroscopy

The use of Raman or IR spectroscopy to monitor the glass structure during indentation would provide more definitive evidence for how shear deformation occurs in glasses. This would enable us to see the unit deformation mechanisms such as formation of NBO or other defect species during indentation which facilitate shear. Structural observations while in the act of indentation would provide the first solid evidence of what the shear mechanism is in CAS or other aluminosilicate glasses.